

**THE APPLICATION OF ATOMIC AND MOLECULAR PHYSICS
IN FUSION PLASMA DIAGNOSTICS**

H. W. DRAWIN

**INSTITUTE OF PLASMA PHYSICS
NAGOYA UNIVERSITY**

NAGOYA, JAPAN

**THE APPLICATION OF ATOMIC AND MOLECULAR PHYSICS
IN FUSION PLASMA DIAGNOSTICS**

H. W. DRAWIN*

Institute of Plasma Physics, Nagoya University
Chikusa-ku, Nagoya 464-01, Japan

July 1988

*On leave from the Association EURATOM-CEA
Centre d'Etudes Nucléaires de Cadarache,
F-13108 St. Paul-lez-Durance/France

This document is prepared as a preprint of compilation of atomic data for fusion research sponsored fully or partly by the IPP/Nagoya University. This is intended for future publication in a journal or will be included in a data book after some evaluations or rearrangements of its contents. This document should not be referred without the agreement of the authors. Enquiries about copyright and reproduction should be addressed to Research Information Center, IPP/Nagoya University, Nagoya, Japan.

Abstract

This report consists of a summary of lecture notes.

Chapter I gives a general presentation of plasma effects caused by impurity species in pure hydrogen (deuterium) plasmas. Diagnostic possibilities based on atomic properties are enumerated. Chapter II contains a detailed derivation of the rate equations for the density of particles (mass), momentum and energy including atomic and molecular processes.

The collisional-radiative terms are discussed. Diagnostic applications of the rate equations are presented and discussed in Chapter III for magnetically confined hot core plasmas and in Chapter IV for edge and divertor plasmas. The heat removal capabilities of molecules are emphasized.

Preface and Acknowledgements

The text presented in this report is a short summary of a series of lectures, which were given while I was a guest professor at the Institute of Plasma Physics (IPP) of Nagoya University from January to April 1988. It has been avoided to treat Atomic and Molecular (A & M) Physics as an independent subject matter, rather has it been tried to see A & M Physics in connection with plasma physical applications..

It was in particular my intention to show how A & M physics can help to get a better understanding of plasmas in magnetic and inertial fusion devices.

Chapter I gives descriptions of plasma physical effects due to atomic and molecular species in high-temperature plasmas.

In Chapter II, the basic rate equations for the density of particles (mass), momentum and energy are developed and put into a form which permits direct application. Chapter III and IV treat particular applications in hot core plasmas and in the colder edge and divertor plasmas.

To give the text a certain homogeneity, pellet injection phenomena and high-density effects in atoms have not been included although they were treated in the lectures.

I would like to thank the Director of the IPP, Professor T. UCHIDA, and in particular Professor A. MIYAHARA who has initiated the invitation, for their continuous support during my stay at the IPP. I am very much obliged to the Director of the Research Information Center, Professor H. OBAYASHI and his collaborators, in particular to Professor H. TAWARA and to Dr. T. KATO. I am indebted to Mrs. ITONAGA who has contributed so much in aiding me to surmount the language problems associated with daily life.

Thanks to every one for making my visit to Japan a pleasant and delightful experience.

H.W. Drawin

Contents

PREFACE AND ACKNOWLEDGEMENTS

CHAPTER I

Introduction

I .1	Atoms and Molecules in Magnetically Confined Plasmas	1
I .1.1.	Radiation losses in hot core plasmas	1
I .1.2.	Further effects due to impurity species	3
	(a) electrical conductivity	3
	(b) particle diffusion	4
	(c) thermal conductivity	5
	(d) viscosity	6
I .1.3.	Pellets and impurity atoms injected by pellets	7
I .1.4.	Impurity atoms in edge plasmas and divertors	9
I .1.5.	Atomic (molecular) impurity species for diagnostic purposes	10
I .1.6.	Verification of atomic structure calculations; data base for plasma diagnostics ..	10
I .2.	Atoms in Laser/Ion Beams-Driven Plasmas	11

CHAPTER II

Basic Equations for Magnetically Confined Plasmas

II .1.	The Basic Electro-Magnetic and Particle Kinetic Equations	15
II .2.	Rate Equations for Particle Densities	17
II .3.	Rate Equations for Mass Density	19
II .4.	Coupling of Rate and Field Equations	19
II .5.	Rate Equations for Momentum Density	20
II .6.	Rate Equations for the Energy Density	22
II .6.1.	Internal energy	22
II .6.2.	Translational energy	26
II .6.3.	Thermal energy	29
II .6.4.	Total energy	31
II .6.5.	The collisional-radiative terms	33

CHAPTER III

Applications to Hot Core Plasmas in Magnetic Confinement Devices

III.1.	Introduction	44
III.2	Determination of Particle Confinement Times τ_p	44
III.3.	Confinement Times τ_p and Diffusion Coefficient D_a	47
III.4.	Determination of Energy Confinement Times τ_E	47
III.5.	The Particle Density Decay Time τ_p^*	49
III.6.	Determination of Particle Fluxes and Velocities.	51
III.7.	Determination of Convection Velocity.	57
III.8.	Radiation Losses	59
III.9.	Further Applications using Atomic Species.	62

CHAPTER IV

Applications to Edge and Divertor Plasmas

IV.1.	Introduction	64
IV.2.	Definition of Boundary and Scrape-off Layer and Divertor Plasmas	64
IV.3.	Formation of the Scrape-off Layer.	67
IV.4.	Recycling Coefficient	70
IV.5.	Properties of Diverted Plasmas	71
IV.6.	Molecules in Recycling Divertor Plasmas	72
IV.7.	Collisional-Radiative Models for Molecules	79
IV.8.	Atomic and Molecular Data for Edge Plasmas	81

REFERENCES	82
----------------------	----

APPENDIX.	86
-------------------	----

CHAPTER I

Introduction

I .1 Atoms and Molecules in Magnetically Confined Plasmas

I .1.1 Radiation losses in hot core plasmas

Atoms and molecules are constituents of all magnetically confined plasmas (tokamak, stellarator, spheromak, reversed field pinch plasmas etc.). Their abundances change with the type of machine, the vacuum conditions, the particular structure and composition of the wall material with which the plasma comes into contact. The atomic and molecular abundances depend strongly on the outgasing conditions and the temporal development of the plasma-wall contact. They are functions of the instantaneous state of the plasma and its spatio-temporal evolution. In other terms: a number of very different effects and parameters influence the atomic and molecular concentrations in both the cold edge plasma and the hot core plasma. And inversely, atoms and molecules have a direct effect on the plasma properties. This effect can be beneficial, for instance in radiating off energy in desired quantities in particular parts of a magnetic confinements device. Ionized impurity atoms can serve as "probes" which give information about the plasma state. The presence of impurity species can on the other hand be very deleterious, just because of the radiation losses and wall erosion they might induce. Increased wall erosion increases the impurity concentration and, thus, the radiation losses.

The ionized atoms are unwanted species in the hot core plasma of machines aiming at realizing the fusion of deuterium (*D*) and tritium (*T*) ions, because they radiate off energy which is needed for maintaining the temperature at a sufficient level which ensures burning of the fuel. Figure 1 may demonstrate this effect. The broken curve shows the total power density \dot{P}_{D-T} of a pure *D-T* plasma of total density $n=2 \times 10^{20} m^{-3}$ ($n_D=n_T=n_e/2=5 \times 10^{19} m^{-3}$). The continuous curve below the broken one represents the power density \dot{P}_α given to the α -particles which are assumed to be confined in the plasma during a sufficient time so that they can transfer their kinetic energy of $3.5 MeV$ to the bulk plasma according to the reaction



The α -particles (4He) heat the bulk plasma and the neutrons escape to the walls.

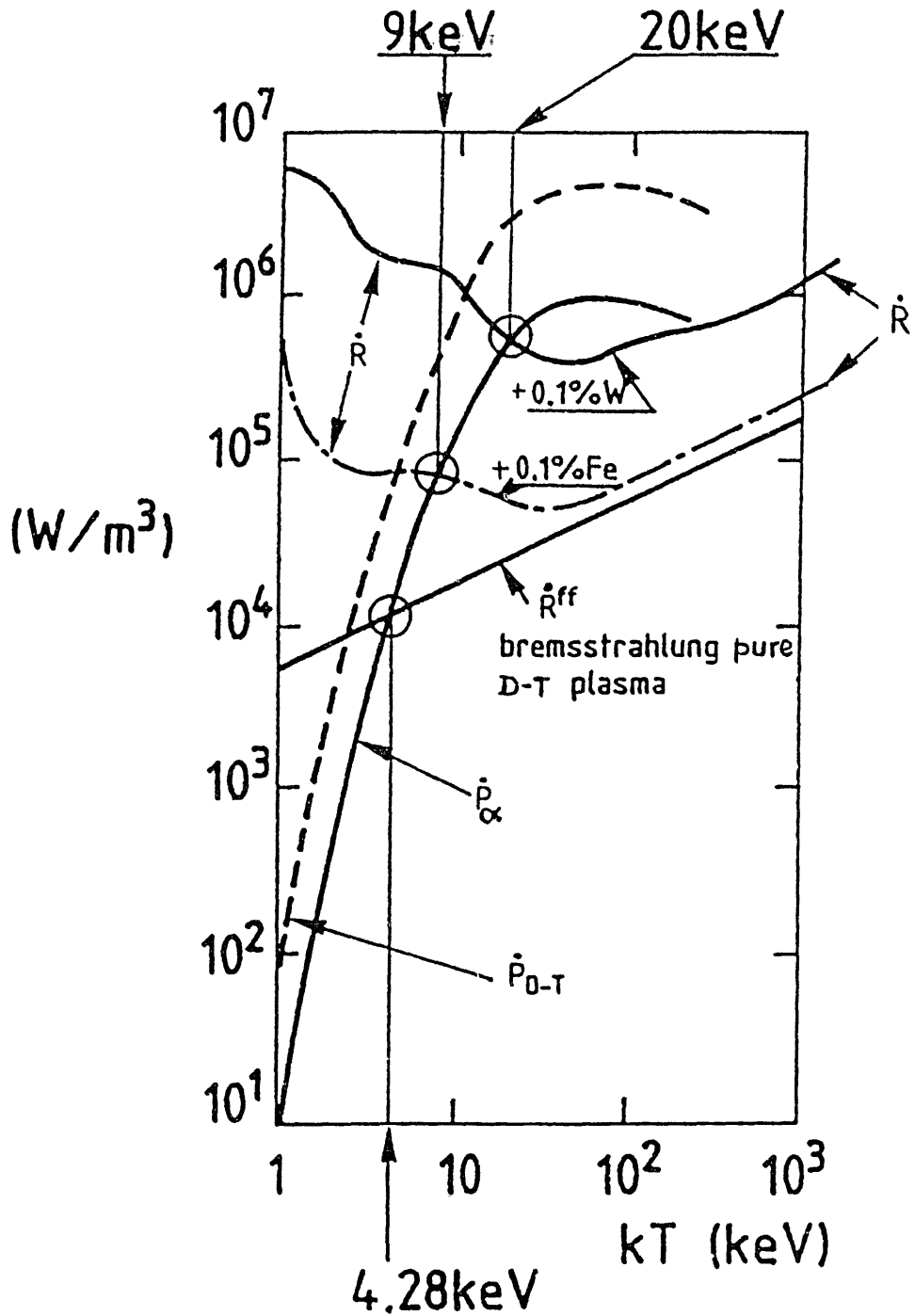


Figure 1 Comparison of power densities due to D-T thermonuclear reactions (\dot{P}_{D-T} and \dot{P}_α) and radiation (\dot{R}^{ff} =free-free or Bremsstrahlung) of a pure D-T plasma, \dot{R} =radiation loss with 0.1% Fe or 0.1% W added. Assumption is made that $n_D = n_T = n_e/2 = 5 \cdot 10^{19} m^{-3}$.

The bulk plasma radiates off energy in form of free-free radiation (bremsstrahlung). When we assume that the α -particle concentration is negligible — which will surely be the case at the beginning of the thermonuclear burning process — the radiation loss is that of a pure $D-T$ plasma according to the relation

$$\dot{R}^{ff} = 4.8 \times 10^{-37} n_e^2 T_e^{1/2} [W/m^3] \quad (1.2)$$

with the electron density n_e in m^{-3} , electron temperature T_e in keV . Assuming no other energy losses, it yields a minimum ignition temperature of $4.28 keV$ for $T_e = T_i$, T_i being the ion temperature. (Intersection where $\dot{R}^{ff} = \dot{P}_a$).

The presence of ionized species of charge state “ z ” having the density n^z increases the radiation losses and decreases the thermonuclear power production rate because of dilution of the fuel. Figure 1 shows the radiation power density R which is lost when 0.1% iron or 0.1% tungsten are present in the plasma. The thermonuclear power density equals the power density lost by radiation at $T = 9 keV$ and $T = 20 keV$, respectively, for the two cases of impurities mentioned above, assuming no dilution of the $D-T$ fuel (which affects \dot{P}_{D-T} and \dot{P}_a) and assuming that the contribution of He^{2+} to the radiation loss is negligible.

Impurities in a $D-T$ plasma increase in particular the energy losses in the colder plasma regions where the thermonuclear power production is insignificant. This means that the thermonuclear core plasma must also compensate these energy losses, hence raising still more the ignition temperature. One can show that a $D-T$ plasma containing approximately $0.6\% \div 1\%$ iron cannot compensate alone all the radiation losses.

Thermal conduction and convection contribute significantly to the energy losses. Since they can very probably not drastically be reduced, the only way of significantly reducing the overall energy losses is to reduce the radiation losses, that is to reduce the concentration of impurities, in particular those with high atomic Z -values. It is because of this situation that the impurity problem is still of major concern in thermonuclear fusion research.

1.1.2 Further effects due to impurity species

The presence of (highly) ionized species causes further effects.

(a) Electrical Conductivity

Species with $z_i > 1$ increase the electrical resistivity by a factor Z_{eff} given by

$$Z_{eff} = \frac{\sum_i n_i z_i^2}{\sum_i n_i z_i} = \frac{\sum_i n_i z_i^2}{n_e} \quad (1.2)$$

where the summation is made over all ion species “ i ” having ionic charge $e_0 z_i$ seen by the bulk electrons.

The generalized Ohm's Law for a magnetized plasma is given by the expression

$$\vec{E} = \eta_{\parallel} \vec{j}_{\parallel} + \eta_{\perp} \vec{j}_{\perp} + \vec{v}_0 \times \vec{B} + \frac{v_{ec} \tau_{ei}}{B} [\vec{j} \times \vec{B} + \vec{\nabla} P_e] \quad (I.3)$$

where \vec{E} is the intensity of the electric field, $\vec{j}_{\parallel(\perp)}$ the current density parallel (perpendicular) to the magnetic induction \vec{B} , \vec{v}_0 the mass velocity, P_e the electron pressure, $v_{ec} = 1/\tau_{ec}$ the electron gyrofrequency ($v_{ec} = 2.8 \times 10^{10} B [T] \text{ sec}^{-1}$) and τ_{ei} the electron-ion 90°-Coulomb deflection time:

$$\tau_{ei} = 2.51 \times 10^8 \frac{A T_e^{3/2}}{Z_{eff}^2 n_e \ell n \Lambda} [s] \quad (I.4)$$

where T_e is the electron temperature in Kelvin, n_e in m^{-3} and $\ell n \Lambda$ the Coulomb logarithm. All terms of the right-hand side (r. h. s.) of eq. (I.3) are influenced by the impurity ions, and even \vec{v}_0 , since the fields acting on the plasma depend on mass and charge. The coefficients of electrical resistivity (η_{\parallel} , η_{\perp}) (conductivity σ_{\parallel} , σ_{\perp}) are given by (T_e in Kelvin, B in Tesla)

$$\eta_{\parallel} = \frac{1}{\sigma_{\parallel}} = 6.87 \times 10^{-1} \frac{Z_{eff} \ell n \Lambda}{T_e^{3/2}} [\Omega \cdot m] \quad (I.5)$$

$$\eta_{\perp} = \frac{1}{\sigma_{\perp}} = 1.37 \times 10^{-2} \frac{Z_{eff} \ell n \Lambda}{T_e^{3/2}} B^2 [\Omega \cdot m] \quad (I.6)$$

A measurement of η_{\parallel} yields an information about Z_{eff} when n_e and T_e are known. n_e intervenes in the expression for $\ell n \Lambda$.

It is not possible to measure in a tokamak E_{\parallel} and j_{\parallel} directly as a function of the radius r . However, a measurement of the total plasma current J_p and of the loop voltage U yields an average value of Z_{eff} , see Eq. (III.56).

(b) Particle Diffusion

Let \vec{v}_0 be the mean local mass velocity of the plasma as a whole and $\langle \vec{V}_s \rangle$ the mean diffusion velocity of the species "s" relative to \vec{v}_0 .

The density of the particle flux of species "s" is given by the relation (see also Eq. (II.10.c))

$$\vec{\Gamma}_s = n_s \vec{v}_0 + n_s \langle \vec{V}_s \rangle \quad (I.7)$$

where $n_s \langle \vec{V}_s \rangle$ represents the density of the so-called "diffusion flux" with regard to the bulk plasma velocity (or mass velocity) \vec{v}_0 . For charged species, the diffusion flux is essentially ambipolar. In a strong uniform magnetic field the density of the diffusion flux (neglecting the Hall and thermoelectric contributions) is expressed by the following relations:

• parallel to \vec{B} :

$$n_e \langle \vec{V}_{amb} \rangle_{\parallel} = -D_{\parallel} \vec{\nabla}_{\parallel} n_e \quad (I.8)$$

with the parallel diffusion coefficient D_{\parallel} given by

$$D_{\parallel} = 2 \times D_{\parallel}^{ions} = 5.62 \times 10^{11} \frac{T_e^{5/2}}{Z_{eff}^3 A^{1/2} n_e \ell n \Lambda} [m^2 s^{-1}] \quad (I.9)$$

• perpendicular to \vec{B} :

$$n_e \langle \vec{V}_{amb} \rangle_{\perp} = -D_{\perp} \vec{\nabla}_{\perp} n_e \quad (I.10)$$

with the perpendicular diffusion coefficient D_{\perp} given by

$$D_{\perp} = 2 \times D_{\perp}^{electrons} = 7.42 \times 10^{-21} \frac{n_e \ell n \Lambda}{B^2 T_e^{1/2}} [m^2 s^{-1}] \quad (I.11)$$

(n_e in m^{-3} , T_e in Kelvin, B in Tesla, A is the relative atomic weight).

(c) *Thermal conductivity*

The density of the thermal heat flux due to thermal conduction (neglecting a term proportional to $\vec{B} \times \vec{\nabla} T$ where T is either T_e or T_i) is given by the expression

$$\vec{q} = -\kappa_{\parallel} \vec{\nabla}_{\parallel} T - \kappa_{\perp} \vec{\nabla}_{\perp} T \quad (I.12)$$

The coefficients of thermal conduction in a strong uniform magnetic field of induction \vec{B} are

• parallel to \vec{B} :

– for the electrons :

$$\kappa_{\parallel}^e = 2.48 \times 10^{-10} \frac{T_e^{5/2}}{\ell n \Lambda} [W \times K^{-1} \times m^{-1}] \quad (I.13)$$

– for the ions :

$$\kappa_{\parallel}^i = 5.82 \times 10^{-12} \frac{T_e^{5/2}}{z_i^4 A_i^{1/2} \ell n \Lambda} [W \times K^{-1} \times m^{-1}] \quad (I.14)$$

• perpendicular to \vec{B} :

– for the electrons :

$$\kappa_{\perp}^e = 7.68 \times 10^{-44} \frac{n_e^2 \ell n \Lambda}{B^2 T_e^{1/2}} [W \times K^{-1} \times m^{-1}] \quad (I.15)$$

– for the ions :

$$\kappa_{\perp}^i = 3.19 \times 10^{-42} \frac{A_i^{2/3} z_i^2 n_i^2 \ell n \Lambda}{B^2 T_i^{1/2}} [W \times K^{-1} \times m^{-1}] \quad (I.16)$$

(d) Viscosity

The coefficient of viscosity (η^e, η^i) for electrons and ions, in the absence of a magnetic field are given by

$$\eta_0^e = 1.09 \times 10^{-17} \frac{T_e^{5/2}}{\ell n \Lambda} \left[\frac{J \times s}{m^3} \right] \quad (I.17)$$

$$\eta_0^i = 4.66 \times 10^{-16} \frac{A_i^{1/2} T_i^{5/2}}{z_i^4 \ell n \Lambda} \left[\frac{J \times s}{m^3} \right] \quad (I.18)$$

In a strong uniform magnetic field of induction \vec{B} (gyrofrequency larger than collision frequency) the components of $\eta^{e,i}$ parallel to \vec{B} are not modified (i.e., $\eta_{\parallel}^e = \eta_0^e, \eta_{\parallel}^i = \eta_0^i$) whereas the components of $\eta^{e,i}$ perpendicular to \vec{B} experience strong modification. The corresponding perpendicular coefficients of viscosity for the electrons and ions are, respectively, given by

$$\eta_{\perp}^e = 3.38 \times 10^{-51} \frac{n_e^2 \ell n \Lambda}{B^2 T_e^{1/2}} \left[\frac{J \times s}{m^3} \right] \quad (I.19)$$

$$\eta_{\perp}^i = 2.64 \times 10^{-46} \frac{z_i^2 A_i^{5/2} n_i \ell n \Lambda}{B^2 T_i^{1/2}} \left[\frac{J \times s}{m^3} \right] \quad (I.20)$$

(n in m^{-3} , T in Kelvin, B in Tesla, A is the relative atomic weight).

Remark

In magnetic confinement devices which have strong nonuniform magnetic field distributions, the measured transport coefficients $D_{\perp}, \kappa_{\perp}, \eta_{\perp}^i$ and η_{\perp}^e are actually larger than the theoretically predicted ones, even when the particular magnetic structure is taken into account. To describe the experimental findings by plasma models one has introduced so-called anomalous transport coefficients. They represent phenomenological coefficients which permit to fit the results of numerical transport codes to experimental data. These transport coefficients are not given by a theory.

I .1.3 Pellets and impurity atoms injected by pellets

The injection of H_2 (D_2) ice pellets is a means to increasing the plasma density of magnetically confined plasmas. Pellet injection can also be applied for plasma diagnostic purposes, either by adding impurity species to H_2 (D_2) pellets or by injecting impurity species in form of an entire impurity pellet (for instance injection of a frozen Ne or Ar pellet or a metal pellet). The advantage of injecting impurities in this way is to create a particle source and a temperature sink which is rather localised and which thus permits measurements which are much more difficult or impossible to realize otherwise.

The pellet plasma proper has some properties which one finds in similar form in the expanding phase of laser/ion-beams irradiated target plasmas. The density is high and the temperature relatively low, at least during the initial stage of the ablation (evaporation). This means that in the high-density phase local thermodynamic equilibrium (L.T.E.) laws can be applied, which considerably facilitates numerical simulation. Also the hydrodynamic evolution has some similarities in both cases. Further, characteristic density effects are quite similar in nature but very different in their absolute values. These differences have their origin in the energy fluxes to which the pellets and targets are submitted. The solid pellets injected into magnetically confined plasmas are subjected to a relatively weak energy flux of electrons, the density of the energy flux being of the order of $(1\sim 10) 10^9 W/m^2$ during the whole ablation process of several hundred microseconds, which is negligible compared to the $10^{18} \sim 10^{20} W/m^2$ to which laser (or ion)-beam targets are exposed during times of the order of a nanosecond or less.

Also during the later expansion phase the two types of plasmas have some common features in so far as both evolve towards a collisional-radiative regime. However, there are also marked differences; the most important one is that the pellet matter ablated in a magnetic confinement device flows into a hot basic plasma by which it is continuously heated up. Therefore its energy density and the flow velocity increase continuously until reaching that of the basic plasma. The flow velocity finally becomes supersonic. The laser (or ion) beams-irradiated target plasmas expand into a gas at low density and low temperature, thus leading to a decrease of the thermal energy density and a decrease of the flow velocity until some collisionless limit is reached.

One can say that both types of high-density plasmas are complementary to each other and represent interesting objects for studying their state and their spatio-temporal evolution.

Figure 2 gives schematic presentations of pellets which have been applied for fueling and diagnostic purposes. The ideal case of a sphere is only realized in the Nagoya experiments, the H_2 (D_2) ice pellets have always the form of a cylinder.

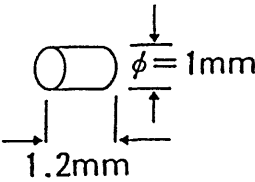
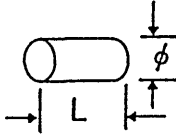
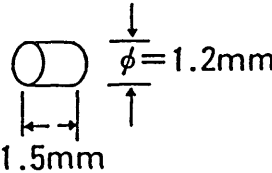
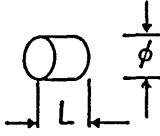

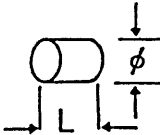
ASDEX		$V_p = 720 \frac{m}{s}$ D_2
TFR		$\phi_1 = 0.6mm$ $L_1 = 2mm$ } $V_p = 600 \frac{m}{s}$ $\phi_2 = 0.85mm$ $L_2 = 1mm$ } $V_p = 700 \frac{m}{s}$ $H_2, D_2 + \text{neon doped}$
PLT		$V_p = 450 \frac{m}{s}$ D_2
JFT-2M		$\phi_1 = L_1 = 1mm$ $\phi_2 = L_2 = 1.65mm$ mixture $H_2 + D_2$ V_p up to $970 \frac{m}{s}$
JIPP-TII		$\phi = 0.5mm, Al$ $\phi = 0.226 \text{ and } 0.46mm$ C (Plastics) $\phi = 0.5mm, \text{ steel SUS}$ $V_p \simeq 400 \frac{m}{s}$
TFTR		$\phi_1 = L_1 = 2.67mm, V_p = 1350 \frac{m}{s}$ $\phi_2 = L_2 = 4mm, V_p = 1300 \frac{m}{s}$

Figure 2. Some types of pellets (listing not exhaustive) which have been injected into various tokamak plasmas.

By including in a larger H_2 (D_2) ice pellet a smaller impurity pellet, for instance a spherical hydrocarbon pellet as shown in Figure 2, it would be possible to introduce deep in the plasma a well defined impurity source without contaminating the outer plasma region with this type of impurity.

I .1.4 Impurity atoms in edge plasmas and divertors

Atoms in low and medium ionization stages have favourable radiation properties, since they can produce huge amounts of radiation. This radiation production represents an energy sink for the plasma particles, in particular the electrons, which furnish the energy by exciting the particles. The presence of impurities in the edge plasma region and in the divertor could therefore have the beneficial property to lower the plasma temperature in front of the material walls and, thus to decrease wall sputtering and wall erosion.

An important problem in the operation of a fusion reactor will be the entire control of the plasma edge region including the plasma in an eventual divertor system or in any other particle and thermal energy exhaust system. This control must consist of optimizing the impurity concentrations in the edge plasma regions in order to cool radiatively as much as possible the plasma in front of the material walls and to minimize the deleterious impurity effects in the hot core plasma where the fusion reactions take place. An enormous task! Neither a physical nor a satisfactory technical solution of this problem have yet been found; also the two requirements are contradictory from the energetic point of view (see Fig. 1 and the corresponding comment there) and some compromise has to be found.

The study of the impurity behaviour in the edge plasma as a function of the parameters and properties of the core plasma on the one side and those of the material walls and the plasma sheath in front of the material walls on the other side is therefore an important task in fusion-oriented plasma diagnostics.

A particular situation is met in the divertor scrape-off layer and in particular in the plasma close to the divertor target plates where the temperature is low (a few eV) and the density high ($\approx 10^{20} \text{ m}^{-3}$). Molecules (H_2 , O_2) have an influence on the radiation and transport properties of that region, see Chapter IV.

I .1.5 Atomic (molecular) impurity species for diagnostic purposes

Impurity atoms and ions represent powerful diagnostic tool. They permit when appropriately chosen and applied, the determination of numerous plasma parameters and quantities of interest. The following methods may be mentioned (not exhaustive) :

<u>Quantity to be determined</u>	<u>Method</u>
– 1-Electron temperature T_e :	measurement of absolute line intensities I_{ij} or of line intensity ratios and interpreted by rate equations.
– 2-Electron density n_e :	Measurement of line intensity ratios and interpreted by rate equations, measurement of absolute line intensities of injected impurities.
– 3-Ion temperature T_i :	measurement of Doppler broadening or line intensity ratios, measurement of “charge-exchange neutrals.”
– 4-Rotation velocity v_r :	measurement of Doppler shift of a spectral line.
– 5-Magnetic fields $ B $:	Measurement of Zeeman splitting.
– 6-Magnetic field direction \vec{B} :	measurement of the polarization angle of the Zeeman components of a spectral line, determination of the pitch angle of the magnetic field lines from striated ablation clouds of injected pellets.
– 7-Confinement times :	measurement of absolute line intensities and interpreted by rate equations; plasma decay measurement.
– 8-Diffusion and convection fluxes :	measurement of line intensities interpreted by rate equations; measurement of fluorescence profiles (for edge plasmas).
– 9-Effective ion charge number Z_{eff} :	measurement of absolute spectral line intensities in connection with the solutions of rate equations; local measurement of intensity ratios of impurity to hydrogen lines populated by charge exchange.

I .1.6 Verification of atomic structure calculations; data base for plasma diagnostics

Several of the diagnostic methods using spectral line emission from impurities rely on atomic models in which both the level structures and the atomic data (cross sections, radiative transition probabilities) intervene. It is essential to possess a reliable data base. The measurement of the wavelengths of impurities emitted from both the hot and cold plasma regions permits identification of impurity species. Their comparison with the theoretical data obtained from atomic (molecular) structure calculations can be useful to

refining the identification. The measurement of both relative and absolute spectral line intensities can be a valuable help in refining the atomic (molecular) data or the plasma models to which the data are applied.

An important quantity is the absolute concentration of the various impurity species as a function of space and time. These are determined from spectral line intensities in connection with rate equations for the atomic processes. Unreliable atomic (molecular) data will lead to unreliable values of the impurity concentrations and of other plasma parameters determined by similar methods.

1.2. Atoms in Laser/Ion Beams-Driven Plasma

Atoms of low- and medium-Z elements generally originate from the particular construction of the solid targets in which the D-T fuel mixture is enclosed. An impurity gas (e.g., argon) is sometimes added for diagnostic purposes. Figures 3 and 4 show typical structures of directly irradiated pellets for specific purposes.

The common features of and the main differences between the expanding plasmas of the pellet ablation clouds in magnetic confinement fusion (MCF) and those applied in inertial confinement fusion (ICF) studies have already been discussed in Section I.1.3. We summarize in Figs. 5a, b the essential parameters of these two types of plasmas.

The diagnostic methods applied for the diagnosis of laser/ion beams-driven plasmas are the same as for plasmas in magnetic confinement devices. There is, however, an important difference: in ICF studies, the duration of a plasma is extremely short, thus, high-speed detection systems have to be applied. Optical absorption can often not be neglected. This introduces a further complication in the evaluation of the measured data, since the radiative transfer equations have to be solved simultaneously with the rate equations for particles (or mass), momentum and energy. In ICF studies, the characteristic time scales are of the order of nanoseconds or less. In MCF studies, the shortest time scale for spectral line measurements is determined by the "saw-tooth period" (several milli-seconds). Only pellet ablation studies require shorter time resolutions (ten to hundred nanoseconds).

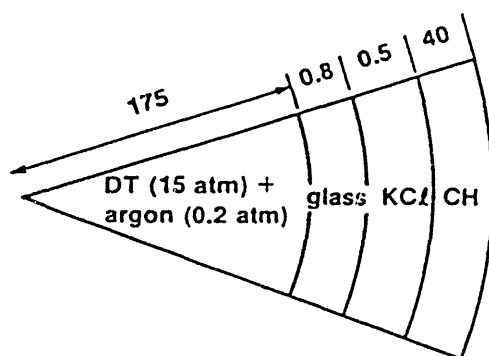


Figure 3. Target for laser radiation implosion studies, after Ref. [1].

All measures
in micrometers

- | | | |
|-----|--|---|
| (1) | | Exploding pusher
(Neutron) |
| (2) | | Ablative compression
(high density compression) |
| (3) | | Multi-layered
(in measurement) |
| (4) | | Shell-target |
| (5) | | Cryo-target |
| (6) | | Large aspect
(stability)
(shock multiplication) |
| (7) | | Corrugated-target
(stability) |

Figure 4. Typical structures of irradiation targets for specific purposes (GMB=glass-micro-balloon), after Ref. [2].

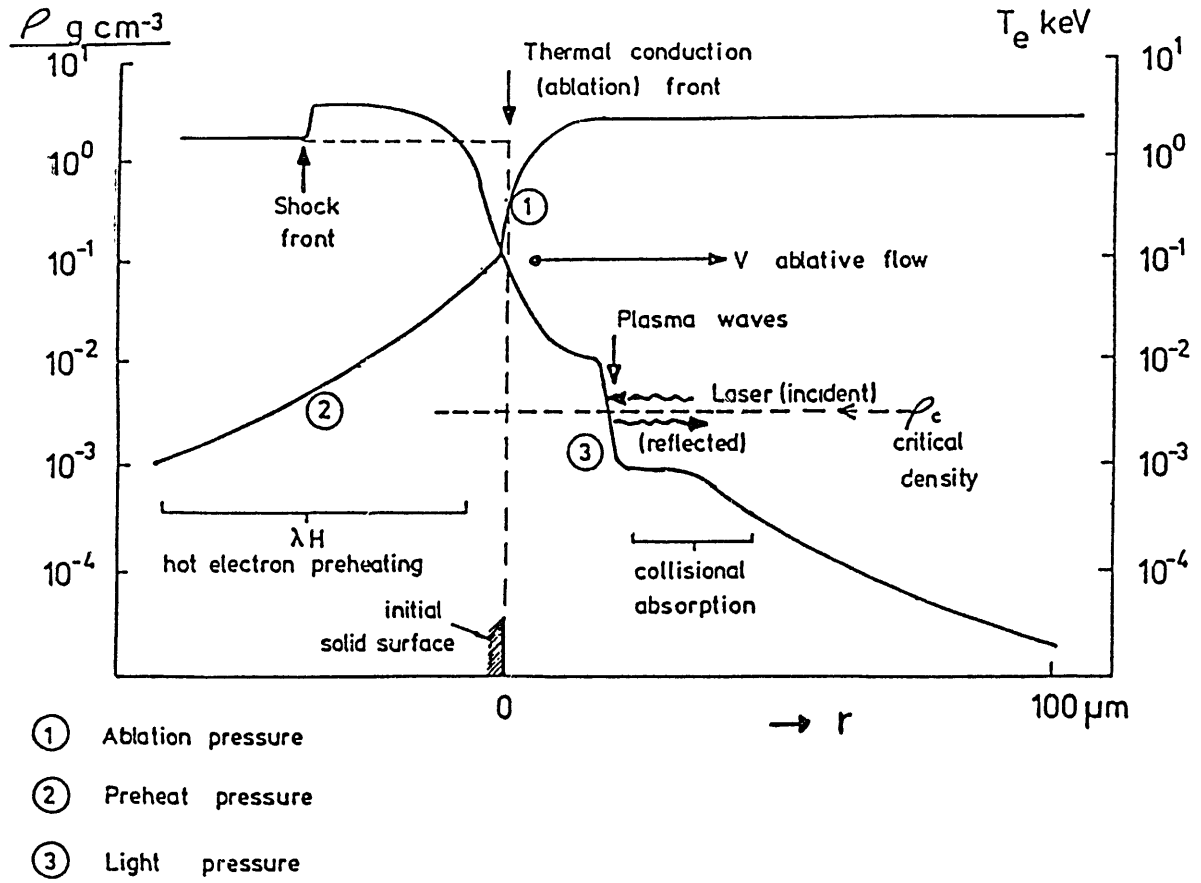


Figure 5a. The essential parameters of the high-density plasma of an ablating pellet in MCF studies. Irradiation conditions: 10^{15} W/cm^2 at wavelength $\lambda=1 \mu\text{m}$ on a $100 \mu\text{m}$ diameter spherical solid target of medium atomic number. 100ps after irradiation the plasma flow would be steady with the parameters shown in this figure. After Ref. [3].

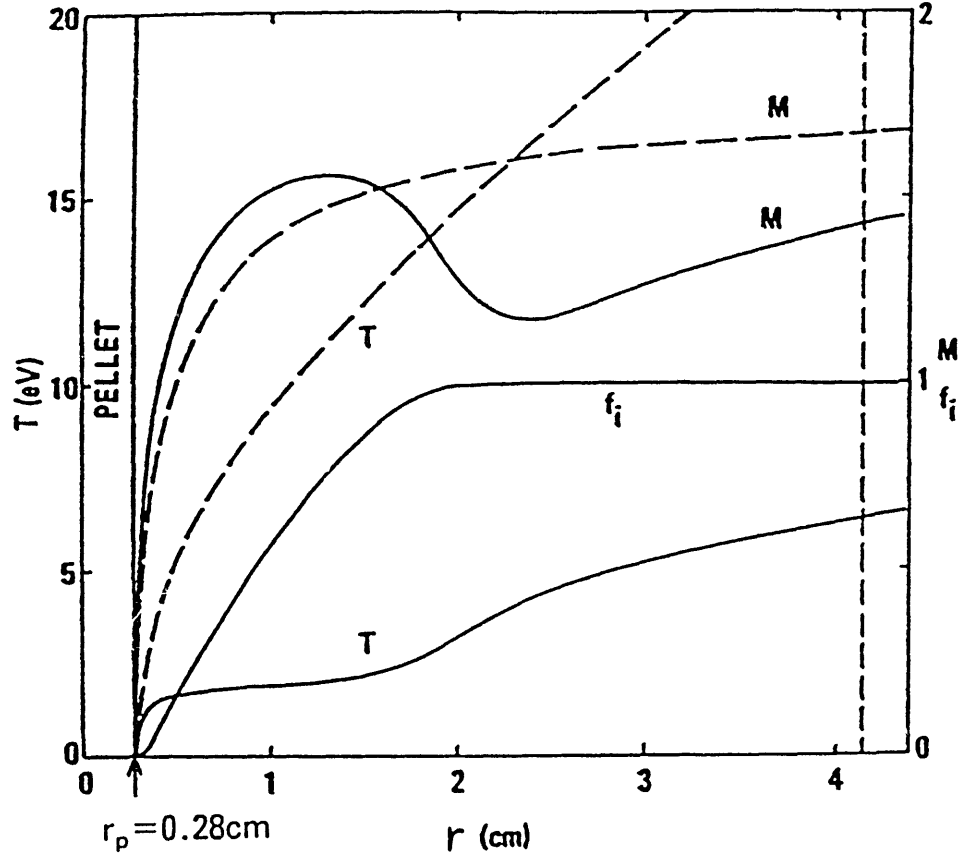


Figure 5b. Temperature T , Mach number $M=v/v_{th}$ and degree of ionization f_i of an ablating H_2 pellet of initial radius $r_p=0.28$ cm injected into a background plasma of $n_e(\infty)=1.01 \times 10^{20} \text{ m}^{-3}$ and $T_e(\infty)=11.5 \text{ keV}$.

----- : with surface dissociation and ionization.

————— : without surface dissociation and ionization.

After Ref. [4].

CHAPTER II

Basic Equations For Magnetically Confined Plasmas

II.1. The Basic Electro-Magnetic and Particle Kinetic Equations

Plasmas in magnetically confined plasma devices are submitted to strong magnetic fields of induction $\vec{B} = \mu \vec{H}$, and to low or medium electric fields of strength \vec{E} which are composed of a stationary and a fluctuating part.

Owing to the high plasma temperature the plasma conductivity is extremely high, thus relative weak stationary or quasi-stationary electric field strengths can produce high current densities, see Eqs. (I .3) and (I .5).

The plasma current of density \vec{j}_p is either a pure electric induction current \vec{j}_{ind} created by the toroidal electric field \vec{E}_ϕ originating from the changing magnetic flux in the poloidal field coils, or a non-inductive current \vec{j}_{nind} sustained by particle injection and/or high-frequency electromagnetic waves converted to particle accelerating wave modes, or it is a combination of both. The inductive current is generally transported by a displaced Maxwellian velocity distribution of the plasma electrons. The non-inductive current produced by high-frequency waves originates from a low-density group of decoupled electrons which are accelerated to relativistic velocities moving in the bulk plasma whose velocity distribution can in a first approximation still be considered as Maxwellian. However, the deviations from the Maxwellian velocity distribution can cause significant atomic physics effects.

The plasma as a highly conducting fluid is globally neutral; i.e., on a macroscopic scale and to a first approximation, the electric charges of the electrons of density n_e and those of all ions of densities $n_{k,i}^z$, compensate each other (z =ionic charge state of particles of chemical element “ k ” in internal quantum state $|i\rangle$). Denoting by the subscript “ s ” either of the negatively ($s=e$) or positively ($s=\{z, k, i\}$) charged species with electric charge q_s and particle density n_s , the quasineutrality condition is given by (e_0 means the elementary charge)

$$\sum_s q_s n_s = e_0 (-n_e + \sum_{i,k,z} z_{k,i} n_{k,i}^z) = 0 \quad (\text{II .1})$$

Further, for an ionized gas, $\varepsilon \approx \varepsilon_0$ and $\mu \approx \mu_0$ hold; thus, the vectors for magnetic induction \vec{B} and electric displacement \vec{D} are given by the following constitutive relations

$$\vec{B} = \mu_0 \vec{H} \quad (\text{a}) \quad ; \quad \vec{D} = \varepsilon_0 \vec{E} \quad (\text{b}) \quad (\text{II .2})$$

where \vec{H} is the magnetic field intensity vector.

The Ampère-Maxwell and Faraday relations couple the material current density \vec{j}_p to the electromagnetic field quantities :

$$\frac{\partial \vec{D}}{\partial t} = \vec{\nabla} \times \vec{H} - \vec{j} \quad (a) \quad ; \quad \frac{\partial \vec{B}}{\partial t} = -\vec{\nabla} \times \vec{E} \quad (b) \quad (II.3)$$

\vec{B} and \vec{D} (because of Eq. (II.1)) are source free :

$$\vec{\nabla} \cdot \vec{B} = 0 \quad (a) \quad ; \quad \vec{\nabla} \cdot \vec{D} = \sum_s q_s n_s \approx 0 \quad (b) \quad (II.4)$$

The density of the plasma current, \vec{j}_p is the sum of inductive (\vec{j}_{ind}) and non-inductive (\vec{j}_{nind}) current densities :

$$\vec{j}_p = \vec{j}_{ind} + \vec{j}_{nind} \quad (II.5)$$

In Eqs. (II.3.a) the toroidal component \vec{j}_ϕ of \vec{j} is the total plasma current density \vec{j}_p . In Eq. (II.3.b) the toroidal component \vec{E}_ϕ of \vec{E} is the inductively created field strength which drives the inductive current of density \vec{j}_{ind} .

The so-called MHD-approximation assumes $\partial \vec{D} / \partial t = 0$.

The particle density $n_s(r, t)$ at space point \vec{r} in the laboratory system, at time t , is the velocity integral over the velocity distribution function $f_s(r, t, \vec{w}_s)$ of species "s", where \vec{w}_s represents the velocity relative to the laboratory system. Then

$$n_s(r, t) = \int_{\vec{w}_s} d^3 w_s f_s(r, t, \vec{w}_s) \quad (II.6)$$

with f_s given by the kinetic non-relativistic Boltzmann equation

$$\frac{\partial f_s}{\partial t} + \vec{w}_s \cdot \frac{\partial}{\partial \vec{r}} f_s + \frac{\vec{F}_s}{m_s} \cdot \frac{\partial f_s}{\partial \vec{w}_s} = \left[\frac{\partial f_s}{\partial t} \right]_{CR} \quad (II.7)$$

\vec{F}_s is the self-consistent force acting on a particle of mass m_s :

$$\vec{F}_s = q_s (\vec{E} + \vec{\omega}_s \times \vec{B}) \quad (II.8)$$

In this expression non-electric and non-magnetic forces have been neglected. \vec{E} is the sum of externally applied electric fields and of fields created in the plasma by the particles themselves (i.e. Debye fields, plasma wave fields, ...).

The expressions of the velocity integrals of the terms in Eq. (II.7) are given in the Appendix.

In magnetic confinement devices, $\vec{B} = \vec{B}_\phi + \vec{B}_\theta + \vec{B}_r$, where \vec{B}_ϕ is the toroidal and \vec{B}_θ the poloidal magnetic induction. \vec{B}_r is the radial component (magnetic ripple) caused by the distance between the toroidal field coils and the vertical field induction. The term on the r.h.s. of Eq. (II.7) is the collisional-radiative term which contains the various collision and radiation processes leading to a change of f_s .

In the following we will use the gradient (Nabla) operators

$$\frac{\partial}{\partial \vec{r}} \equiv \vec{\nabla} \quad \text{and} \quad \frac{\partial}{\partial \vec{w}_s} \equiv \vec{\nabla}_w$$

II.2 Rate Equations for Particle Densities

Integrating Eq. (II. 7) over \vec{w}_s yields the rate or balance equation for the particle density $n_s(r, t)$ see e.g. ref. [5], pp. 155~159 or ref. [6] :

$$\frac{\partial n_s}{\partial t} + \vec{\nabla} \cdot (n_s \langle \vec{w}_s \rangle) = \left[\frac{\partial n_s}{\partial t} \right]_{CR} \quad (\text{II.9})$$

where $\langle \vec{w}_s \rangle$ is the mean species velocity. We introduce the mean local mass velocity* $\vec{v}_0(r, t)$ of the plasma as a whole and the peculiar velocity $\vec{V}_s(r, t)$ relative to \vec{v}_0 . The vector $\vec{V}_s(r, t)$ has two contributions, one originating from the mean diffusion velocity $\langle \vec{V}_s(r, t) \rangle$ relative to \vec{v}_0 , the other one is a random velocity $\vec{v}_s(r, t)$ whose average is zero. This latter part represents the particle motion due to heat and yields the hydrostatic pressure p . We thus have

$$\vec{w}_s = \vec{v}_0 + \vec{V}_s(r, t) = \vec{v}_0(r, t) + \langle \vec{V}_s(r, t) \rangle + \vec{v}_s(r, t) \quad (\text{II.10.a})$$

$$\langle \vec{w}_s \rangle = \vec{v}_0 + \langle \vec{V}_s \rangle \quad (\text{II.10.b})$$

because of $\langle \vec{v}_s \rangle = 0$, and

$$\vec{v}_0(r, t) = \frac{\sum_s n_s m_s \langle \vec{w}_s \rangle}{\sum_s n_s m_s} \equiv \frac{\sum_s \rho_s \langle \vec{w}_s \rangle}{\sum_s \rho_s} \quad (\text{II.10.c})$$

Note that

$$\sum_s n_s m_s \langle \vec{V}_s \rangle = 0 \text{ and } \sum_s n_s m_s \langle \vec{V}_s \rangle \langle \vec{V}_s \rangle \neq 0 \quad (\text{II.10.d})$$

Then the Eq. (II.9) becomes

$$\frac{\partial n_s}{\partial t} + \vec{\nabla} \cdot (n_s \vec{v}_0) + \vec{\nabla} \cdot (n_s \langle \vec{V}_s \rangle) = \left[\frac{\partial n_s}{\partial t} \right]_{CR} \equiv \int_{w_s} d^3 w_s \left[\frac{\partial f_s}{\partial t} \right]_{CR} \quad (\text{II.11})$$

\vec{v}_0 and $\langle \vec{V}_s \rangle$ depend in a complicated manner on the particular collision processes and the forces acting on the particles.

For the electron density we have in particular the rate equation

$$\frac{\partial n_e}{\partial t} + \vec{\nabla} \cdot (n_e \vec{v}_0) + \vec{\nabla} \cdot (n_e \langle \vec{V}_e \rangle) = \left[\frac{\partial n_e}{\partial t} \right]_{CR} \quad (\text{II.12})$$

* One can also introduce a mean local particle velocity by $\vec{u}_0 = \sum_s n_s \langle \vec{w}_s \rangle / \sum_s n_s$ and the peculiar and mean velocities respectively by $\vec{w}_s = \vec{u}_0 + \vec{U}_s$, $\langle w_s \rangle = \vec{u}_0 + \langle \vec{U}_s \rangle$.

Then $\partial n_s / \partial t + \vec{\nabla} \cdot (n_s \vec{u}_0) + \vec{\nabla} \cdot (n_s \langle \vec{U}_s \rangle) = [\partial n_s / \partial t]_{CR}$ but (compare with Eq. (II.14))

$$\partial n / \partial t + \vec{\nabla} \cdot (n \vec{u}_0) = [\partial n / \partial t]_{CR}$$

because $\sum_s n_s \langle \vec{U}_s \rangle = 0$ and $\sum_s n_s m_s \langle \vec{V}_s \rangle = 0$, but $\langle \vec{U}_s \rangle \neq \langle \vec{V}_s \rangle$.

These differences may become important in analyzing particle velocities and fluxes.

The r. h. s. of Eqs. (II.11, 12) describes the instantaneous local rate with which the density n_s (respectively n_e) changes due to collision and radiation processes.

The r. h. s. of Eq. (II. 12) writes

$$\left[\frac{\partial n_e}{\partial t} \right] = \left[\begin{array}{c} \text{sum of all volume} \\ \text{ionization rates} \end{array} \right] - \left[\begin{array}{c} \text{sum of all volume} \\ \text{recombination rates} \end{array} \right] \quad (\text{II.13})$$

Summation of all equations (II.11) yields the following rate equation for the total particle density $n = \sum_s n_s$:

$$\boxed{\frac{\partial n}{\partial t} + \vec{\nabla} \cdot (n \vec{v}_0) + \sum_s \vec{\nabla} \cdot (n_s \langle \vec{V}_s \rangle) = \left[\frac{\partial n}{\partial t} \right]_{CR}} \quad (\text{II.14})$$

When one writes on the r. h. s. all the individual terms one obtains

$$\begin{aligned} \left[\frac{\partial n}{\partial t} \right]_{CR} = & \left[\begin{array}{c} \text{sum of all molecular} \\ \text{volume dissociation rates} \end{array} \right] - \left[\begin{array}{c} \text{sum of all atomic} \\ \text{volume recombination rates} \end{array} \right] \\ & + \left[\begin{array}{c} \text{sum of all volume} \\ \text{ionisation rates} \end{array} \right] - \left[\begin{array}{c} \text{sum of all volume} \\ \text{recombination rates} \end{array} \right] \\ & + \left[\begin{array}{c} \text{sum of all volume} \\ \text{nuclear particle creation rates} \end{array} \right] - \left[\begin{array}{c} \text{sum of all volume} \\ \text{nuclear particle capture rates} \end{array} \right] \end{aligned}$$

This last equation can also be written in the following compact form :

$$\left[\frac{\partial n}{\partial t} \right]_{CR} = \left[\frac{\partial n_{A,M}}{\partial t} \right]_{CR} + \left[\frac{\partial n_e}{\partial t} \right]_{CR} + \left[\frac{\partial n_{nucl}}{\partial t} \right]_{CR} \quad (\text{II.16})$$

where the terms on the r. h. s. account respectively for the following processes :

- (i) creation and disappearance of heavy particles (atoms, molecules)
- (ii) creation and disappearance of electrons
- (iii) creation and disappearance of particles due to nuclear reactions.

Plasma exhaust and particle injection for additional heating must be accounted for either in the boundary conditions or as additional source terms or sinks on the r. h. s. of the rate equations. In the case of pellet fueling one has in any case to add a local source term which corresponds to the local deposition rate for the particle density.

At this point it may be useful to mention that the collisional - radiative terms can be the origin of forces leading to particle fluxes. For instance, during the radiative recombination process a particle (the electron) disappears and a photon is created (which we assume to escape from the plasma). The disappearance of the particle represents a sink in the rate equations for particle and energy transfer. These sinks lead to forces (e. g. to a difference in pressure) which drive the fluxes.

In the rate for three-body recombination, also an electron disappears; however, the total energy is conserved because the third body (an electron) takes over the thermal energy of

the recombining electron and the internal recombination energy. Thus, all the energy is taken over by the third body in form of translational energy, which means that the thermal energy is not conserved but increases, thus causing a pressure increase which can drive fluxes too.

II.3 Rate Equations for Mass Density

From Eq. (II.9) follows for the mass density $\rho_s = m_s n_s$ of species "s" the rate equation

$$\left[\frac{\partial \rho_s}{\partial t} \right] + \vec{\nabla} \cdot (\rho_s \vec{w}_s) = \left[\frac{\partial \rho_s}{\partial t} \right]_{CR} \quad (\text{II.17})$$

In the absense of nuclear reactions, $[\partial \rho_s / \partial t]_{CR} = m_s [\partial n_s / \partial t]_{CR}$ holds.

Summing up all, Eqs. (II.17) yields the rate equation for the total mass density

$\rho = \sum_s \rho_s$:

$$\frac{\partial \rho}{\partial t} + \vec{\nabla} \cdot (\rho \vec{v}_0) = \left[\frac{\partial \rho}{\partial t} \right]_{CR} = \left[\frac{\partial \rho_{nucl}}{\partial t} \right]_{CR} \quad (\text{II.18})$$

In the absence of nuclear reactions $[\partial n_{nucl} / \partial t]_{CR} = 0$.

In a *D-T* plasma, $[\partial n_{nucl} / \partial t]_{CR}$ accounts for the escape of the neutron from the plasma.

The effect of particle injection and exhaust is taken into account by chosing appropriate boundary conditions or by adding corresponding source terms (sinks) on the r. h. s. of Eqs. (II.17, 18). The change of mass due to pellet injection is taken into account by additional source terms.

II.4 Coupling of Rate and Field Equations

Assuming $f_s(r, t, \vec{w}_s)$ to be known one can calculate the density of the diffusion flux :

$$\vec{\Gamma}_s(r, t) = n_s \langle \vec{w}_s \rangle = \int_{\vec{w}_s} d^3 w_s \vec{w}_s f_s(r, t, \vec{w}_s). \quad (\text{II.19})$$

Multiplying by the charge q_s and summing all equations "s" yields the total electric current density :

$$\vec{j}(r, t) = \sum_s \rho_s n_s \langle \vec{w}_s \rangle = -e_0 n_e \langle \vec{V}_e \rangle + \sum_{i,k,z} e_0 z_{k,i} n_{k,i}^z \langle \vec{V}_{k,i}^z \rangle \quad (\text{II.20})$$

where Eqs. (II.1) and (II.10.b) have been applied.

The toroidal component of Eq. (II.20) represents the plasma current density. Eq. (II.20) is the link between the rate equations for the particle densities and the electromagnetic field equations. $\vec{j}(r, t)$ multiplied by the electric voltage yields $\dot{\Omega}$, see Eqs. (II.51, 54).

When neutral particles are absent, $\langle \vec{V}_e \rangle$ and $\langle \vec{V}_{k,i}^z \rangle$ are exclusively determined by momentum transfer through Colomb collisions and the fields acting on the particles.

II.5 Rate Equations for Momentum Density

The rate equation for the momentum density $n_s m_s \langle \vec{w}_s \rangle$ of the species "s" is obtained by multiplying in Eq. (II.7) f_s by $m_s \vec{w}_s$ and integrating over \vec{w}_s . We introduce the mass density ρ_s of the species "s" and the mass density ρ of the plasma as a whole by

$$\rho_s = n_s m_s, \quad \rho = \sum_s \rho_s.$$

The general rate equation for the momentum density $\rho_s \langle \vec{w}_s \rangle$ in the laboratory system becomes :

$$\left[\frac{\partial}{\partial t} (\rho_s \langle \vec{w}_s \rangle) + \vec{\nabla} \cdot (\rho_s \langle \vec{w}_s \vec{w}_s \rangle) - n_s \langle \vec{F}_s \rangle \right] = \left[\frac{\partial}{\partial t} (\rho_s \langle \vec{w}_s \rangle) \right]_{CR} \quad (\text{II.21})$$

The mean value $\langle \vec{w}_s \rangle$ is defined by Eq. (II.10.b), see also Eq. (II.31.a).

The r.h.s. describes again the rate of change of the momentum density due to collisional-radiative processes. It may be split into two terms :

$$\left[\frac{\partial}{\partial t} (\rho_s \langle \vec{w}_s \rangle) \right]_{CR} = \langle \vec{w}_s \rangle \left[\frac{\partial \rho_s}{\partial t} \right]_{CR} + \rho_s \left[\frac{\partial \langle \vec{w}_s \rangle}{\partial t} \right]_{CR} \quad (\text{II.22})$$

Every spatially non equilibrated volume process contributes in principle to the r.h.s. of Eqs. (II.21, 22). For instance, the collisional momentum transfer between neutral beam injected particles and plasma particles is described by the CR-term.

Multiplying Eq. (II.17) by $\langle \vec{w}_s \rangle$ and subtracting the result from Eq. (II.21) yields the equation of motion for the species "s" in the laboratory system.

$$\rho_s \frac{\partial \langle \vec{w}_s \rangle}{\partial t} + \vec{\nabla} \cdot (\rho_s \langle \vec{w}_s \vec{w}_s \rangle) - \langle \vec{w}_s \rangle \vec{\nabla} \cdot (\rho_s \langle \vec{w}_s \rangle) - n_s \langle \vec{F}_s \rangle = \rho_s \left[\frac{\partial \langle \vec{w}_s \rangle}{\partial t} \right]_{CR} \quad (\text{II.23})$$

We put in the hydrodynamic terms $\vec{w}_s = \vec{v}_0 + \vec{V}_s$ (see Eq. (II.10.a)) and introduce the momentum flux tensor \overleftrightarrow{P}_s for the species "s" with the components:

$$\overleftrightarrow{P}_s = \rho_s \langle \vec{V}_s \vec{V}_s \rangle = \begin{pmatrix} P_{sxx} & P_{sxy} & P_{sxz} \\ P_{syx} & P_{syy} & P_{syx} \\ P_{sxx} & P_{szy} & P_{szz} \end{pmatrix} \quad (\text{II.24})$$

The component p_{sxx} is, for instance, given by $p_{sxx} = \rho_s \langle V_s \rangle_x \langle V_s \rangle_x + \rho_s \langle v_{sx} v_{sx} \rangle$. The first term is related to the kinetic diffusion energy in x-direction ($(1/2) \rho_s \langle V_s^2 \rangle_x$), the second term is related to the kinetic energy due to the random velocity and represents heat energy. For a maxwellian velocity distribution function the following relations between species' temperature T_s and the scalar (hydrostatic) partial pressure p_s holds :

$$\frac{3}{2} kT_s \equiv \frac{1}{2} m_s \langle v_s^2 \rangle = \frac{1}{n_s} \frac{1}{2} m_s \int_{-\infty}^{+\infty} v_s^2 f_s(\vec{v}_s) d^3 v_s \quad (\text{II.25.a})$$

The equation of state is given by

$$p_s = n_s kT_s \quad (\text{II.25.b})$$

and the scalar pressure of the plasma as a whole by

$$p = \sum_s p_s \quad (\text{II.25.c})$$

Thus, the scalar pressure p_s is equal to each of the diagonal components of the hydrostatic pressure tensor $\overleftrightarrow{p}_s = \rho_s \langle \vec{v}_s \vec{v}_s \rangle$; hence :

$$p_s = \frac{1}{3} (\rho_s \langle v_{sx} \cdot v_{sx} \rangle + \rho_s \langle v_{sy} \cdot v_{sy} \rangle + \rho_s \langle v_{sz} \cdot v_{sz} \rangle) \quad (\text{II.25.d})$$

Making use of the relation $\rho_s \langle \vec{v}_s \vec{v}_s \rangle = \rho_s \langle \vec{v}_s \rangle \langle \vec{v}_s \rangle + \rho_s \langle \vec{v}_s \vec{v}_s \rangle$, the Eq. (II.23) becomes

$$\rho_s \frac{\partial \langle \vec{w}_s \rangle}{\partial t} + \rho_s \langle \vec{w}_s \rangle \cdot \vec{\nabla} \langle \vec{w}_s \rangle + 3 \vec{\nabla} p_s - n_s \langle \vec{F}_s \rangle = \rho_s \left[\frac{\partial \langle \vec{w}_s \rangle}{\partial t} \right]_{CR} \quad (\text{II.26})$$

The rate equation for the momentum transfer of the plasma as a whole is obtained by summing the Eq. (II.21) over all species "s". It follows the rate equation

$$\frac{\partial}{\partial t} (\rho \vec{v}_0) + \vec{\nabla} \cdot (\rho \vec{v}_0 \vec{v}_0) + \vec{\nabla} \cdot \vec{P} - \sum_s n_s \langle \vec{F}_s \rangle = \left[\frac{\partial}{\partial t} \rho \vec{v}_0 \right]_{CR} \quad (\text{II.27})$$

with the mass density ρ and the momentum flux tensor \vec{P} for the plasma as a whole given by

$$\rho = \sum_s \rho_s \quad (\text{a}) \quad \vec{P} = \sum_s \vec{P}_s \quad (\text{b})$$

where the components of \vec{P} are given by

$$\vec{P} = \begin{pmatrix} P_{xx} & P_{xy} & P_{xz} \\ P_{yx} & P_{yy} & P_{yz} \\ P_{zx} & P_{zy} & P_{zz} \end{pmatrix} \quad (\text{c}) \quad (\text{II.28.a-c})$$

Because of Eqs. (II.10.d) and (II.25.d) the diagonal components of \vec{P} represent the total scalar pressure p plus the total kinetic diffusion energy $(1/2) \sum_s \rho_s \langle V^2 \rangle$.

The Eq. (II.27) can be simplified when one applies the Eq. (II.18) multiplied by \vec{v}_0 ; it results the local vector force equation for the plasma as a whole :

$$\rho \frac{\partial \vec{v}_0}{\partial t} + \rho \vec{v}_0 \cdot \vec{\nabla} \vec{v}_0 + \vec{\nabla} \cdot \vec{P} - \sum_s n_s \langle \vec{F}_s \rangle = \left[\frac{\partial \vec{v}_0}{\partial t} \right]_{CR} \quad (\text{II.29})$$

The r. h. s. of this equation is generally zero, since collisions and radiation processes (assumed to be distributed isotropically) alone cannot modify \vec{v}_0 . However, when a plasma is submitted to an external particle and/or photon flux, the r. h. s. of Eq. (II.29) can become different from zero. The increased toroidal rotation of a tokamak plasma during tangential particle injection is due to a non vanishing value of this term. In such a case the non

diagonal components of \vec{P} can have a great influence on the velocity (friction).

We will use Eq. (II.29) to modify the Eq. (II.26). This last equation refers to the laboratory frame. The first term of Eq. (II.26) is, for instance composed of two terms, $\rho_s \partial \langle \vec{w}_s \rangle / \partial t = \rho_s \partial \vec{v}_0 / \partial t + \rho_s \partial \langle \vec{V}_s \rangle / \partial t$, the first one is due to a velocity change of the plasma as a whole, the second one accounts for a velocity change relative to \vec{v}_0 . We can eliminate that part which is connected to changes of \vec{v}_0 by multiplying Eq. (II.29) by ρ_s / ρ and subtracting the result from Eq. (II.26); one obtains

$$\begin{aligned} \rho_s \frac{\partial \langle \vec{V}_s \rangle}{\partial t} + \rho_s \langle \vec{V}_s \rangle \cdot \vec{\nabla} \langle \vec{V}_s \rangle + \rho_s \vec{v}_0 \cdot \vec{\nabla} \langle \vec{V}_s \rangle + \rho_s \langle \vec{V}_s \rangle \cdot \vec{\nabla} \vec{v}_0 + 3 \vec{\nabla} p_s \\ - \frac{\rho_s}{\rho} \vec{\nabla} \cdot \vec{P} - n_s \langle \vec{F}_s \rangle + \frac{\rho_s}{\rho} \sum_s n_s \langle \vec{F}_s \rangle = \rho_s \left[\frac{\partial \langle \vec{V}_s \rangle}{\partial t} \right]_{CR} \end{aligned} \quad (\text{II.30})$$

which represents the equation of motion of the species "s" in a coordinate system moving with the mass velocity \vec{v}_0 . The third and fourth term on the l. h. s. account for interactions of the velocity fields \vec{v}_0 and $\langle \vec{V}_s \rangle$.

The mean velocity $\langle \vec{w}_s \rangle$ is calculated from

$$\langle \vec{w}_s \rangle = \vec{v}_0 + \frac{1}{n_s} \int_{V_s} V_s f_s(r, t, V_s) dV_s = \vec{v}_0 + \langle V_s \rangle \quad (\text{II.31.a})$$

and the collisional-radiative term is given by

$$\left[\frac{\partial \langle \vec{w}_s \rangle}{\partial t} \right]_{CR} = \frac{1}{\rho_s} \int_{\vec{w}_s} d^3 w_s m_s \vec{w}_s \left[\frac{\partial f_s}{\partial t} \right]_{CR} \quad (\text{II.31.b})$$

The values of $[\partial f_s / \partial t]_{CR}$ depend on the atomic (molecular) and/or Colomb cross sections.

II.6 Rate Equations for the Energy Density

A plasma possesses translational energy of density E^{tr} and internal energy of density E^{int} stocked in the excitation and ionization (dissociation) levels. We will first consider the equations governing E^{int} .

II.6.1 Internal Energy

The simplest way to establish the rate equations is to give all internal energy to the heavy particles (molecules, atoms, molecular ions, atomic ions). Thus the electrons possess only translational energy.

Let $E_{k,i}^z$ be the internal energy of a z-times ionized particle of chemical species "k" in quantum state $|i\rangle$.

The definition of $E_{k,i}^z$ is given in Fig. 6 where we have assumed that the energetically

lowest state (the “reference state” for the internal energy of species “ k ”) is the atomic state. When atoms can originate from molecules, and when the molecular internal energies play a role in the energy balance, then the reference state is given by the ground state energy of the molecular system. This is for instance the case for D_2 and for hydrocarbons found near the walls of carbon limiters in tokamaks. The molecules can radiate off energy, therefore their internal energy state must be taken into account.

For ionized species, $E_{k,i}^z$ contains the sum of the ionization energies of all lower lying stages of ionization.

The total internal energy density of all heavy particles is then given by

$$\bar{E}^{int} = \sum_z \sum_k \sum_i n_{k,i}^z E_{k,i}^z \equiv \sum_s n_s E_s^{int} \equiv \sum_s \bar{E}_s^{int} \quad (\text{II.32})$$

where “ s ” stands for $s=\{z, k, i\}$. E_s^{int} is the energy density of a particular species $s=\{z, k, i\}$.

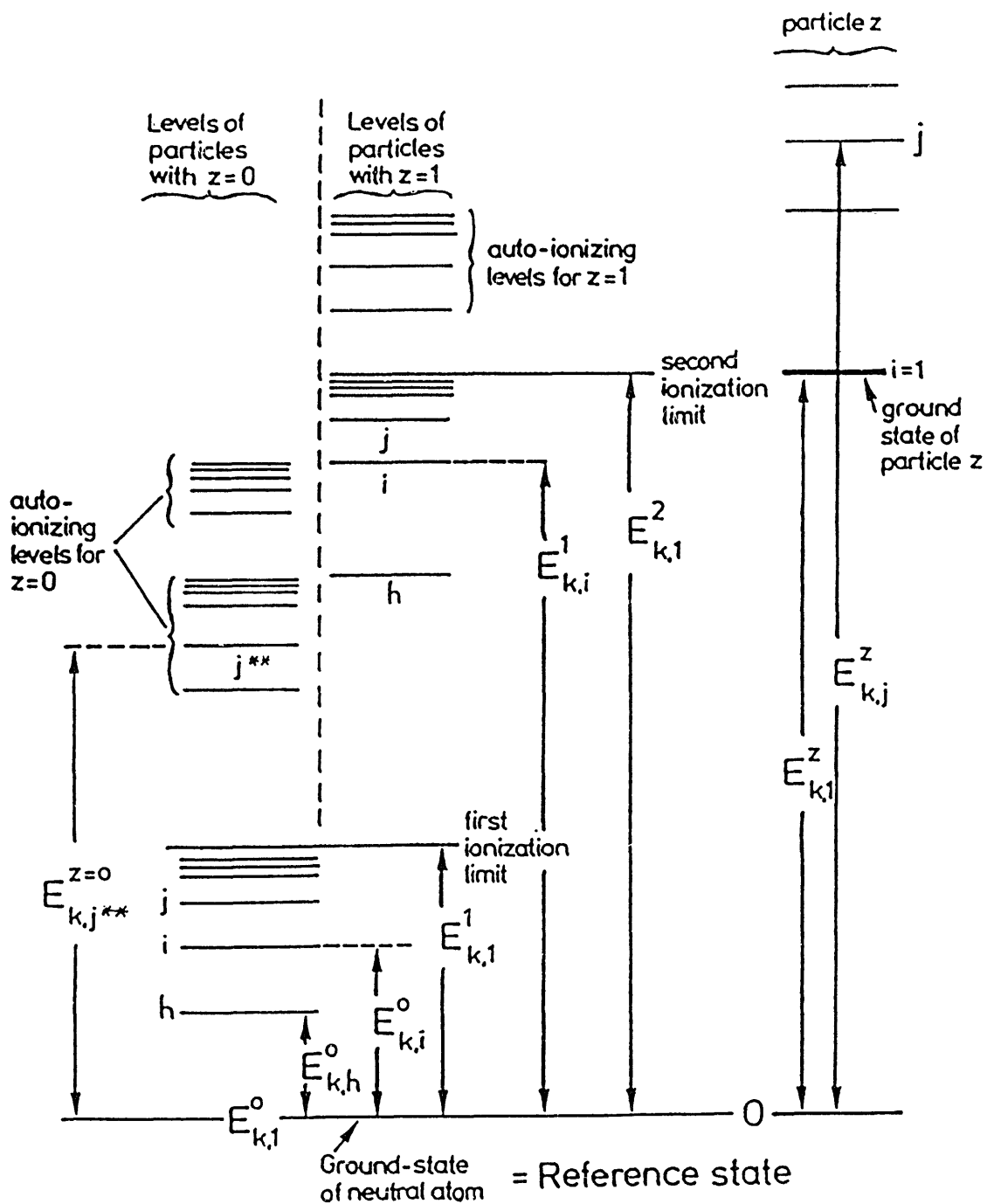


Fig. 6 Definition of the internal energy $E_{k,i}^z$ of a z -times ionized particle of chemical element k in quantum state $|i\rangle$. When nuclear reactions become important, the relativistic energy $m_{k,i}^z c^2$ must be included in $E_{k,i}^z$. After ref. [7].

Since the excited and ionized particles are mobile they can diffuse in space. With the internal energy is thus associated a particular flux vector describing the transport of internal energy (sometimes also termed "reaction energy"). Let $n_s E_s^{int} < \vec{w}_s >$ be the flux density of internal energy associated with the species $s = \{z, k, i\}$. The rate equation of the internal energy density of species "s" then follows from Eq. (II.9) by replacing the particle density n_s by the internal energy density $n_s E_s^{int}$:

$$\frac{\partial n_s E_s^{int}}{\partial t} + \vec{\nabla} \cdot (n_s E_s^{int} < \vec{w}_s >) = \left[\frac{\partial n_s E_s^{int}}{\partial t} \right]_{CR} \quad (II.33.a)$$

which is identical with the expression

$$E_s^{int} \left[\frac{\partial n_s}{\partial t} + \vec{\nabla} \cdot (n_s < \vec{w}_s >) \right] = \left[\frac{\partial n_s E_s^{int}}{\partial t} \right]_{CR} \quad (II.33.b)$$

substituting the expression in the parenthesis of the l. h. s. by the l. h. s. of Eq. (II.9) yields

$$E_s^{int} \left[\frac{\partial n_s}{\partial t} \right]_{CR} = \left[\frac{\partial n_s E_s^{int}}{\partial t} \right]_{CR} \quad (II.33.c)$$

In other terms : the rate equation for the internal energy of species "s" is equal to the rate equation for the particle density n_s multiplied by the internal energy E_s^{int} of one particle.

Summing Eqs. (II.33.a) over all species "s" yields the rate equation for the total internal energy density :

$$\frac{\partial \bar{E}^{int}}{\partial t} + \vec{\nabla} \cdot \left[\sum_s \bar{E}_s^{int} < \vec{w}_s > \right] = \left[\frac{\partial \bar{E}^{int}}{\partial t} \right]_{CR} \quad (II.34)$$

The expression in the parenthesis [] contains the species' density and mean diffusion velocity :

$$\sum_s \bar{E}_s^{int} < \vec{w}_s > = \sum_s E_s^{int} n_s (\vec{v}_0 + < \vec{V}_s >) \quad (II.35)$$

where $n_s E_s^{int} \vec{v}_0$ is a flux vector associated with the plasma as a whole, whereas $n_s E_s^{int} < \vec{V}_s >$ is a flux vector transporting internal energy in a coordinate frame moving with \vec{v}_0 .

We now define a flux vector \vec{Q}_s^{int} for the transport of internal energy relative to \vec{v}_0 by

$$\vec{Q}_s^{int} = n_s E_s^{int} < \vec{V}_s > \equiv \bar{E}_s^{int} < \vec{V}_s > \quad (II.36.a)$$

The flux vector representing the transport of the whole internal energy density is

$$\vec{Q}^{int} = \sum_s \vec{Q}_s^{int} \quad (II.36.b)$$

Thus, the Eqs. (II.33.a) and (II.34) become, respectively

$$\frac{\partial \bar{E}_s^{int}}{\partial t} + \vec{\nabla} \cdot (\bar{E}_s^{int} \vec{v}_0) + \vec{\nabla} \cdot \vec{Q}_s^{int} = \left[\frac{\partial \bar{E}_s^{int}}{\partial t} \right]_{CR}$$

(II.37.a)

$$\frac{\partial \bar{E}^{int}}{\partial t} + \vec{\nabla} \cdot (\bar{E}^{int} \vec{v}_0 + \vec{Q}^{int}) = \left[\frac{\partial \bar{E}^{int}}{\partial t} \right]_{CR} \quad (\text{II.37.b})$$

The r. h. s. of these equations ensure the coupling with the translational energy and with the radiation field, since any collisional - radiative change of the total internal energy density \bar{E}^{int} leads to a change of translational (thermal) and/or of radiation energy, and vice versa. Details will be given in Chapter II.6.5.

II.6.2 Translational Energy

It is useful to make a distinction between the directional and random velocities and the translational energies which are associated with these two types of movement. Particle diffusion of velocity $\langle \vec{V}_s \rangle$ also means diffusion of "diffusion kinetic energy" $(1/2) \rho_s \langle V_s^2 \rangle$. The sum of all these "diffusion kinetic energies" is generally small but not zero; furthermore, the plasma as a whole will generally have some directional kinetic energy $(1/2) \rho v_0^2$. And finally, the random velocity \vec{v}_s whose average is zero is related to heat and pressure, see Eqs. (II.25).

The multiplication of f_s in Eq. (II.7) by $m_s \vec{w}_s \vec{w}_s$ and integration over the velocity yields the rate equation for the tensor of twice the translational (or kinetic) energy density of species "s" in the laboratory system, that is :

$$\frac{\partial}{\partial t} (\rho_s \langle \vec{w}_s \vec{w}_s \rangle) + \vec{\nabla} \cdot (\rho_s \langle \vec{w}_s \vec{w}_s \vec{w}_s \rangle) - 2n_s \langle \vec{F}_s \vec{w}_s \rangle = \left[\frac{\partial (\rho \langle \vec{w}_s \vec{w}_s \rangle)}{\partial t} \right]_{CR} \quad (\text{II.38})$$

Owing to the Eqs. (II.10) and (II.24), this equation can be expressed as a function of \vec{v}_0 and \vec{P}_s and a flux tensor \vec{Q}_s^{tr} for the species "s" defined by

$$\vec{Q}_s^{tr} = \rho_s \langle \vec{V}_s \vec{V}_s \vec{V}_s \rangle \quad (\text{II.39})$$

After the development of the various terms, the Eq. (II.38) becomes :

$$\begin{aligned} & \frac{\partial}{\partial t} \{ \rho_s \vec{v}_0 \vec{v}_0 + \rho_s \vec{v}_0 \langle \vec{V}_s \rangle + \rho_s \langle \vec{V}_s \rangle \vec{v}_0 + \vec{P}_s \} \\ & + \vec{\nabla} \cdot \{ \rho_s [\vec{v}_0 \vec{v}_0 \vec{v}_0 + \vec{v}_0 \vec{v}_0 \langle \vec{V}_s \rangle + \vec{v}_0 \langle \vec{V}_s \rangle \vec{v}_0 + \langle \vec{V}_s \rangle \vec{v}_0 \vec{v}_0 + \langle \vec{V}_s \vec{v}_0 \vec{V}_s \rangle] \} \\ & + \vec{\nabla} \cdot \{ \vec{v}_0 \vec{P}_s + \vec{P}_s \vec{v}_0 + \vec{Q}_s^{tr} \} - 2n_s \langle \vec{F}_s \rangle \vec{v}_0 - 2n_s \langle \vec{F}_s \vec{V}_s \rangle \\ & = \left[\frac{\partial}{\partial t} \rho_s \vec{v}_0 \vec{v}_0 \right]_{CR} + \left[\frac{\partial}{\partial t} \rho_s \langle \vec{V}_s \rangle \vec{v}_0 \right]_{CR} + \left[\frac{\partial}{\partial t} \rho_s \vec{v}_0 \langle \vec{V}_s \rangle \right]_{CR} + \left[\frac{\partial}{\partial t} \vec{P}_s \right]_{CR} \end{aligned} \quad (\text{II.40})$$

The terms have the following meaning :

$(\partial / \partial t) \rho_s \vec{v}_0 \vec{v}_0$ and $\vec{\nabla} \cdot (\rho_s \vec{v}_0 \vec{v}_0 \vec{v}_0)$ are connected with the temporal and spatial variations of the

kinetic energy of the species "s" due to changes of the translational energy of the plasma as a whole in which the species "s" are imbedded. The first term on the r. h. s. is the collisional-radiative counter part.

$(\partial/\partial t)\vec{P}_s$ and $\vec{\nabla} \cdot \vec{Q}^{tr}$ are connected with the temporal and spatial variations of the kinetic energy of the species "s" relative to a coordinate frame moving with \vec{v}_0 . The last term on the r. h. s. is the collisional-radiative counterpart.

$-2n_s \langle \vec{F}_s \cdot \vec{V}_s \rangle$ represents twice the tensor of the work done against the force \vec{F}_s by the particles moving with \vec{V}_s relative to \vec{v}_0 ; $-2n_s \langle \vec{F}_s \rangle \cdot \vec{v}_0$ is the corresponding tensor for particles moving with \vec{v}_0 .

The term $n_s \langle \vec{F}_s \cdot \vec{V}_s \rangle$ represents the power density due to ohmic heating of the species "s".

All other terms represent changes of kinetic and thermal energy due to the fact that the fluid "s" moves with the velocity $\langle \vec{V}_s \rangle$ in the fluid of all other species.

When one sums the Eqs. (II.40) for all species "s" one obtains the tensor of twice the translational energy density of the plasma as a whole :

$$\begin{aligned} & \frac{\partial}{\partial t} (\rho \vec{v}_0 \vec{v}_0) + \frac{\partial}{\partial t} \vec{P} + \vec{\nabla} \cdot (\rho \vec{v}_0 \vec{v}_0 \vec{v}_0) + \vec{\nabla} \cdot \vec{Q}^{tr} + \vec{\nabla} \cdot \left(\sum_s \rho_s \langle \vec{V}_s \vec{v}_0 \vec{V}_s \rangle \right) \\ & + \vec{\nabla} \cdot \{ \vec{v}_0 \vec{P} + \vec{P} \vec{v}_0 \} - 2 \sum_s n_s \langle \vec{F}_s \rangle \cdot \vec{v}_0 - 2 \sum_s n_s \langle \vec{F}_s \vec{V}_s \rangle \\ & = \left[\frac{\partial}{\partial t} (\rho \vec{v}_0 \vec{v}_0) \right]_{CR} + \left[\frac{\partial \vec{P}}{\partial t} \right]_{CR} \end{aligned} \quad (II.41)$$

where use has been made of Eq. (II.10d).

The rate equation for the translational energy density of the plasma as a whole is obtained by taking the trace of Eq. (II.41) and dividing by two; this leads to the following expression :

$$\begin{aligned} & \frac{\partial}{\partial t} \left(\frac{1}{2} \rho v_0^2 \right) + \frac{\partial}{\partial t} \left(\text{Trace} \frac{1}{2} \vec{P} \right) + \vec{\nabla} \cdot \left(\frac{1}{2} \rho v_0^2 \vec{v}_0 \right) + \text{Trace} \left\{ \frac{1}{2} \vec{\nabla} \cdot \vec{Q}^{tr} \right\} \\ & + \text{Trace} \left\{ \frac{1}{2} \vec{\nabla} \cdot \left(\sum_s \rho_s \langle \vec{V}_s \vec{v}_0 \vec{V}_s \rangle \right) + \frac{1}{2} \vec{\nabla} \cdot (\vec{v}_0 \vec{P}) + \frac{1}{2} \vec{\nabla} \cdot (\vec{P} \vec{v}_0) \right\} \\ & - \sum_s n_s \langle \vec{F}_s \rangle \cdot \vec{v}_0 - \sum_s n_s \langle \vec{F}_s \cdot \vec{V}_s \rangle = \left[\frac{\partial}{\partial t} \left(\frac{1}{2} \rho v_0^2 \right) \right]_{CR} + \left[\frac{\partial}{\partial t} \text{Trace} \frac{1}{2} \vec{P} \right]_{CR} \end{aligned} \quad (II.42)$$

No approximations have been made so far. Thus Eq. (II.42) represents the full continuity equation for the density of the translational energy of a plasma as a whole.

The individual Trace terms of Eq. (II.42) write without making approximations :

$$Trace \left\{ \frac{1}{2} \vec{P} \right\} = \frac{3}{2} p + \sum_s \frac{1}{2} \rho_s \langle V_s \rangle^2 \quad (\text{II.43.a})$$

$$Trace \left\{ \frac{1}{2} \vec{V} \cdot \vec{Q}^{tr} \right\} = \vec{V} \cdot \vec{q}^{th} + \vec{V} \cdot \left(\sum_s \frac{1}{2} \rho_s \langle V_s \rangle^2 \langle \vec{V}_s \rangle \right) \quad (\text{II.43.b})$$

with the thermal heat flux vector \vec{q}^{th} given by

$$\vec{q}^{th} = \sum_s \frac{5}{2} p_s \langle \vec{V}_s \rangle = \sum_s \frac{5}{2} n_s k T_s \langle \vec{V}_s \rangle \quad (\text{II.43.c})$$

$$Trace \left\{ \frac{1}{2} \vec{V} \cdot (\vec{v}_0 \vec{P}) \right\} = \vec{V} \cdot \left(\frac{3}{2} p \vec{v}_0 \right) + \vec{V} \cdot \left(\frac{1}{2} \rho_s \langle V_s \rangle^2 \vec{v}_0 \right) \quad (\text{II.43.d})$$

$$Trace \left\{ \frac{1}{2} \vec{V} \cdot (\vec{P} \vec{v}_0) \right\} = \vec{V} \cdot \left(\frac{1}{2} \vec{P} \cdot \vec{v}_0 \right) = \frac{1}{2} \vec{V} \cdot (\vec{P} \vec{v}_0) \quad (\text{II.43.e})$$

$$Trace \left\{ \frac{1}{2} \vec{V} \cdot \sum_s \rho_s \langle \vec{V}_s \vec{v}_0 \vec{V}_s \rangle \right\} = \vec{V} \cdot \left(\frac{1}{2} \vec{P} \cdot \vec{v}_0 \right) = \frac{1}{2} \vec{V} \cdot (\vec{P} \vec{v}_0) \quad (\text{II.43.f})$$

In calculating the trace we have made use of the Eqs. (II.10.d). We now neglect all terms associated with the "diffusion kinetic energies". The Eq. (II.42) thus reduces to the following expression

$$\begin{aligned} & \frac{\partial}{\partial t} \left\{ \frac{1}{2} \rho v_0^2 + \frac{3}{2} p \right\} + \vec{V} \cdot \left\{ \frac{1}{2} \rho v_0^2 \vec{v}_0 + \vec{q}^{th} \right\} + \vec{V} \cdot \left(\frac{5}{2} p \vec{v}_0 \right) \\ & - \sum_s n_s \langle \vec{F}_s \rangle \cdot \vec{v}_0 - \sum_s n_s \langle \vec{F}_s \cdot \vec{V}_s \rangle = \left[\frac{\partial}{\partial t} \frac{1}{2} \rho v_0^2 \right]_{CR} + \left[\frac{\partial}{\partial t} \frac{3}{2} p \right]_{CR} \end{aligned} \quad (\text{II.44})$$

The collisional-radiative term $[(\partial/\partial t) \rho v_0^2/2]_{CR}$ is only different from zero when the plasma is submitted to an external energy flux which increases the kinetic energy $(1/2) \rho v_0^2$ of the plasma via collision and/or radiation processes, thus

$$\left[\frac{\partial}{\partial t} \frac{1}{2} \rho v_0^2 \right]_{CR} = 0 \quad (\text{II.45})$$

except cases in which collisional-radiative volume processes are responsible for an increase of the kinetic energy $(1/2) \rho v_0^2$.

The collisional-radiative term $[(\partial/\partial t) 3p/2]_{CR}$ is for a plasma always different from zero. One contribution to this term originates from free-free transitions (bremsstrahlung) and synchrotron radiation. Free-free transitions transforms thermal energy into photon energy which can escape from the plasma. Another contribution originates from free-bound transitions (spontaneous recombination). The photon $h\nu$ created in this event radiates off thermal plus ionization energy. The thermal contribution to $h\nu$ is taken into account in $[(\partial/\partial t) 3p/2]_{CR}$, the disappearance of ionization energy in the recombination process is taken

into account in the collisional-radiative term for the internal energy. The last term on the r.h.s. of Eq. (II.44) contains also all energy rates due to collisional excitation, ionization, and three-body recombination. Excitation and ionization processes consume thermal energy to the profit of internal energy which is increased. Thermal energy is not consumed in heating newly created electrons, however the temperature decreases due to this heating. In a three-body recombination process, internal energy is transformed into thermal energy which appears as a positive contribution on the r. h. s. of Eq. (II.44) and as a negative one in the collisional-radiative term of the rate equation for the internal energy.

Neutral beam injection is used to heat plasmas. The kinetic beam energy is transferred to the plasma particles via collisions, i.e., a corresponding rate contributes to the terms on the r. h. s. of Eq. (II.44). That part of the neutral beam energy which leads to an increase of directional energy of the plasma as a whole ($\rho v_0^2/2$) is taken into account in the first term of the r. h. s. It is evident that this contribution is then lost for the heating process proper ($3p/2$).

In the present context it may be useful to remember that the omission of the non diagonal components of \hat{P} can have consequences in evaluating the energy balance when viscous-stresses contribute to the energy transfer. The components of the viscous-stress tensor T are given by the following relation

$$\begin{aligned} T_{\alpha\beta} \equiv \tau_{\alpha\beta} &= \sum_s \tau_{s,\alpha\beta} = - \sum_s (p_{s,\alpha\beta} - p_s \delta_{\alpha\beta}) \\ &= \sum_s \left[\rho_s \langle V_{s,\alpha} V_{s,\beta} \rangle - \frac{1}{3} \rho_s \langle V_{s,\alpha} V_{s,\alpha} \rangle \delta_{\alpha\beta} \right] \end{aligned}$$

where the summation is over all species "s". Further, α and β represent the three components x, y, z , and $\delta_{\alpha\beta}$ is the Kronecker delta symbol

$$\delta_{\alpha\beta} = \begin{cases} 0 & \text{if } \alpha \neq \beta \\ 1 & \text{if } \alpha = \beta \end{cases}$$

II.6.3 Thermal Energy

Changes of the thermal energy are described by the change of the momentum flux tensor \hat{P} alone. To obtain the rate equation for \hat{P} one subtracts from the tensor equation (II.41) the two tensor equations which are obtained when Eq. (II.27) is multiplied from the right by \vec{v}_0 and Eq. (II.28) from the left by \vec{v}_0 . The resulting equation writes

$$\begin{aligned} \frac{\partial \hat{P}}{\partial t} + \vec{\nabla} \cdot \hat{Q}^{tr} + \vec{\nabla} \cdot \{ \vec{v}_0 \hat{P} + \sum_s \rho_s \langle \vec{V}_s \vec{v}_0 \vec{V}_s \rangle \} + \hat{P} \cdot \vec{\nabla} \vec{v}_0 - \vec{v}_0 \vec{\nabla} \cdot \hat{P} \\ - \sum_s n_s (\langle \vec{F}_s \rangle \vec{v}_0 - \vec{v}_0 \langle \vec{F}_s \rangle) - 2 \sum_s n_s \langle \vec{F}_s \vec{V}_s \rangle = \left[\frac{\partial \hat{P}}{\partial t} \right]_{CR} \end{aligned} \quad (II.46)$$

The rate equation for the thermal energy density of the plasma as a whole is obtained by taking from Eq. (II.46) the trace and dividing by two. The result is :

$$\left[\frac{\partial}{\partial t} \left(\frac{3}{2} p + \sum_s \frac{1}{2} p_s \langle V_s^2 \rangle \right) + \vec{\nabla} \cdot \left(\frac{5}{2} p \vec{v}_0 + \vec{q}^{th} \right) + \vec{\nabla} \cdot \left(\sum_s \frac{1}{2} p_s \langle V_s^2 \rangle \langle \vec{V}_s \rangle \right) + \frac{1}{2} \vec{\nabla} : (\vec{P} \vec{v}_0) \right. \\ \left. + \frac{1}{2} \vec{P} : \vec{\nabla} \vec{v}_0 - \frac{1}{2} \vec{v}_0 \vec{\nabla} : \vec{P} - \sum_s n_s \langle \vec{F}_s \cdot \vec{V}_s \rangle = \left[\frac{\partial}{\partial t} \frac{3}{2} p \right]_{CR} + \left[\frac{\partial}{\partial t} \sum_s \frac{1}{2} p_s \langle V_s^2 \rangle \right]_{CR} \right] \quad (\text{II.47})$$

Since no approximations have been introduced so far, this equation represents the exact rate equation for the total thermal plus "diffusion kinetic energy" densities. In Eq. (II.47) we have made use of Eqs. (II.43) and of

$$\text{Trace} \left\{ \frac{1}{2} \vec{P} \cdot \vec{\nabla} \vec{v}_0 \right\} = \frac{1}{2} \vec{P} : \vec{\nabla} \vec{v}_0 \quad (\text{II.48.a})$$

$$\text{Trace} \left\{ \frac{1}{2} \vec{v}_0 \vec{\nabla} \cdot \vec{P} \right\} = \frac{1}{2} v_0 \cdot \vec{\nabla} : \vec{P} \quad (\text{II.48.b})$$

We now neglect all contributions associated with the "diffusion kinetic energy". Then the Eq. (II.47) becomes

$$\left[\frac{\partial}{\partial t} \left(\frac{3}{2} p \right) + \vec{\nabla} \cdot \left(\frac{5}{2} p \vec{v}_0 + \vec{q}^{th} \right) - \vec{v}_0 \cdot \vec{\nabla} p - \sum_s n_s \langle \vec{F}_s \cdot \vec{V}_s \rangle = \left[\frac{\partial}{\partial t} \frac{3}{2} p \right]_{CR} \right] \quad (\text{II.49})$$

This equation can be written in other useful forms. We apply the equation of state

$$p = \sum_s p_s = \sum_s n_s k T_s = n k T \quad (\text{II.50})$$

and put for the ohmic power density

$$\dot{\Omega} = \sum_s n_s \langle \vec{F}_s \cdot \vec{V}_s \rangle \quad (\text{II.51})$$

By using the relations $-kT \vec{v}_0 \cdot \vec{\nabla} n = -kT \vec{\nabla} \cdot (n \vec{v}_0) + nkT \vec{\nabla} \cdot \vec{v}_0$ and

$[\partial / \partial t \ 3p/2]_{CR} = (3/2)nk [\partial T / \partial t]_{CR} + (3/2)kT [\partial n / \partial t]_{CR}$, the Eq. (II.49) becomes

$$\frac{3}{2} nk \frac{\partial T}{\partial t} + \frac{3}{2} kT \frac{\partial n}{\partial t} + \frac{3}{2} nk \vec{v}_0 \cdot \vec{\nabla} T + \frac{3}{2} kT \vec{\nabla} \cdot (n \vec{v}_0) + \vec{\nabla} \cdot \vec{q}^{th} \quad (\text{II.52})$$

$$+ kT n \vec{\nabla} \cdot \vec{v}_0 = \frac{3}{2} nk \left[\frac{\partial T}{\partial t} \right]_{CR} + \frac{3}{2} kT \left[\frac{\partial n}{\partial t} \right]_{CR} + \dot{\Omega}$$

We make now use of Eq. (II.14) and obtain

$$\frac{3}{2} nk \frac{\partial T}{\partial t} + \frac{3}{2} kn \vec{v}_0 \cdot \vec{\nabla} T + nkT \vec{\nabla} \cdot \vec{v}_0 + \vec{\nabla} \cdot \vec{q}^{th} - \frac{3}{2} kT \vec{\nabla} \cdot \left(\sum_s n_s \langle \vec{V}_s \rangle \right) \quad (\text{II.53})$$

$$= \frac{3}{2} nk \left[\frac{\partial T}{\partial t} \right]_{CR} + \dot{\Omega}$$

The fourth and fifth terms can be contracted (see the Eq. (II.43.c)). We thus obtain the following "rate equation" for the temperature T :

$$\boxed{\begin{aligned} \frac{3}{2}nk \frac{\partial T}{\partial t} + \sum_s \frac{3}{2}n_s k (\vec{v}_0 + \langle \vec{v}_s \rangle) \cdot \vec{\nabla} T + \sum_s n_s k \langle \vec{v}_s \rangle \cdot \vec{\nabla} T + nk T \vec{\nabla} \cdot \vec{v}_0 \\ = \frac{3}{2}nk \left[\frac{\partial T}{\partial t} \right]_{CR} + \dot{Q} \end{aligned}} \quad (II.54)$$

where $\vec{v}_0 + \langle \vec{v}_s \rangle = \langle \vec{w}_s \rangle$, see Eq. (II.10.b). We introduce the density of the diffusion flux in the laboratory system by

$$\vec{I}_s = n_s (\vec{v}_0 + \langle \vec{v}_s \rangle) = n_s \langle \vec{w}_s \rangle \quad (II.55)$$

Then

$$\boxed{\frac{3}{2}nk \frac{\partial T}{\partial t} + \frac{3}{2}k \sum_s \left(\vec{I}_s + \frac{2}{3}n_s \langle \vec{v}_s \rangle \cdot \vec{\nabla} T + nk T \vec{\nabla} \cdot \vec{v}_0 \right) = \frac{3}{2}nk \left[\frac{\partial T}{\partial t} \right]_{CR} + \dot{Q}} \quad (II.56)$$

The Eq. (II.49) can be put into another useful form:

$$\boxed{\vec{v}_0 \cdot \vec{\nabla} p = \frac{\partial}{\partial t} \left(\frac{3}{2}p \right) + \vec{\nabla} \cdot \left(\sum_s \frac{5}{2}kT_s \vec{I}_s \right) - \dot{Q} - \sum_s \frac{3}{2}kn_s \left[\frac{\partial T_s}{\partial t} \right]_{CR} + \sum_s \frac{3}{2}kT_s \left[\frac{\partial n_s}{\partial t} \right]_{CR}} \quad (II.57)$$

We remember that effects due to viscous-shear stresses have been neglected. When their influence cannot be omitted one must take into account the non diagonal components in the corresponding terms of Eq. (II.47). This is not difficult but introduces complications and makes applications more complex. For further details see Eqs. (II.84.b) (II.85) and Chapter III.7 where Eq. (II.57) is applied to determine \vec{v}_0 .

II.6.4 Total Energy

The rate equation for the total energy density is equal to the sum of the rate equations for translational and internal energy densities. Only the corresponding equations for the plasma as a whole and the sum of the thermal and internal energy densities for the plasma as a whole are of physical relevancy. The energy equation for individual species "s" is too complex and will hardly be applied.

We add the Eq. (37.b) to Eq. (II.42) and obtain the rate equation for the total energy density of a plasma as a whole; this equation writes without any approximations :

$$\begin{aligned}
& \left[\frac{\partial}{\partial t} \left\{ \frac{1}{2} \rho v_0^2 + \bar{E}^{int} + \text{Trace} \frac{1}{2} \hat{P} \right\} + \vec{\nabla} \cdot \left\{ \frac{1}{2} \rho v_0^2 \vec{v}_0 + \bar{E}^{int} \vec{v}_0 + \vec{Q}^{int} \right\} + \text{Trace} \left\{ \frac{1}{2} \vec{\nabla} \cdot \vec{Q}^{tr} \right\} \right. \\
& \left. + \text{Trace} \left\{ \frac{1}{2} \vec{\nabla} \cdot \left(\sum_s \rho_s \langle \vec{V}_s \vec{v}_0 \vec{V}_s \rangle \right) + \frac{1}{2} \vec{\nabla} \cdot (\vec{v}_0 \hat{P}) + \frac{1}{2} \vec{\nabla} \cdot (\hat{P} \vec{v}_0) \right\} - \sum_s n_s \langle \vec{F}_s \rangle \cdot \vec{v}_0 - \dot{\Omega} \right] \\
& = \left[\frac{\partial}{\partial t} \frac{1}{2} \rho v_0^2 \right]_{CR} + \left[\frac{\partial}{\partial t} \text{Trace} \frac{1}{2} \hat{P} \right]_{CR} + \left[\frac{\partial}{\partial t} \bar{E}^{int} \right]_{CR}
\end{aligned} \tag{II.58}$$

When only the diagonal components of \hat{P} and their derivatives are retained, and contributions from the "diffusion kinetic energy" are neglected, Eq. (II.58) leads to the following expression :

$$\begin{aligned}
& \left[\frac{\partial}{\partial t} \left\{ \frac{1}{2} \rho v_0^2 + \frac{3}{2} p + \bar{E}^{int} \right\} + \vec{\nabla} \cdot \left\{ \frac{1}{2} \rho v_0^2 \vec{v}_0 + \bar{E}^{int} \vec{v}_0 + \frac{5}{2} p \vec{v}_0 + \vec{q}^{th} + \vec{Q}^{int} \right\} - \sum_s n_s \langle \vec{F}_s \rangle \cdot \vec{v}_0 - \dot{\Omega} \right] \\
& = \left[\frac{\partial}{\partial t} \frac{1}{2} \rho v_0^2 \right]_{CR} + \left[\frac{\partial}{\partial t} \frac{3}{2} p \right]_{CR} + \left[\frac{\partial}{\partial t} \bar{E}^{int} \right]_{CR}
\end{aligned} \tag{II.59}$$

Apart from particular situations (e.g. neutral beam injection or current drive) the first term on the r. h. s. is zero, i.e. the Eq. (II.45) holds.

When one is only interested in the thermal plus the internal energy density the corresponding rate equation writes without approximations :

$$\begin{aligned}
& \left[\frac{\partial}{\partial t} \left\{ \bar{E}^{int} + \text{Trace} \frac{1}{2} \hat{P} \right\} + \vec{\nabla} \cdot (\bar{E}^{int} \vec{v}_0 + \vec{Q}^{int}) + \text{Trace} \left\{ \frac{1}{2} \vec{\nabla} \cdot \vec{Q}^{tr} + \frac{1}{2} \vec{\nabla} \cdot (\vec{v}_0 \hat{P}) \right\} \right. \\
& \left. + \text{Trace} \left\{ \frac{1}{2} \vec{\nabla} \cdot \left(\sum_s \rho_s \langle \vec{V}_s \vec{v}_0 \vec{V}_s \rangle \right) + \frac{1}{2} \hat{P} \cdot \vec{\nabla} \vec{v}_0 - \frac{1}{2} \vec{v}_0 \vec{\nabla} \cdot \hat{P} \right\} - \dot{\Omega} \right] \\
& = \left[\frac{\partial}{\partial t} \text{Trace} \frac{1}{2} \hat{P} \right]_{CR} + \left[\frac{\partial}{\partial t} \bar{E}^{int} \right]_{CR}
\end{aligned} \tag{II.60}$$

In the expressions for the Traces we will omit all non diagonal components of \hat{P} and their derivatives and all contributions from the "diffusion kinetic energy". The Eq. (II.60) then leads to (see also Eq. (II.83)) :

$$\begin{aligned}
& \left[\frac{\partial}{\partial t} \left(\frac{3}{2} p + \bar{E}^{int} \right) + \vec{\nabla} \cdot \left(\frac{5}{2} p \vec{v}_0 + \bar{E}^{int} \vec{v}_0 + \vec{q}^{th} + \vec{Q}^{int} \right) - \vec{v}_0 \cdot \vec{\nabla} p \right] \\
& = \left[\frac{\partial}{\partial t} \frac{3}{2} p \right]_{CR} + \left[\frac{\partial}{\partial t} \bar{E}^{int} \right]_{CR} + \dot{\Omega}
\end{aligned} \tag{II.61}$$

Thermal energy considerations of a plasma have to be based on this rate equation,

because changes of the thermal energy are not independent of changes of the internal energy. A simpler rate equation for energy considerations does not exist.

We will now discuss the processes which contribute to the collisional-radiative terms of the r. h. s. of Eqs. (II.12, 14), (II.57) and of Eq. (II.61). Particular forms of the rate equations (II.9) and (II.14) will be discussed in the Chapters III and IV.

II.6.5 The Collisional - Radiative Terms

The two collisional - radiative terms on the r. h. s. of Eq. (II.61) are intimately linked by numerous collision and radiation processes. Both elastic, inelastic and superelastic processes contribute to the collisional - radiative terms which shall therefore be decomposed in two parts. Separating the first term on the r. h. s. of Eq. (II.61) into an electronic (e) and a heavy particle (h) terms, the two collisional-radiative terms can be decomposed as follows :

$$\begin{aligned} & \left[\frac{\partial}{\partial t} \frac{3}{2} P \right]_{CR} + \left[\frac{\partial}{\partial t} \bar{E}^{int} \right]_{CR} \\ &= \left[\frac{\partial}{\partial t} \frac{3}{2} P_e \right]_{CR} + \left[\frac{\partial}{\partial t} \frac{3}{2} P_h \right]_{CR} + \left[\frac{\partial}{\partial t} \bar{E}^{int} \right]_{CR} = \phi_{ela} + \psi \end{aligned} \quad (\text{II.62})$$

where ϕ_{ela} accounts for elastic and ψ for inelastic and superelastic collisions and all radiation processes. A contribution to ψ can still originate from nuclear reactions, for instance from the production of α -particles in D - T collisions. When nuclear reactions represent an energy source or sink, the reference level of the internal energies (see Fig. 6) must be changed by the amount $m_s c^2$. In this particular case, \bar{E}^{int} must contain the mass energy density ${}_s \Sigma n_s m_s c^2$. In the D - T nuclear reaction, ${}_s \Sigma n_s m_s c^2$ decreases; the difference $\Delta {}_s \Sigma n_s m_s c^2$ appears as translational energy of the α -particles and of the neutrons. The latter escape immediately whereas the α -particles appear as a new species in the plasma in which deuterons and tritons have disappeared. This disappearance of deuterons and tritons additionally causes a disappearance of their thermal energies, $(3/2)n_D k T_D$ and $(3/2)n_T k T_T$, which must be distributed amongst the α 's and neutrons. When intense neutral beam injection produces additional D - T reactions they must be accounted for in ψ .

In the following we shall assume that the plasma nuclear reaction rates can be neglected. We shall also assume that there is no neutral beam heating causing additional nuclear reactions and transfer of kinetic beam energy into plasma translational energy. In the presence of neutral beam heating the term $[\partial \rho v_0^2 / 2 \partial t]_{CR}$ must be taken into account, which causes further complications and has no direct relevancy to the atomic and molecular processes proper.

We will assume a sufficient maxwellisation of the random velocity distribution functions so that we can talk of a temperature T_e and T_h of the electrons and heavy particles, respectively. We first show that $\phi_{ela} = 0$ holds.

The elastic processes simply account for energy transfer between electrons and heavy particles due to elastic collisions. In a coordinate frame moving with \vec{v}_0 one obtains for the electronic part of ϕ_{ela} the relation

$$\phi_{ela,e} = -n_e \sum_h \frac{2m_e}{m_h} v_e^h \frac{3}{2} k (T_e - T_h) \quad (\text{II.63.a})$$

where v_e^h is the average collision frequency for elastic collisions between one electron and the heavy particle species whose masse and temperature are, respectively, m_h and T_h . The corresponding values for the electrons are m_e and T_e . n_e is the electron density. Eq. (II.63.a) describes the exchange of thermal energy between electrons and heavy particles, leading to energy loss of the electrons. The same amount of energy is given to the heavy particles and appears in the contribution to $\phi_{ela,h}$ with a positive sign :

$$\phi_{ela,h} = +n_e \sum_h \frac{2m_e}{m_h} v_e^h \frac{3}{2} k (T_e - T_h) = -\phi_{ela,e} \quad (\text{II.63.b})$$

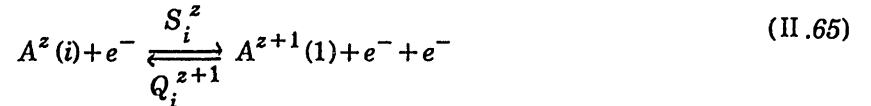
Thus

$$\phi_{ela} = \phi_{ela,e} + \phi_{ela,h} = 0 \quad (\text{II.64})$$

which means that elastic collisions alone cannot change the thermal energy density, they can only redistribute thermal energy amongst the different species.

We will now consider the processes contributing to ψ . For the inelastic, superelastic and radiative processes, the following collisional-radiative processes shall be taken into account. (Symbols above and below the arrows denote rate coefficients for the relevant processes. The following reactions apply to "ordinary", doubly, triply ... excited states, with the subscript k dropped) :

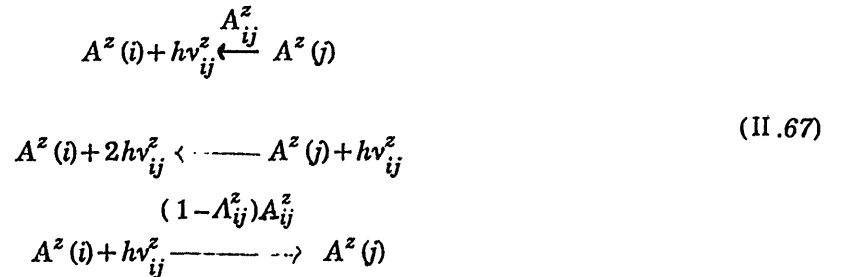
a. electronic ionization and 3-body collisional recombination :



b. electronic excitation and de-excitation



c. spontaneous emission, induced emission and photo-excitation due to radiative absorption :

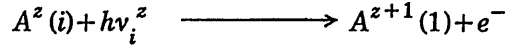
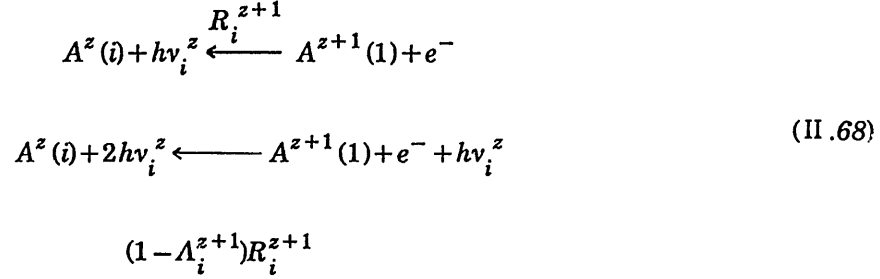


The effective radiative de-excitation rate is $\Lambda_{ij}^z A_{ij}^z n_j^z$, where A_{ij}^z is the Einstein coefficient for spontaneous de-excitation $j \rightarrow i$ and Λ_{ij}^z the optical

escape factor for this particular transition. The Λ_{ij}^z can be calculated according to a procedure given by Holstein [8], see also Refs. [9] and in which intervenes the equation of radiative transfer. For completely optically thin transitions (no reabsorption) $\Lambda_{ij}^z = 1$ holds. When all radiation is absorbed (complete radiative equilibrium) one has $\Lambda_{ij}^z = 0$.

d. radiative recombination, stimulated recombination and photoionization :

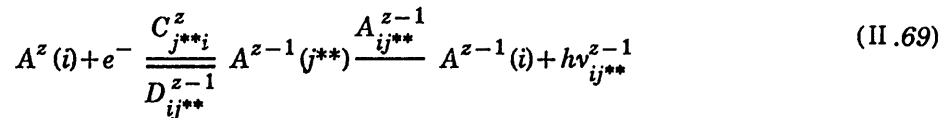
These processes are symbolically described by



The effective two-body recombination rate into level i is $\Lambda_i^{z+1} R_i^{z+1} n_i^{z+1} n_e$, where Λ_i^{z+1} is the optical escape factor for free-bound radiation of the i -th continuum. It can be estimated according to a procedure given in Ref. [9]. R_i^{z+1} is the rate coefficient for radiative (spontaneous) recombination.

e. dielectronic recombination

This effect is de-composed into two individual reactions, namely excitation of an ion simultaneously with electron capture into an autoionizing state of the formed doubly excited particle, followed either by autoionization or radiative decay of one of the two excited electrons; symbolically :



For all levels (i, j) lying below the ordinary (or simple) ionization limit of the corresponding ion, the rate coefficients are zero. For the passage from $A^z(i)$ to $A^{z-1}(j^{**})$ the internal energy is increased by $E_{j^{**}}^{z-1} - E_i^z$; the same amount is lost as internal energy in the autoionizing process $A^{z-1}(j^{**}) \rightarrow A^z(i) + e^-$ and returned to the electrons in form of thermal energy. The system itself does not loose any energy. The plasma can only loose energy in the radiative process $A^{z-1}(j^{**}) \rightarrow A^{z-1}(i) + h\nu_{ij}^{z-1}$. The quantity of energy radiated off depends on the population density $n_{j^{**}}^{z-1}$ of $A^{z-1}(j^{**})$. This density, however depends on the collision and radiation processes in which both $A^{z-1}(j^{**})$ and $A^{z-1}(i)$ are involved. $A^{z-1}(j^{**})$ can in particular be submitted to intense collisional ionization, thus leading to a reduction of $n_{j^{**}}^z$ and to a reduced radiation rate. From a principal point of view it is therefore not reasonable to separate so-called "dielectronic

recombination radiation" from usual bound-bound radiation. When doubly, triply, ... excited states are taken into account in a collisional-radiative model, the bound-bound radiative transitions should automatically contain the effect of dielectronic recombination through the spontaneous de-excitation from a doubly excited state above the ionization limit to an ordinary excited state below the ionization limit. Similar arguments hold for transitions from triply to doubly excited states.

Only when the doubly (multiply) excited states created by electronic excitation with capture decay radiatively before suffering other collisions, can the "dielectronic recombination radiation" be calculated without detailed collisional-radiative model calculations for the doubly (multiply) excited states. In this particular case the following relation exists between the densities n_i^z of $A^z(i)$ and $n_{j^{**}}^z$ of $A^{z-1}(j^{**})$:

$$n_e C_{j^{**}i}^z n_i^z = [D_{ij^{**}}^{z-1} + A_{ij^{**}}^{z-1}] n_{j^{**}}^{z-1} \quad (\text{II.70})$$

$C_{j^{**}i}^z$ can be expressed by the Saha equation and by $D_{ij^{**}}^{z-1}$ (by invoking the principle of detailed balancing) :

$$C_{j^{**}i}^z = D_{ij^{**}}^{z-1} \frac{g_{j^{**}}^{z-1}}{2g_i^z} \frac{1}{X_{j^{**}}^z(T_e)} \quad (\text{II.71})$$

where

$$\frac{1}{X_{j^{**}}^z(T_e)} = \frac{h^3}{(2\pi m_e k T_e)^{3/2}} \exp\left(\frac{E_{j^{**}}^{z-1} - E_i^z}{k T_e}\right) \quad (\text{II.72})$$

It follows that

$$n_{j^{**}}^{z-1} = n_i^z n_e \frac{g_{j^{**}}^{z-1}}{2g_i^z} \frac{1}{X_{j^{**}}^z(T_e)} \frac{D_{ij^{**}}^z}{D_{ij^{**}}^z + A_{ij^{**}}^{z-1}} \quad (\text{II.73})$$

The power density radiated off by this particular level j^{**} of $A^{z-1}(j^{**})$ is $A_{ij^{**}}^{z-1} n_{j^{**}}^{z-1} h\nu_{ij^{**}}^{z-1}$. The total power density due to this "unperturbed dielectronic recombination radiation" is obtained by summing over all possible radiative transitions $A^{z-1}(j^{**}) \rightarrow A^{z-1}(i) + h\nu_{ij^{**}}^{z-1}$.

In the following we will not consider "dielectronic recombination radiation" as an independent radiation phenomenon. It simply represents a particular type of bound-bound radiative transitions — which can under particular conditions (low electron density, high electron temperature) be additive to bound-bound radiative transitions in which only simply excited states are involved.

f. Charge exchange

In the most general case we have to write

$$A^z(i) + B^{z+n}(h) \rightleftharpoons A^{z+n}(j) + B^z(h) \quad (\text{II.74.a})$$

submitted to the energy condition

$$\Sigma(\text{internal energies}) + \Sigma(\text{transl. energies}) = 0 \quad (\text{II.74.b})$$

In a charge exchange reaction, internal energy can in principal be partly transformed into thermal energy, and vice versa. However, the largest reaction rates are obtained for resonance or quasi-resonance charge transfer reactions in which neither the sum of the thermal nor the sum of the internal energy is changing noticeably. The most important reaction is the one between ionized impurity species $A^z(1)$ in the ground state "1" and a neutral hydrogen atom $H^0(i)$ in its ground state ($i=1$) or in an excited state ($i>1$) :



This reaction does not produce radiation, it primarily redistributes only internal energy of the reaction partners : the internal energy of hydrogen is increased by the amount of $13.6/i^2$ eV. The same amount is taken away from $A^z(1)$ yielding the species $A^{z-1}(j)$ in the excited state "j". This state may radiate off energy, however, it may also undergo electronic collisions leading to reionization. We have quite a similar situation as for dielectronic recombination.

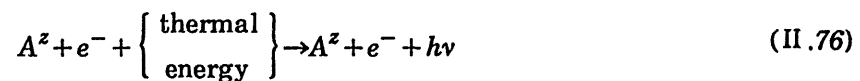
Only at low electron densities is the probability for spontaneous radiative decay of $A^{z-1}(j)$ so high that electronic collisions can be neglected. The collision rate of reaction (II.75) multiplied by $h\nu_{ij}$ then yields the so-called "charge exchange recombination radiation" which is additive to the other radiation rates.

We will not consider "charge exchange recombination radiation" as an independent radiation process.

The effect of charge exchange reactions in the radiative power loss will be included in the bound-bound radiative rate.

g. Inelastic electron-ion collisions leading to bremsstrahlung (free-free radiation)

We have symbolically



We neglect absorption and inverse bremsstrahlung which are important in laser beam-plasma interactions at high electron densities.

h. Collisions between heavy particles

Collisional excitation and ionization of impurity species by hydrogen ions can modify the population densities. The corresponding reactions are described by (II.65, 66) with e^- replaced by H^+ .

The source term ψ of Eq. (II.62) can now be expressed as a function of the particle densities, the rate coefficients and the energies involved. When one writes down all terms one sees that all collision terms cancel each other. (This has been demonstrated in Ref. [7]). Only radiation processes contribute to ψ which may be put into the following form

including electron-synchrotron (sy) radiation :

$$\psi = -\dot{R} = -\dot{R}^{sy} - \dot{R}^{ff} - \dot{R}^{fb} - \dot{R}^{bb} \quad (\text{II.77})$$

where the three last terms on the r. h. s. represent, respectively, the radiation power per unit volume which is lost due to free-free (ff), free-bound (fb) and bound-bound (bb) transitions. One has the following expressions :

For synchrotron radiation

$$\dot{R}^{sy} = \frac{e_0^2 \omega_{ec}^2}{3\pi\epsilon_0 c} \left(\frac{kT_e}{m_e c^2} \right) n_e \left(1 + \frac{5}{2} \frac{kT_e}{m_e c^2} + \dots \right) \quad (\text{II.78})$$

The spectrum of this radiation consists of many harmonics of ω_{ec} , most of the energy being emitted in harmonics higher than the first one. The angular distribution is complicated. Much of the energy can be redirected back into the plasma by using the first wall as a reflector.

For free-free radiation one has (with the subscript "k" reintroduced)

$$\dot{R}^{ff} = \frac{32\pi e_0^6}{3(4\pi\epsilon_0)^3 c^3 m_e h} \left(\frac{2\pi kT_e}{3m_e} \right)^{1/2} n_e \sum_z \sum_k \sum_i z^2 n_{k,i}^z \quad (\text{II.79})$$

An optically thin plasma has been assumed for this radiation.

Free-bound radiation loss is given by

$$\dot{R}^{fb} = \sum_z \sum_k \sum_i \Lambda_{k,i}^z R_{k,i}^z n_e n_{k,1}^z (E_{k,i}^{z-1} + \beta_{k,i}^{z-1} kT_e) \quad (\text{II.80})$$

The summation over z begins with $z=0$ (neutrals) and ends with $z=Z$, Z being the charge number of the bare nucleus. The $f-b$ radiation for $z=0$ represents radiation due to electron attachment. When molecules or molecular ions are present they have to be included in Eq. (II.80). For optically thin transitions $\Lambda_{k,i}^z=1$ holds.

The coefficient $\beta_{k,i}^{z-1}$ is of order of unity, the exact value depends on the recombination cross sections and the velocity distribution.

Bound-bound radiation is given by

$$\dot{R}^{bb} = \sum_z \sum_k \sum_{i,j} \Lambda_{k,ij}^z A_{k,ij}^z n_{k,j}^z (E_{k,j}^z - E_{k,i}^z) \quad (\text{II.81})$$

The summation over i and j includes the ground level ($i, j=1$) and the singly and multiply excited states ($i, j>1$). A cut-off value for the summation can for instance be introduced by using the Inglis-Teller relation, or by applying some other criterion. For an optically thin transition, $\Lambda_{k,ij}^z=1$ holds. It should be born in mind that \dot{R}^{bb} also contains the so-called "charge exchange" and "dielectronic recombination" radiation.

We remember that the subscript "k" denotes the chemical type of the species. When molecules and molecular ions can contribute to the radiation losses, they must be included in Eq. (II.81) by assigning a k -value to these molecules and molecular ions.

In the particular case of coronal excitation, the densities of the excited states $j>1$ are

proportional to those for the ground state $i=1$; for singly excited levels and multiply excited levels below the ionization limit :

$$n_{k,j}^z = \frac{C_{k,j1}^z n_{k,1}^z n_e}{\sum_{i<j} A_{k,ij}^z} \quad (\text{II.82})$$

Doubly excited levels formed by electron excitation with capture have population densities given by Eq. (II.73). Quite a similar expression is obtained for inner-shell excited levels.

In conclusion, the two collisional-radiative terms of Eq. (II.61) represent, in the absence of nuclear reactions and of neutral-beam heating, the power density of the radiation losses. The heating effects due to nuclear reactions and neutral beam injection can formally be taken into account by two additional terms. \dot{N} and \dot{I} , respectively. We then have :

$$\left[\frac{\partial}{\partial t} \frac{3}{2} p \right]_{CR} + \left[\frac{\partial \bar{E}^{int}}{\partial t} \right]_{CR} = -\dot{R} + \dot{N} + \dot{I} \quad (\text{II.83})$$

\dot{R} , \dot{N} and \dot{I} are positive quantities.

The term $[\partial \bar{E}^{int}/\partial t]_{CR}$ can be decomposed in a collisional and a radiative contribution :

$$\left[\frac{\partial \bar{E}^{int}}{\partial t} \right]_{CR} = \left[\frac{\partial \bar{E}^{int}}{\partial t} \right]_C + \left[\frac{\partial \bar{E}^{int}}{\partial t} \right]_R \quad (\text{II.84})$$

The first term of the r.h.s. describes the volume production rate of \bar{E}^{int} due to collisions alone, the second term is the corresponding rate due to radiation processes alone. For instance, the increase of \bar{E}^{int} due to collisional dissociation and ionization or the decrease of \bar{E}^{int} due to radiative recombination is taken into account in $[\partial \bar{E}^{int}/\partial t]_C$. The decrease of \bar{E}^{int} due to spontaneous de-excitation, for instance, contributes to the last term of Eq. (II.84).

In the following we neglect \dot{I} and \dot{N} . From the development of Eq. (II.83)

$$\left[\frac{\partial}{\partial t} \frac{3}{2} p \right]_{CR} + \left[\frac{\partial \bar{E}^{int}}{\partial t} \right]_{CR} = \sum_s \frac{3}{2} \left\{ kT_s \left[\frac{\partial n_s}{\partial t} \right]_{CR} + n_s k \left[\frac{\partial T_s}{\partial t} \right]_{CR} \right\} + \left[\frac{\partial \bar{E}^{int}}{\partial t} \right]_{CR} = -\dot{R} \quad (\text{II.85})$$

it follows that

$$\sum_s \frac{3}{2} n_s k \left[\frac{\partial T_s}{\partial t} \right]_{CR} = -\dot{R} - \left[\frac{\partial \bar{E}^{int}}{\partial t} \right]_{CR} - \sum_s \frac{3}{2} kT_s \left[\frac{\partial n_s}{\partial t} \right]_{CR} \quad (\text{II.86})$$

When atom production by dissociation is negligible we have $\Sigma[\partial n_s/\partial t]_{CR} = [\partial n_e/\partial t]_{CR}$. When in addition the collisional-radiative processes do not modify the heavy particle temperature, the relation

$$\sum_s \frac{3}{2} kT_s \left[\frac{\partial n_s}{\partial t} \right]_{CR} = \frac{3}{2} kT_e \left[\frac{\partial n_e}{\partial t} \right]_{CR} \quad (\text{II.87})$$

holds and the Eq. (II.86) can be written in the following form:

$$\sum_s \frac{3}{2} n_s k \left[\frac{\partial T_s}{\partial t} \right]_{CR} = -\dot{R} - \left[\frac{\partial \bar{E}^{int}}{\partial t} \right]_{CR} - \frac{3}{2} k T_e \left[\frac{\partial n_e}{\partial t} \right]_{CR} \quad (II.88)$$

The terms of the r. h. s. have, respectively, the following meanings: power density lost by radiation, power density consumed in changing \bar{E}^{int} , power density consumed in heating volume-created electrons to the temperature T_e .

CHAPTER III

Application To Hot Core Plasmas In Magnetic Confinement Devices

III.1 Introduction

We will now apply atomic physics to hot core plasmas in magnetic confinement devices with emphasis on tokamaks. The hot core plasma is that part of the plasma which lies inside the so-called separatrix. The separatrix is defined as the outermost magnetic surface which is made up of magnetic field lines which do not hit a material wall or leave the configuration without returning to it. An electron, for instance, of extremely low velocity will travel for a very long time on such a surface before leaving it. Under actual conditions, however, we have a less ideal situation. The finite gyro-radius (or cyclotron radius) r_c given by

$$r_c = \frac{mw_{\perp}}{ze_0B} \Rightarrow \langle r_c \rangle = \frac{(2mkT)^{1/2}}{ze_0B} \quad (\text{III.1})$$

has the consequence that the particles are only bound to the magnetic surface within a width of $\pm \langle r_c \rangle$ for the electrons (because of charge neutrality). Further, electric fields of strength \vec{E}_{\perp} perpendicular to \vec{B} cause the particles to drift perpendicularly to \vec{E}_{\perp} and \vec{B} with the velocity

$$w_{DE} = \frac{\vec{E}_{\perp} \times \vec{B}}{B^2} \quad (\text{III.2})$$

Furthermore, a curvature of the magnetic field lines causes a centrifugal force which leads to particle drift \vec{w}_{DR} perpendicularly to \vec{B} and to the radius of curvature \vec{R} given by

$$\vec{w}_{DR} = 2 \frac{\frac{1}{2} mw_{\parallel}^2}{e_0 R^2 B^2} (\vec{R} \times \vec{B}) \Rightarrow \langle \vec{w}_{DR} \rangle = \frac{kT}{e_0 R^2 B^2} (\vec{R} \times \vec{B}) \quad (\text{III.3})$$

From the plasma physical point of view the separatrix defines a "region" rather than a "surface" in which the plasma parameters change strongly and where plasma-wall interaction has a direct influence on the plasma properties. — This property will in Chapter IV be used to define the plasma boundary and edge region. That part of the plasma which lies inside the outermost closed magnetic surface (the separatrix) defines in the following the hot core plasma.

III.2 Determination of Particle Confinement Times τ_p

One has introduced the concept of the confinement times τ in order to describe qualitatively and rather phenomenologically transport properties which are still an enigma. The knowledge of τ does not mean that one has understood the physical phenomena which

are responsible that a certain τ -value exists and not another one. Low (high) values of the particle confinement τ_p only mean that particles are transported with high (low) velocity across the plasma volume.

The determination of τ_p is based on the measurement of spectral line intensities.

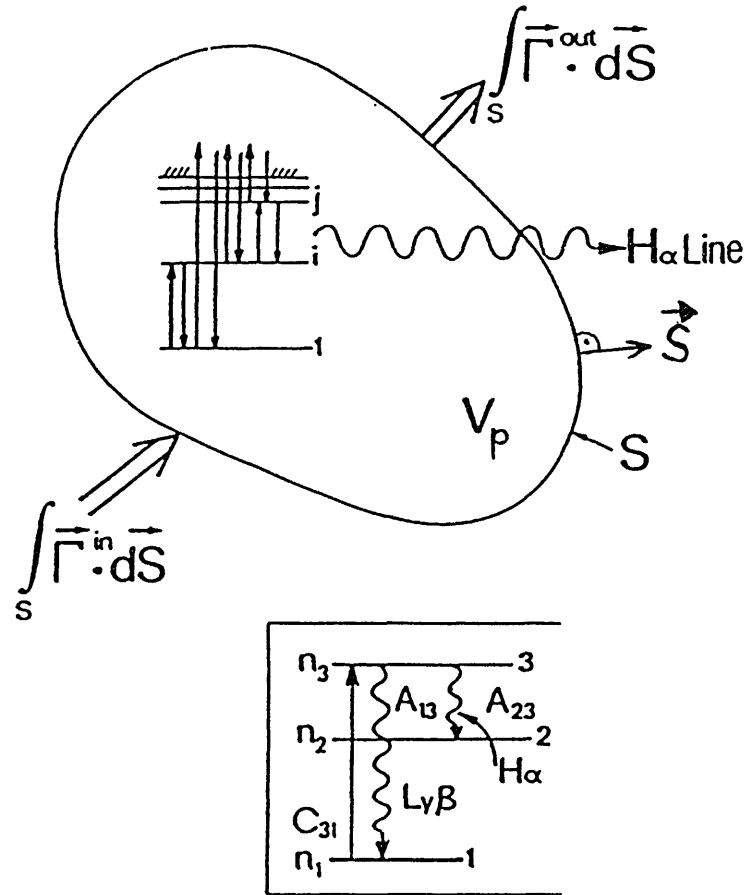


Figure 7. Particle diffusion fluxes $\vec{\Gamma}^{in}$ in and $\vec{\Gamma}^{out}$ across the surface S enclosing the plasma volume V_p . Hydrogen atoms are excited and emit radiation, e.g. H_α . The lower part shows coronal excitation of the $n=3$ level of atomic hydrogen leading to the emission of $Ly\beta$ and H_α . After Ref. [10].

a. The local particle confinement time τ_p

Consider a volume V_p containing a pure hydrogen plasma (see Fig. 7). We have particle fluxes $\vec{\Gamma}^{in}$ and $\vec{\Gamma}^{out}$, with $\vec{\Gamma} = \vec{\Gamma}^{in} + \vec{\Gamma}^{out}$. Charge neutralization forces electrons and protons to diffuse together with equal flux densities, i.e., $\vec{\Gamma}_e = \vec{\Gamma}_+$. In the stationary state, the constancy of the plasma pressure requires the following relation to be fulfilled for

the neutral and charged flux densities, $\vec{\Gamma}_0 = -(1/2)(\vec{\Gamma}_e + \vec{\Gamma}_+) = -\vec{\Gamma}_e$.

The rate equations for the neutral hydrogen atoms and the electrons are (see Eqs. (II. 11, 12) and (II. 55))

$$\frac{\partial n_0}{\partial t} + \vec{\nabla} \cdot \vec{\Gamma}_0 = -n_0 n_e S_0 + n_+ n_e \alpha_+ = \left[\frac{\partial n_0}{\partial t} \right]_{CR} \quad (\text{III. 4.a})$$

$$\frac{\partial n_e}{\partial t} + \vec{\nabla} \cdot \vec{\Gamma}_e = +n_0 n_e S_0 - n_+ n_e \alpha_+ = \left[\frac{\partial n_e}{\partial t} \right]_{CR} \quad (\text{III. 4.b})$$

where S_0 and α_+ are the ionization and recombination coefficients, respectively. In the stationary state, $\partial n_0/\partial t = 0$ and $\partial n_e/\partial t = 0$ hold. One now replaces the divergency of the diffusion flux by the relations

$$\frac{n_0}{\tau_{p,0}} = \vec{\nabla} \cdot \vec{\Gamma}_0, \quad \frac{n_e}{\tau_{p,e}} = \vec{\nabla} \cdot \vec{\Gamma}_e \quad (\text{III. 5})$$

which define the local particle confinement time of the neutral atoms, $\tau_{p,0}$, and the electrons, $\tau_{p,e}$. Because of the charge neutrality, electrons and protons diffuse together (ambipolar diffusion). Therefore, the confinement time of the protons is the same as that for the electrons. The Eqs. (III. 4 a, b) thus yield in the stationary state

$$\frac{n_0}{\tau_{p,0}} = -n_0 n_e S_0 + n_+ n_e \alpha_+ \quad (\text{III. 6.a})$$

$$\frac{n_e}{\tau_{p,e}} = -n_0 n_e S_0 + n_+ n_e \alpha_+ \quad (\text{III. 6.b})$$

hence, owing to $\vec{\Gamma}_0 = -\vec{\Gamma}_e = -\vec{\Gamma}_+$, it follows that

$$\tau_{p,0} = \tau_{p,e} = \tau_{p,+} = \frac{1}{n_0 S_0 - n_+ \alpha_+} \equiv \tau_p \quad (\text{III. 7})$$

It is thus possible to determine τ_p when the local values of $n_0, n_+ = n_e, S_0$ and α_+ are known. In the general case, S_0 and α_+ must be calculated from a collisional-radiative model. However, at low electron densities and high temperatures, the coronal ionization model can be applied, i.e., S_0 is equal to the rate coefficient for ionization from the ground level, and α_+ is the sum of all rate coefficients for recombination into the ground and excited states :

$$S_0 = S_{H,1}^0(T_e), \quad \alpha_+ = \sum_{i=1}^{\infty} R_{H,i}^1(T_e)$$

The crucial point is the determination of the neutral hydrogen particle density n_0 which practically equals that of the particles in the ground state ($i=1$), $n_{H,1}^0$. The most exact way of determining $n_{H,1}^0$ is by laser excitation from the ground level and then measuring the fluorescence light, for instance of H_α or $Ly_{\alpha,\beta}$. This method is only

possible at sufficient but not too high particle densities, not too a high temperature (because of too a large absorption line profile) and sufficient laser beam energy in the desired frequency range.

In general $n_{H,1}^0$ is determined by measuring the emission coefficient ε of a hydrogen spectral line. For instance for the H_α line we have in the optically thin case :

$$\varepsilon_{H,23}^0 = \frac{1}{4\pi} A_{H,23}^0 n_{H,3}^0 h\nu_{H,23}^0 \quad (\text{III.8})$$

where $A_{H,23}^0$ is the Einstein coefficient for spontaneous de-excitation. When we assume corona excitation conditions (see Fig. 7), the particle density $n_{H,3}^0$ of the level with principal quantum number $j=3$ is given by the condition that

$$n_e C_{H,31}^0 n_{H,1}^0 = [A_{H,13}^0 + A_{H,23}^0] n_{H,3}^0 \quad (\text{III.9})$$

which yields

$$n_0 = n_{H,1}^0 = \frac{4\pi}{n_e C_{H,31}^0} \frac{A_{H,13}^0 + A_{H,23}^0}{A_{H,23}^0} \frac{\varepsilon_{H,23}^0}{h\nu_{H,23}^0} \quad (\text{III.10})$$

where $C_{H,31}^0(T_e)$ is the rate coefficient for electronic excitation of level $j=3$ from the ground state $i=1$. This relation also shows how many atomic data are necessary for the determination of n_0 : frequencies, transition probabilities and excitation coefficients.

In conclusion, a measurement of $T_e(r)$, $n_e(r)$ and the emission coefficient ε of a hydrogen line permits a determination of the local particle confinement time $\tau_{p,e} = \tau_p$.

In the transient state, the rate Eq. (III. 4.b) yields for $\tau_{p,e}$ the expression

$$\tau_{p,e} = \frac{1}{n_0 S_0 - n_+ \alpha_+ - (1/n_e) \partial n_e / \partial t} \quad (\text{III.11.a})$$

When impurity species are present $\tau_{p,e}$ must be valuated from the expression

$$\tau_{p,e} = \frac{n_e}{[\partial n_e / \partial t]_{CR} - \partial n_e / \partial t} \quad (\text{III.11.b})$$

b. The mean or global particle confinement time $\bar{\tau}_p$

The mean (or global) particle confinement time refers to some mean value of τ_p related to the total particle content in a discharge.

Let $\int n_e dV_p = N_e$ be the total number of electrons in the plasma volume V_p enclosed by the separatrix. The integration over V_p of Eq. (III. 4.b) yields

$$-\frac{\partial N_e}{\partial t} + \int \vec{\nabla} \cdot \vec{\Gamma}_e dV_p = \int \left[\frac{\partial n_e}{\partial t} \right]_{CR} dV_p + C_e = \left[\frac{\partial N_e}{\partial t} \right]_{CR} + C_e \quad (\text{III.12})$$

where C_e is the integration constant. The second term on the *l.h.s.* is the electron flux crossing the plasma surface S , that is

$$\int \vec{\nabla} \cdot \vec{\Gamma}_e dV_p = \oint \vec{\Gamma}_e \cdot d\vec{S} \quad (\text{III.13})$$

The mean particle confinement time $\bar{\tau}_{p,e}$ of the electrons may be defined by

$$\frac{N_e}{\bar{\tau}_{p,e}} = \int \vec{\nabla} \cdot \vec{\Gamma}_e dV_p = \oint \vec{\Gamma}_e \cdot d\vec{S} \quad (\text{III.14})$$

Further, $C_e=0$, since no additional particle source is deposited in the volume V_p . One thus obtains

$$\bar{\tau}_{p,e} = \frac{1}{\frac{1}{N_e} \left[\frac{\partial N_e}{\partial t} \right]_{CR} - \frac{1}{N_e} \frac{\partial N_e}{\partial t}} \quad (\text{III.15})$$

where $[\partial N_e / \partial t]_{CR}$ is the volume integrated value of $[\partial n_e / \partial t]_{CR}$. The effect of recycling and gas puffing is automatically taken into account in these expressions since the collisional-radiative term accounts also for the electron production due to recycled neutral atoms and gas-puffed neutrals entering the plasma. Consider for instance a plasma with a recycling coefficient R equal to one, $R=1$. Then $\partial N_e / \partial t = 0$, since the electron density is constant. But $\partial N_e / \partial t = 0$ can also be obtained with $R < 1$, when the missing flux is compensated by external gas puffing.

For further details, see Chapter IV.

c. Particle confinement times of impurity ions $\tau_{p,z}$

The particle confinement of the ionic impurity species can be determined in the same manner as that of the electrons. It is sufficient to consider the particles in the ground state. Their density is $n_{k,1}^z \approx \sum_i n_{k,i}^z$. The rate equation for $n_{k,1}^z$ writes

$$\frac{\partial n_{k,1}^z}{\partial t} + \vec{\nabla} \cdot \vec{\Gamma}_{k,1}^z = \left[\frac{\partial n_{k,1}^z}{\partial t} \right]_{CR} \quad (\text{III.16})$$

We define a local particle confinement time $\tau_{p,k}$ by

$$\frac{n_{k,1}^z}{\tau_{p,k}^z} = \vec{\nabla} \cdot \vec{\Gamma}_{k,1}^z \quad (\text{III.17})$$

and obtain for particles of the chemical element "k" in the ion charge state "z"

$$\tau_{p,k}^z = \frac{1}{\frac{1}{n_{k,1}^z} \left[\frac{\partial n_{k,1}^z}{\partial t} \right]_{CR} - \frac{1}{n_{k,1}^z} \frac{\partial n_{k,1}^z}{\partial t}} \quad (\text{III.18})$$

One can also define a mean or global particle confinement time $\bar{\tau}_{p,k}^z$. However, the individual charge states "z" of the heavier elements are concentrated in an annulus of limited radial width. Therefore $\bar{\tau}_{p,k}^z$ will not much deviate from $\tau_{p,k}^z$. It is physically more

interesting to consider the particle confinement of the ensemble of all ion charge states "z" of a given impurity species "k". Their mean confinement time $\bar{\tau}_{p,k}$ can be obtained from the following system of rate equations:

$$\begin{aligned} \frac{\partial n_{k,1}^{z=1}}{\partial t} + \vec{\nabla} \cdot \vec{\Gamma}_{k,1}^{z=1} &= \left[\frac{\partial n_{k,1}^{z=1}}{\partial t} \right]_{CR} \\ \vdots \\ \frac{\partial n_{k,1}^{z=Z}}{\partial t} + \vec{\nabla} \cdot \vec{\Gamma}_{k,1}^{z=Z} &= \left[\frac{\partial n_{k,1}^{z=Z}}{\partial t} \right]_{CR} \end{aligned} \quad (\text{III.19})$$

After summation and integration over the plasma volume V_p one has

$$\sum_{z=1}^Z \left\{ \frac{\partial N_{k,1}^z}{\partial t} + \int \nabla \cdot \Gamma_{k,1}^z dV_p \right\} = \sum_{z=1}^Z \left[\frac{\partial N_{k,1}^z}{\partial t} \right]_{CR} \quad (\text{III.20})$$

We define a mean particle confinement time $\bar{\tau}_{p,k}^z$ for the individual charge state "z" and a mean particle confinement $\bar{\tau}_{p,k}$ for the ensemble of all ionized impurity species "k" within the plasma volume V_p by

$$\frac{N_{k,1}^z}{\bar{\tau}_{p,k}^z} = \int \vec{\nabla} \cdot \vec{\Gamma}_{k,1}^z dV_p \quad (\text{III.21.a})$$

$$\frac{\sum_z N_{k,1}^z}{\bar{\tau}_{p,k}} = \sum_z \frac{N_{k,1}^z}{\bar{\tau}_{p,k}^z} \quad (\text{III.21.b})$$

The Eqs. (III.20) and (III.21.a, b) then lead to

$$\bar{\tau}_{p,k} = \frac{\sum_z N_{k,1}^z}{\sum_z \left\{ \left[\frac{\partial N_{k,1}^z}{\partial t} \right]_{CR} - \frac{\partial N_{k,1}^z}{\partial t} \right\}}$$

(III.22)

The determination of $\bar{\tau}_{p,k}$ requires the radial distribution $n_{k,1}^z(r)$ of all impurity ions to be known experimentally. This is practically impossible. Under actual situations one will only know the r -distributions for a few ion charge states "z" from a limited number of spectral lines for which an Abel inversion can be performed. Therefore the measurement must be complemented by solutions of a numerical code which gives the solutions for $n_{k,1}^z$ over the radius for measured radial electron temperature and electron density distributions which are needed for the calculation of the collisional-radiative rates, see e.g. Eq. (III.19)

For the measurement of $n_{k,1}^z$ the excitation coefficients and the Einstein transition probabilities are needed (unless the resonance line is used and cascading is neglected). For

the evaluation of $[\partial n_{k,1}^z / \partial t]_{CR}$ the ensemble of rate coefficients for ionization, excitation with electron capture recombination and charge exchange processes must be known.

III.3 Confinement Time τ_p and Diffusion Coefficient D_a

We apply Fick's law which states that the diffusion flux is proportional to $\vec{\nabla}n$ and proportional to a coefficient D termed particle diffusion coefficient. For electron-ion pair diffusion, D is the ambipolar diffusion coefficient D_a . We thus have

$$\vec{\Gamma}_e = -D_a \vec{\nabla}n_e \quad (\text{III.23})$$

Inserting this into Eq. (III.14) yields

$$\frac{1}{\bar{\tau}_{p,e}} \int n_e dV_p = - \int \vec{\nabla} \cdot D_a \vec{\nabla}n_e dV_p = - \oint D_a (\vec{\nabla}n) \cdot d\vec{S} \quad (\text{III.24})$$

For toroidal geometry, with a torus length $L=2\pi R_0$ and a plasma radius a , we have

$$\int n_e dV_p = \bar{n}_e L \pi a^2 \quad (\text{III.25})$$

where \bar{n}_e is the mean electron density of the whole discharge volume. We will in particular assume that

$$n_e(r) = n_e(0) \left(1 - \frac{r^2}{a^2}\right)^a \quad \text{with } a=1 \quad (\text{III.26})$$

We then find the following relation

$$\bar{\tau}_{p,e} = \frac{1}{4} \frac{\bar{n}_e}{n_e(0)} \frac{a^2}{D_a} = \frac{1}{8} \frac{a^2}{D_a} \quad (\text{III.27})$$

where D_a represents some space-averaged electron-ion diffusion coefficient. Eq. (III.27) can be considered as a "scaling law" for tokamaks ; when we assume that D_a does not vary much change with the dimensions and with the plasma parameters (within certain n_e , T_e -limits) then the global particle confinement is proportional to a^2 .

Measurements on Alcator-C and TFR have shown that $\bar{\tau}_{p,e} \propto n_e$, hence

$$\bar{\tau}_{p,e} \propto a^2 n_e \quad (\text{III.28})$$

When we assume this relation to be valid, then the same $\bar{\tau}_{p,e}$ -value can be obtained in a tokamak of smaller size with plasmas of higher electron density.

III.4 Determination of Energy Confinement Times τ_E

The rate equation for the total energy density is given by Eq. (II.59). We define a local energy confinement time τ_E by

$$\frac{\frac{1}{2} \rho v_0^2 + \frac{3}{2} p + \bar{E}^{int}}{\tau_E} = \vec{\nabla} \cdot \left\{ \frac{1}{2} \rho v_0^2 \vec{v}_0 + \bar{E}^{int} \vec{v}_0 + \frac{5}{2} p \vec{v}_0 + \vec{q}^{th} + \vec{Q}^{int} \right\} + R \quad (\text{III.29})$$

When we introduce this expression into Eq. (II. 59) and apply the Eq. (II. 83) we obtain

$$\tau_E = \frac{\frac{1}{2} \rho v_0^2 + \frac{3}{2} p + \bar{E}^{int}}{\left[\frac{\partial}{\partial t} \frac{1}{2} \rho v_0^2 \right]_{CR} + \dot{\Omega} + \dot{I} + \dot{N} + \sum_s n_s \langle \vec{F}_s \rangle \cdot \vec{v}_0 - \frac{\partial}{\partial t} \left(\frac{1}{2} \rho v_0^2 + \frac{3}{2} p + \bar{E}^{int} \right)} \quad (\text{III.30})$$

We remember that the effect due to shear stresses is not contained in this relation. For low impurity concentrations and simultaneously high plasma temperatures we can put

$$\frac{1}{2} \rho v_0^2 + \frac{3}{2} p + \bar{E}^{int} \approx \frac{3}{2} p \quad (\text{III.31})$$

We assume Eq. (II. 45) to be valid and put $\sum_s n_s \langle \vec{F}_s \rangle \cdot \vec{v}_0 = 0$, hence

$$\tau_E = \frac{\frac{3}{2} \sum_s n_s k T_s}{\dot{\Omega} + \dot{I} + \dot{N} - \frac{\partial}{\partial t} \left\{ \frac{3}{2} \sum_s n_s k T_s \right\}} \quad (\text{III.32})$$

It can be seen from the values given in Table 1 that the omission of the internal energy is in particular at high plasma temperatures practically always allowed (which does not mean that bound-bound radiation can be neglected).

The local energy confinement time due to thermal and convective transport alone is obtained in omitting \dot{R} in Eq. (III.29), hence the definition for the local energy confinement time τ_E^{tr} due to convection and diffusion alone is

$$\frac{\frac{1}{2} \rho v_0^2 + \frac{3}{2} p + \bar{E}^{int}}{\tau_E^{tr}} = \nabla \cdot \left\{ \frac{1}{2} \rho v_0^2 v_0 + \bar{E}^{int} v_0 + \frac{5}{2} p v_0 + q^{th} + Q^{int} \right\} \quad (\text{III.33})$$

TABLE 1

Internal energy $E^{int,z}$ in [eV] carried by one iron ion in the ion charge state "z", with values from Ref. [11] *								
Fe^{z+}	$z=1$	2	3	4	5	6	7	8
$E^{int,z}$	7.87	24.05	54.65	109.8	184.5	283.6	408.6	559.7
Fe^{z+}	$z=9$	10	11	12	13	14	15	
$E^{int,z}$	793.3	1055.4	1345.7	1676.5	2037.5	2429.7	2886.7	
Fe^{z+}	$z=16$	17	18	19	20	21	22	
$E^{int,z}$	3375.9	4641.9	5999.9	7455.9	9037.9	10726.9	12525.9	
Fe^{z+}	$z=23$	24	25	26				
$E^{int,z}$	14475.9	16501.3	25329.3	34607				
*with $Fe \text{ XXIV} \rightarrow Fe \text{ XXV}$: 2025.4 eV ; $Fe \text{ XXVI} \rightarrow Fe \text{ XXVII}$: 9277.65 eV								

The Eq. (II. 59) then leads to (with the same approximation as for Eq. (III. 32)

$$\tau_E^{tr} = \frac{\frac{3}{2} \sum_s n_s k T_s}{-\dot{R} + \dot{\Omega} + \dot{I} + \dot{N} - \frac{\partial}{\partial t} \left\{ \frac{3}{2} \sum_s n_s k T_s \right\}} \quad (\text{III.34})$$

One has $\tau_E^{tr} > \tau_E$.

Owing to difficulties in measuring $\dot{\Omega}$ one often considers only the mean energy confinement times. In applying the same method as for the particle confinement times one finds for the mean values of τ_E and τ_E^{tr} the relations

$$\bar{\tau}_E = \frac{\int_0^a \frac{3}{2} \sum_s n_s k T_s r dr}{\int_0^a \left[\dot{\Omega} + \dot{I} + \dot{N} - \frac{\partial}{\partial t} \left\{ \frac{3}{2} \sum_s n_s k T_s \right\} \right] r dr} \quad (\text{III.35})$$

$$\bar{\tau}_E^{tr} = \frac{\int_0^a \frac{3}{2} \sum_s n_s k T_s r dr}{\int_0^a \left[-\dot{R} + \dot{\Omega} + \dot{I} + \dot{N} - \frac{\partial}{\partial t} \left\{ \frac{3}{2} \sum_s n_s k T_s \right\} \right] r dr} \quad (\text{III.36})$$

where

$$J_p U = L \int_0^a \dot{\Omega} 2\pi r dr \quad (\text{III.37})$$

represents the total ohmic power input (J_p =total plasma current, U =loop voltage, $L=2\pi R_0$ =length of the torus, a =plasma radius) and can easily be measured.

The atomic physics problem in the determination of τ_E^{tr} consists mainly in the evaluation of the radiative loss term $-\dot{R}$. In the presence of impurity atoms one must know their radial density distribution in order to be able to calculate reliable values for \dot{R} .

However, atomic physics is also involved in the determination of the heavy particle temperatures T_s , either by charge exchange measurements or by spectroscopic means.

III.5 The Particle Density Decay Times τ_p^*

Whether the particle density in a discharge can be maintained on a constant level depends both on the divergency of the diffusion fluxes and on the source of ionization. We will now consider the decay of the plasma density due to an imbalance between the particle fluxes and the ionization sources.

Integration of the Eqs. (III.4.a, b) over the plasma volume yields owing to Eq. (III.14)

$$\frac{\partial N_0}{\partial t} + \oint \vec{\Gamma}_0 \cdot d\vec{S} = \left[\frac{\partial N_0}{\partial t} \right]_{CR} \quad (\text{III.38.a})$$

$$\frac{\partial N_e}{\partial t} + \frac{N_e}{\tau_{p,e}} = \left[\frac{\partial N_e}{\partial t} \right]_{CR} \quad (\text{III.38.b})$$

The integration constants are zero, since no particle sources have been placed inside the plasma volume. Apart from their signs, the *r. h. s.* are equal, hence

$$\left[\frac{\partial N_0}{\partial t} \right]_{CR} = - \left[\frac{\partial N_e}{\partial t} \right]_{CR} \quad (\text{III.38.c})$$

and Eq. (III.38.b) can be given the form

$$\frac{\partial N_e}{\partial t} = - \frac{\partial N_e}{\tau_{p,e}} - \oint \vec{\Gamma}_0 \cdot d\vec{S} - \frac{\partial N_0}{\partial t} \quad (\text{III.39})$$

The total neutral particle flux

$$-\phi_0 = \oint \vec{\Gamma}_0 \cdot d\vec{S} = \oint (\vec{\Gamma}_{0,R} + \vec{\Gamma}_{0,G}) \cdot d\vec{S} \quad (\text{III.40})$$

which crosses the plasma surface S and flows into the plasma can be thought to be composed of two parts :

1. Recycling

The part R of the electron-ion pairs leaving the plasma returns as neutral atoms to the plasma. The total flux of this part is

$$\oint \vec{\Gamma}_{0,R} \cdot d\vec{S} = -R \oint \vec{\Gamma}_e \cdot d\vec{S} = -R \frac{N_e}{\tau_{p,e}} \quad (\text{III.41})$$

R is the recycling coefficient.

2. Gas Puffing

By artificially increasing the pressure outside the plasma by additional gas puffing it is possible to increase the neutral particle flux into the plasma. This gas puffing flux is $-\phi_{0,G} = \oint \vec{\Gamma}_{0,G} \cdot d\vec{S}$. The total flux of neutral particles is thus given by

$$-\phi_0 = -R \frac{N_e}{\tau_{p,e}} - \phi_{0,G} \quad (\text{III.42})$$

The minus sign indicates inward direction of the flux. We replace $-\phi_0$ in Eq. (III.40) by the *r.h.s.* of Eq. (III.42), introduce that expression into Eq. (III.39) and obtain, after dividing by N_e ,

$$\frac{1}{N_e} \frac{\partial N_e}{\partial t} = - \frac{1-R}{\tau_{p,e}} + \frac{1}{N_e} \phi_{0,G} - \frac{1}{N_e} \frac{\partial N_0}{\partial t} \quad (\text{III.43})$$

This equation determines the temporal behaviour of the total number of plasma electrons.

For a tokamak discharge, $N_0 \ll N_e$ holds in the core plasma. The last term can in that particular case be neglected. We will assume that $R < 1$. After switch-off of the gas puffing, $\phi_{0,G}=0$, and N_e decays according to

$$N_e(t) = N_e(0) e^{-t(1-R)/\bar{\tau}_{p,e}} \quad (\text{III.44})$$

We define an effective electron density decay time $\bar{\tau}_p^*$ by

$$\bar{\tau}_p^* = \frac{\bar{\tau}_{p,e}}{1-R} \quad (\text{III.45})$$

and obtain

$$N_e(t) = N_e(0) e^{-t/\bar{\tau}_p^*} \quad (\text{III.46})$$

By measuring separately $\bar{\tau}_{p,e}$ and $\bar{\tau}_p^*$ it is possible to determine the recycling coefficient R .

Only for $R=0$ is the mean particle confinement time $\bar{\tau}_{p,e}$ equal to the decay time $\bar{\tau}_p^*$.

This offers another possibility of determining $\bar{\tau}_{p,e}$: by wall gettering it is possible to fix the particles on the walls and to obtain a recycling R very close to zero, hence $\bar{\tau}_p^* \approx \bar{\tau}_{p,e}$ in this particular case.

III.6 Determination of Particle Fluxes and Velocities

The density of the particle flux of species " s " = $\{z, k, i\}$ can be determined when one is able to solve the Eq. (II. 9). We consider the ground state particle ($i=1$) of ions in the charge state " z ". With the subscript " k " dropped the rate equation writes

$$\frac{\partial n_1^z}{\partial t} + \vec{\nabla} \cdot \vec{\Gamma}_1^z = \left[\frac{\partial n_1^z}{\partial t} \right]_{CR} \quad (\text{III.47})$$

with the density of the diffusion flux given by

$$\vec{\Gamma}_1^z = n_1^z (\vec{v}_0 + \langle \vec{V}_1^z \rangle) \quad (\text{III.48})$$

The collisional-radiative term writes

$$\left[\frac{\partial n_1^z}{\partial t} \right]_{CR} = -n_e [S_1^z + \alpha_1^z] n_1^z + n_e S_1^{z-1} n_1^{z-1} + n_e \alpha_1^{z+1} n_1^{z+1} \quad (\text{III.49})$$

$$-n_1^z \sum_i C_i^{z \rightarrow z-1} n_{H,i}^0 + n_1^{z+1} \sum_i C_i^{z+1 \rightarrow z} n_{H,i}^0$$

The $S_1^z, \alpha_1^z \dots$ are, respectively, the ionization and recombination coefficients (including the effect of dielectronic recombination) and the C_i 's are the rate coefficients for charge exchange between neutral hydrogen atoms $H^0(i)$ in quantum state i and the ion species in the ground state $i=1$. It is assumed that all captured electrons end in the ground level of the recombined ion. When the cross sections and the temperature are known, the rate

coefficients can be calculated.

For a cylindrically symmetric plasma follows

$$\Gamma_1^z(r) = \frac{1}{r} \int_{r'=0}^{r'=r} r' \left\{ \left[\frac{\partial n_1^z(r, t)}{\partial t} \right]_{CR} - \left(\frac{\partial n_1^z}{\partial t} \right)_{t_0} \right\} dr' \quad (\text{III.50})$$

where $(\partial n_1^z / \partial t)_{t_0}$ is to be taken at time t_0 for which Γ_1^z shall be determined. Provided, all cross sections and the radial distributions of n_e , T_e , n_1^{z-1} , n_1^z and n_1^{z+1} are known the integral can be evaluated and $\Gamma_1^z(r)$ be determined. A direct experimental determination of the diffusion flux of an impurity species in a limited radial region is therefore principally possible. In practice, however, this way is not gone, since the data are not sufficiently precise to permit a reliable evaluation. It is in particular necessary to measure precisely n_1^{z-1} , n_1^z and n_1^{z+1} on an absolute scale over the region of interest, which poses still considerable instrumental problems and difficulties.

At present, diffusion fluxes are determined "more globally" in the following manner which is based on the empirical expression

$$\Gamma_1^z(r) = - \left[f(r) v_0^* + D_{\perp} \frac{1}{n_1^z} \frac{\partial n_1^z}{\partial r} \right] n_1^z \quad (\text{III.51})$$

for the radial component of a "cylindrical" tokamak plasma. Eq. (III.51) was empirically found to fit the impurity transport in the ASDEX tokamak [12] and was subsequently confirmed by other laboratories as a way to describe the experimental findings. The reasons for this particular choice of Γ_1^z may for instance be found in Refs. [13–15]. The general structure of Eq. (III.51) is in agreement with the structure of Eq. (III.48), with the radial component of v_0 and $\langle V_1^z \rangle$ approximated by

$$v_{0,r} = -f(r) v_0^* \quad (\text{a}) ; \quad \langle V_1^z \rangle_r = -D_{\perp} \frac{1}{n_1^z} \frac{\partial n_1^z}{\partial r} \quad (\text{b}) \quad (\text{III.52})$$

Why, for instance, only the gradient due to self-diffusion determines $\langle V_1^z \rangle_r$ is not clear.

The ASDEX-team has found $f(r) v_0^* = D_{\perp} 2r / a^2$ to be a convenient choice (with only D_{\perp} to be determined experimentally). Other groups put $f(r) = r/a$ and chose independently the value for v_0^* and D_{\perp} .

All tokamak impurity transport studies yield approximately the same values for D_{\perp} and v_0^* in the case of ohmic heating:

$$D_{\perp} \approx 0.4 - 1 \left[\frac{m^2}{s} \right] ; \quad v_0^* \approx 4 - 50 \left[\frac{m}{s} \right]$$

We will consider the effect of diffusion on the radial particle distributions. The Figure

8 shows typical radial distributions of n_e and T_e as they are measured in medium-sized tokamaks. The Figure 9 shows the radial density distributions $n_{Fe_1}^z$ of Fe^{z+} ions obtained from a 1-D transport code. In Figure 9.a, no diffusion has been assumed ($D_{\perp}=0$), the ion distribution is determined by the local values of n_e and T_e by assuming coronal ionization—recombination equilibrium to be valid. In Figure 9.b, diffusion with $D_{\perp}=1\text{ m}^2/\text{s}$ has been assumed. Diffusion spreads the particles over wider radial regions, because $\partial n_1^z/\partial r$ has a positive and a negative sign : the particles diffuse inward and outward. The inward diffusion leads to a retardation in ionization, the outward diffusion to a retardation of recombination, compared to Figure 9.a.

Superimposing a convective inward velocity leads to a peaking of the radial distributions of intrinsic and completely recycling impurities, that means that one obtains a situation lying between the Figures 9.a and 9.b.

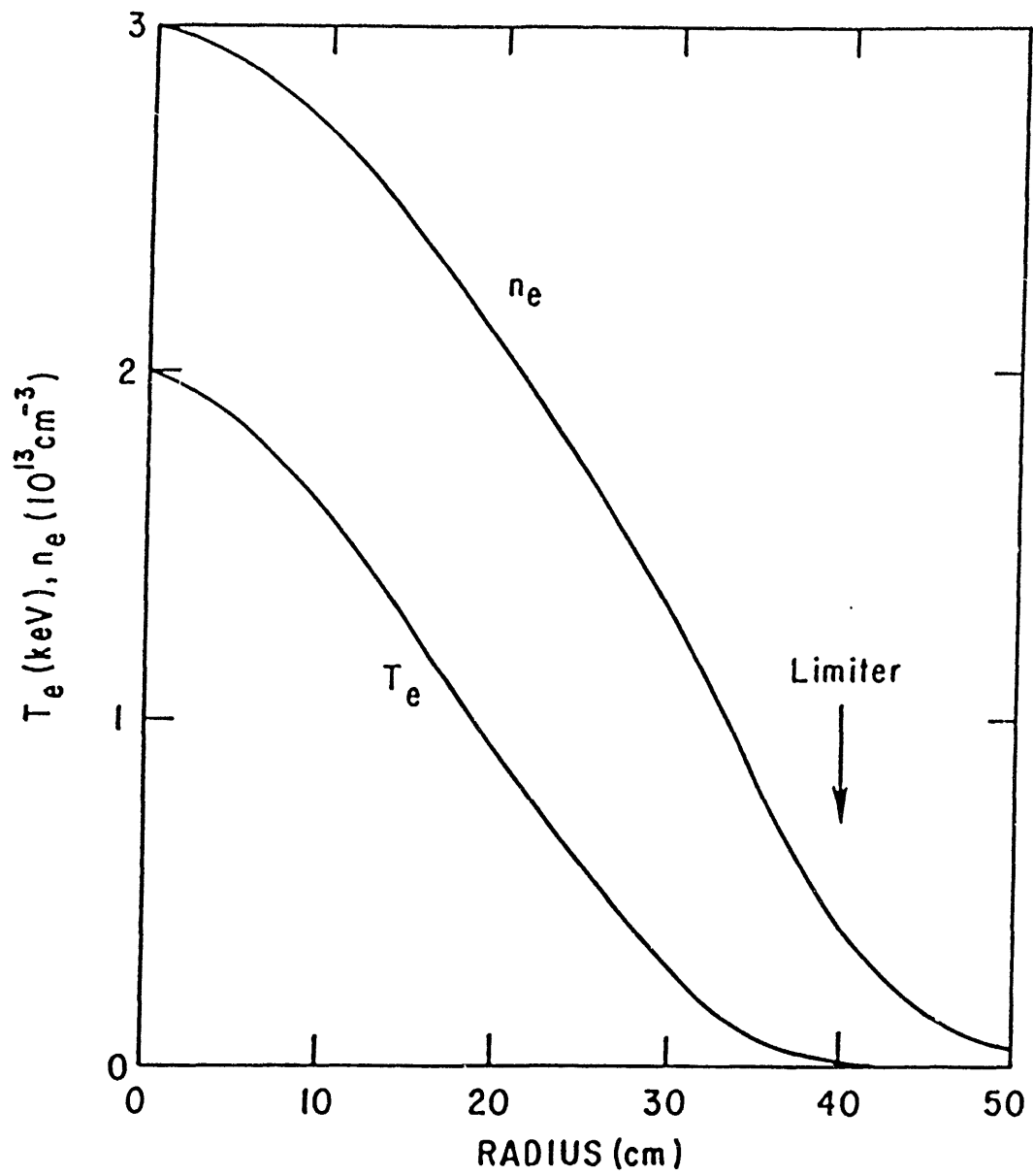


Figure 8. Typical radial distributions of electron temperature T_e and electron density n_e , from Ref. [16]

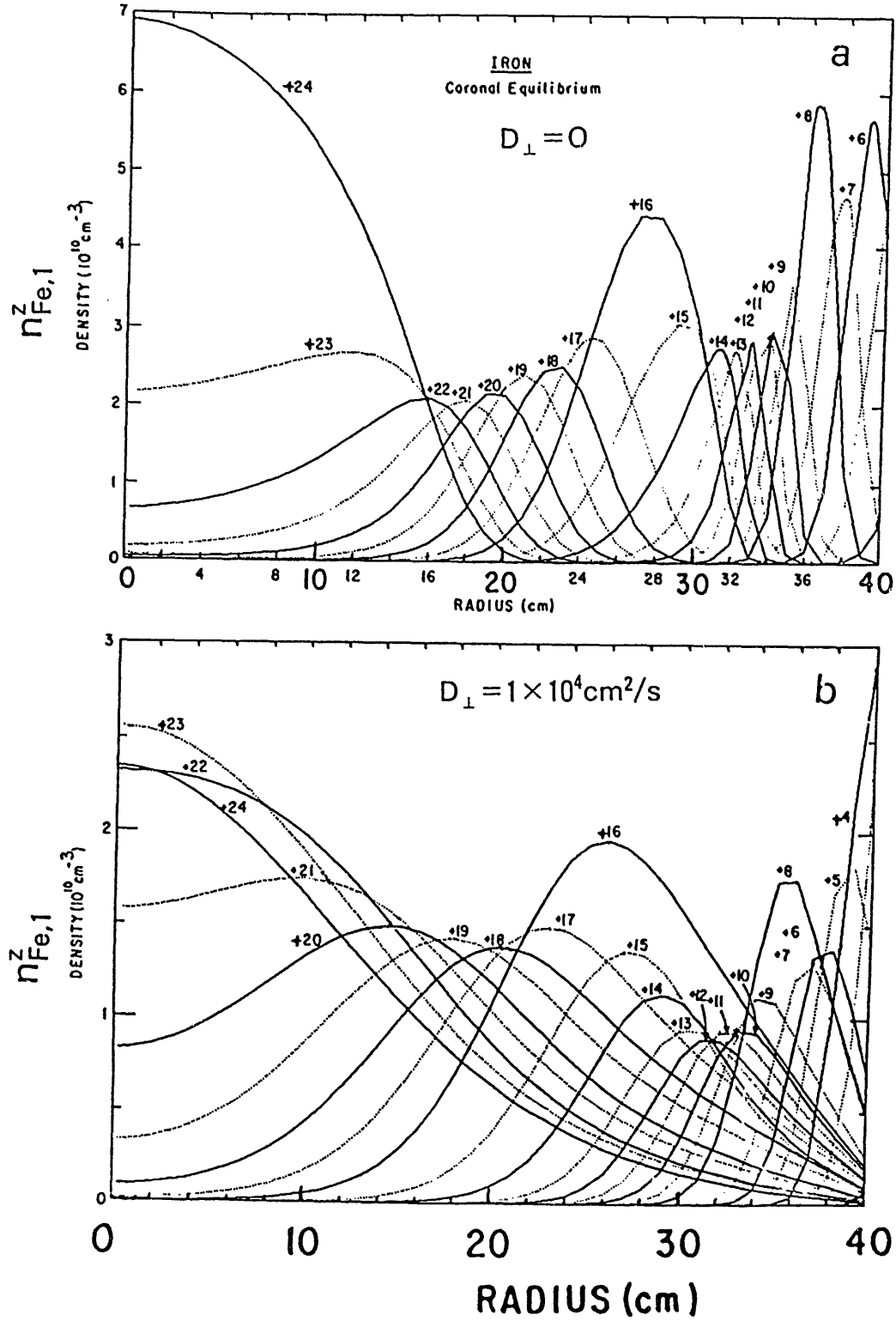


Figure 9. Radial distributions of n_1^z for the T_e, n_e –distributions of Fig. 8, with the total iron density $\sum n_{Fe,1}^z = 1 \times 10^{11} \text{ cm}^{-3}$.

a : coronal equilibrium ($D_{\perp} = 0$);

b : ions submitted to diffusion with $D_{\perp} = 1 \text{ m}^2/\text{s}$.

After Ref. [16]

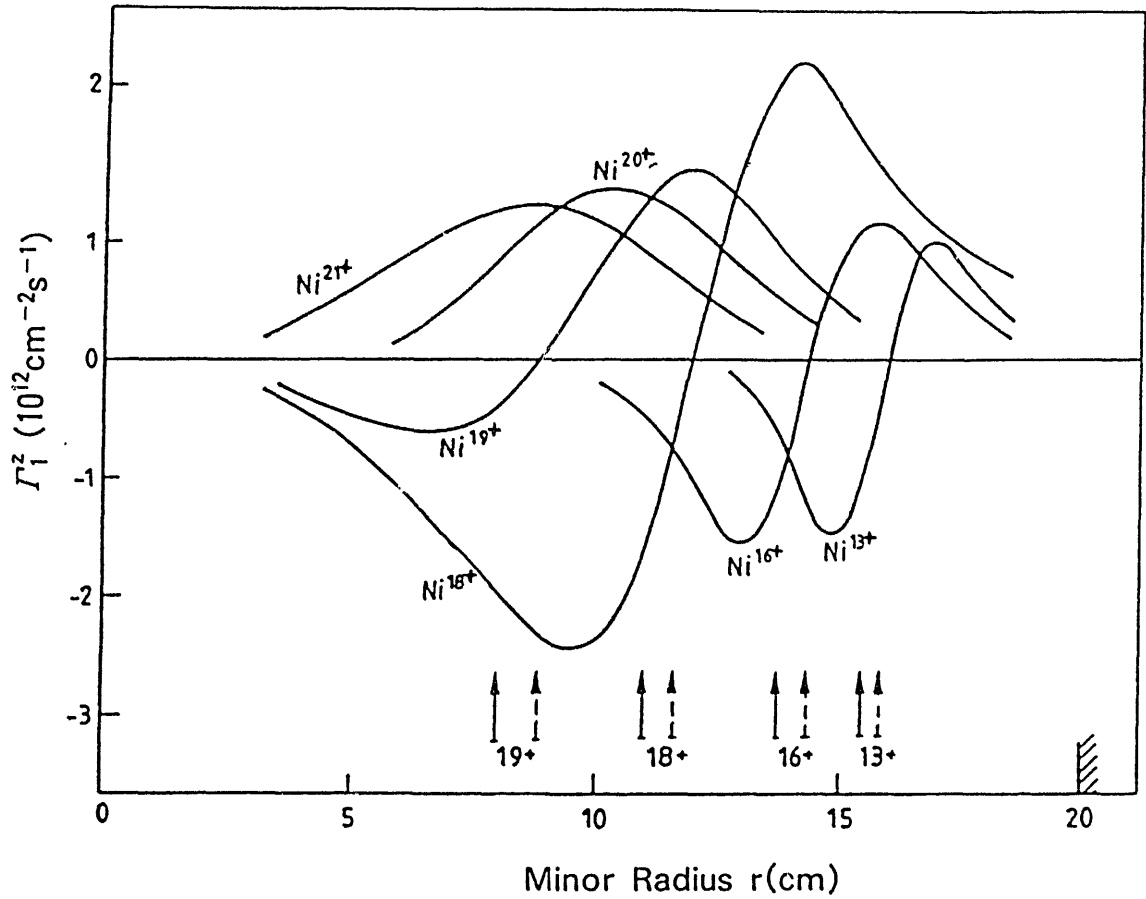


Figure 10. Radial distributions of the particle flux densities Γ_1^z of intrinsic nickel ions in a TFR discharge obtained from a 1-D transport code, with $D_{\perp} = 0.4 \text{ m}^2/\text{s}$ and $v_0^* = 4 \text{ m/s}$.

Full arrows indicate the measured maximum ion density radial position, broken arrows indicate this maximum when coronal ionization–recombination is assumed. After Ref. [17]

The experimental determination of D_{\perp} and v_0^* is performed in the following manner for intrinsic impurities. One constructs the radial profile of $n_1^z(r)$ from Abel-inverted chord-measurements of spectral line intensities pertaining to different charge stages “ z ” (only a limited number of charge stages “ z ” is considered in the case of medium–and high- Z elements). One then compares – for measured n_e, T_e distributions – the experimentally determined n_1^z -distributions with those delivered by a transport code. By modifying D_{\perp} and v_0^* in the code one finds a best fit to the experimental data. The method is somewhat ambiguous, since D_{\perp} and v_0^* cannot be determined independently. However, there is some reliability in processing in this way. The diffusion coefficient D_{\perp} determines primarily the location and the width of the individual distributions $n_1^z(r)$. The convective term influences the peaking, and in particular the relative concentrations of two widely separated ion

species. It is thus possible to obtain within certain limits reliable values for D_{\perp} and v_0^* .

For non-intrinsic impurities, for instance introduced by "laser-blow-off", the values of v_0^* and D_{\perp} can be determined from the spatio-temporal evolution of the ion species. For further details the reader is referred to Refs. [14, 15, 18] in which the methods have been reviewed.

Figure 10 shows the radial distributions of $\Gamma_1^z(r)$ for intrinsic nickel ions in TFR plasmas calculated with a 1D-transport code with $D_{\perp} = 0.4 m^2/s$ and $v_0^* = 4 m/s$, for measured n_e, T_e -profiles similar to those shown in Fig. 8. Ions whose density $n_1^z(r)$ increases continuously towards the center of the discharge show a flux vector which only points outward radially ($\Gamma_1^z > 0$), whereas those ions which have a maximum somewhere between the limiter and the center show inward and outward fluxes ($\Gamma_1^z < 0$ and $\Gamma_1^z > 0$).

In the stationary state, the Eq. (III. 51) can be solved for the total impurity density.

Once $\Gamma_1^z(r)$ is known, the radial flux velocity $\langle w_1^z(r) \rangle$ can be calculated :

$$\langle w_1^z(r) \rangle_r = v_{0,r} + \langle V_1^z \rangle_r = \frac{\Gamma_1^z(r)}{n_1^z(r)} \quad (\text{III. 53})$$

We would like to emphasize that the expression (III. 51) has no theoretical foundation. Neither the proton-electron density gradient nor the temperature gradient intervene as driving forces for the diffusion flux. Also the presence of other ion species seems to have no effect on $\Gamma_1^z(r)$. This is not satisfactory from a physical point of view. Therefore a determination of Γ_1^z from Eq. (III. 47) should not be discarded without having really tested the potentiality of this method.

Diffusion fluxes of the main plasma species, protons (deuterons) and electrons are also determined from Eq. (III. 51) by using measured radial n_e -distributions. For v_0^* and D_{\perp} , quite similar values as for the heavier impurity species are found.

III.7 Determination of Convection Velocity

The rate equation for the particle densities n_1^z yields only the entire flux density $\vec{\Gamma}_1^z$ relative to the laboratory system. It is composed of two parts, the flux density due to convection, and the flux density originating from diffusion relative to the mass velocity $\vec{v}_0(r)$ of the plasma as a whole. To separate the two effects one needs a second equation.

In Chapter II an equation for $\vec{v}_0 \cdot \vec{\nabla} p$ was found which should permit a determination of \vec{v}_0 , at least in principle. We will assume a cylindrical plasma column. The Eq. (II. 57) yields for the radial component of the mass velocity \vec{v}_0 the expression

$$v_{0,r} = \frac{1}{\rho} \left\{ \frac{3}{2} \frac{\partial p}{\partial r} + \vec{\nabla} \cdot \left(\sum_s \frac{5}{2} k T_s \vec{\Gamma}_s \right) - \dot{\Omega} - \frac{3}{2} k \sum_s \left(n_s \left[\frac{\partial T_s}{\partial t} \right]_{CR} + T_s \left[\frac{\partial n_s}{\partial t} \right]_{CR} \right) \right\} \quad (\text{III. 54})$$

Again we are faced with atomic physical problems :

1. The expression for $[\partial T_s / \partial t]_{CR}$ contains the local production rates $[\partial n_e / \partial t]_{CR}$ and $[\partial \bar{E}^{int} / \partial t]_{CR}$, see Eq. (II. 88). The determination of these quantities requires the knowledge of at least the ground state density $n_{k,1}^z$ of all chemical species "k" which contribute to $[\partial n_e / \partial t]_{CR}$ and $[\partial \bar{E}^{int} / \partial t]_{CR}$ in the radial region for which Eq. (III. 54) is to be evaluated.
2. The sum of all flux densities in radial direction, $\Sigma \Gamma_{k,1}^z(r)$, must be known. The determination of this quantity relies in principle also on the knowledge of atomic data, see Chapter III. 6.
3. Finally we must know the local power density $\dot{\Omega}$ for ohmic heating which depends on the mean effective ion charge state $\bar{Z}_{eff}(r)$ at radial position r . $\bar{Z}_{eff}(r)$ is a function of the $n_{k,1}^z(r)$.

A precise knowledge of the relevant densities $n_{k,1}^z(r)$, to be determined spectroscopically, and of the radial n_e, T_e -distributions should at least in principle allow the determination of $v_{0,r}$.

A particularly favourable situation arises for the stationary state. Then $\partial p / \partial t = 0$ holds. We apply the Eqs. (II. 87, 88) and the Eq. (III. 54) becomes

$$v_{0,r} = \frac{1}{\partial p / \partial r} \left\{ \vec{\nabla} \cdot \left(\sum_s \frac{5}{2} k T_s \vec{\Gamma}_s \right) + \dot{\Omega} + \dot{R} - \left[\frac{\partial \bar{E}^{int}}{\partial t} \right]_{CR} \right\} \quad (\text{III. 55})$$

The total ohmic power can be measured precisely, see Eq. (III. 37). Using measured radial n_e, T_e -distributions it is thus possible to determine an average value of Z_{eff} from

$$\bar{Z}_{eff} = \frac{J_p U}{L \int_0^a \dot{\Omega}_1 2\pi r dr} \quad (\text{III. 56})$$

where $\dot{\Omega}_1$ is the calculated power density with $Z_{eff}=1$. Assuming \bar{Z}_{eff} to be the same throughout the plasma, $\dot{\Omega}(r)$ in Eq. (III. 55) is known for any position r . The value of \bar{Z}_{eff} thus determined can also be used for the calculation of the bremsstrahlung losses in the expression for \dot{R} . Thus, the crucial point is the determination of $[\partial n_e / \partial t]_{CR}$ and $[\partial \bar{E}^{int} / \partial t]_{CR}$ appearing in Eq. (II. 55).

The calculation of $[\partial n_e / \partial t]_{CR}$ could be by-passed when one knows the local particle confinement $\tau_{p,e}$ for the stationary state from independent measurements, since according to Eq. (III. 11.b) :

$$\tau_{p,e}(r) = \frac{n_e(r)}{[\partial n_e / \partial t]_{CR}} \quad (\text{III. 57})$$

However, the determination of $\tau_{p,e}$ is based on this relation. It is thus not possible to avoid the atomic physics problems in the determination of $v_{0,r}$ from the Eqs. (III. 54, 55).

In Eq. (III. 55) the terms on the r. h. s. have different values at different radii. It would therefore be interesting to seek for situations in which a reversal of the sign of $v_{0,r}$ takes place. It should be mentioned that Eqs. (III. 54, 55) contain the pinch effect, since the r.h.s. depend on the "pinch force."

III. 8 Radiation Losses

The power densities lost by radiation are given by the Eqs. (II. 77–81). Synchrotron radiation can in almost all cases be neglected and it will probably play only a minor role in $D-T$ fusion reactors. For a $D-D$ reactor however, which will work at much higher temperature than a $D-T$ reactor, energy losses due to synchrotron radiation may become a serious problem.

Radiation losses (neglecting synchrotron radiation) have been calculated by many authors. We give two examples. Figure 11 shows the calculated loss rates for the two radial iron ion distributions of Figures 9.a and 9.b. Diffusion increases the radiation loss in the central part of the plasma compared to the case without diffusion.

The Figure 12 shows the different contributions to the power loss per electron and per iron atom as a function of T_e under the assumption that the plasma is in the state of coronal ionization-recombination (i.e., no diffusion) and that the coronal excitation model is applicable. To obtain the radiation losses one has first to solve the coupled system of rate equations which gives the particle densities in the ground level, $n_{k,1}$. These densities are used to calculate the radiation losses. In the limit of coronal excitation, the expression for the power loss due to bound-bound radiation is particularly simple, since all collisionally excited electrons return to the ground level via spontaneous de-excitations. Details of the cascading back to the ground level need not be known.

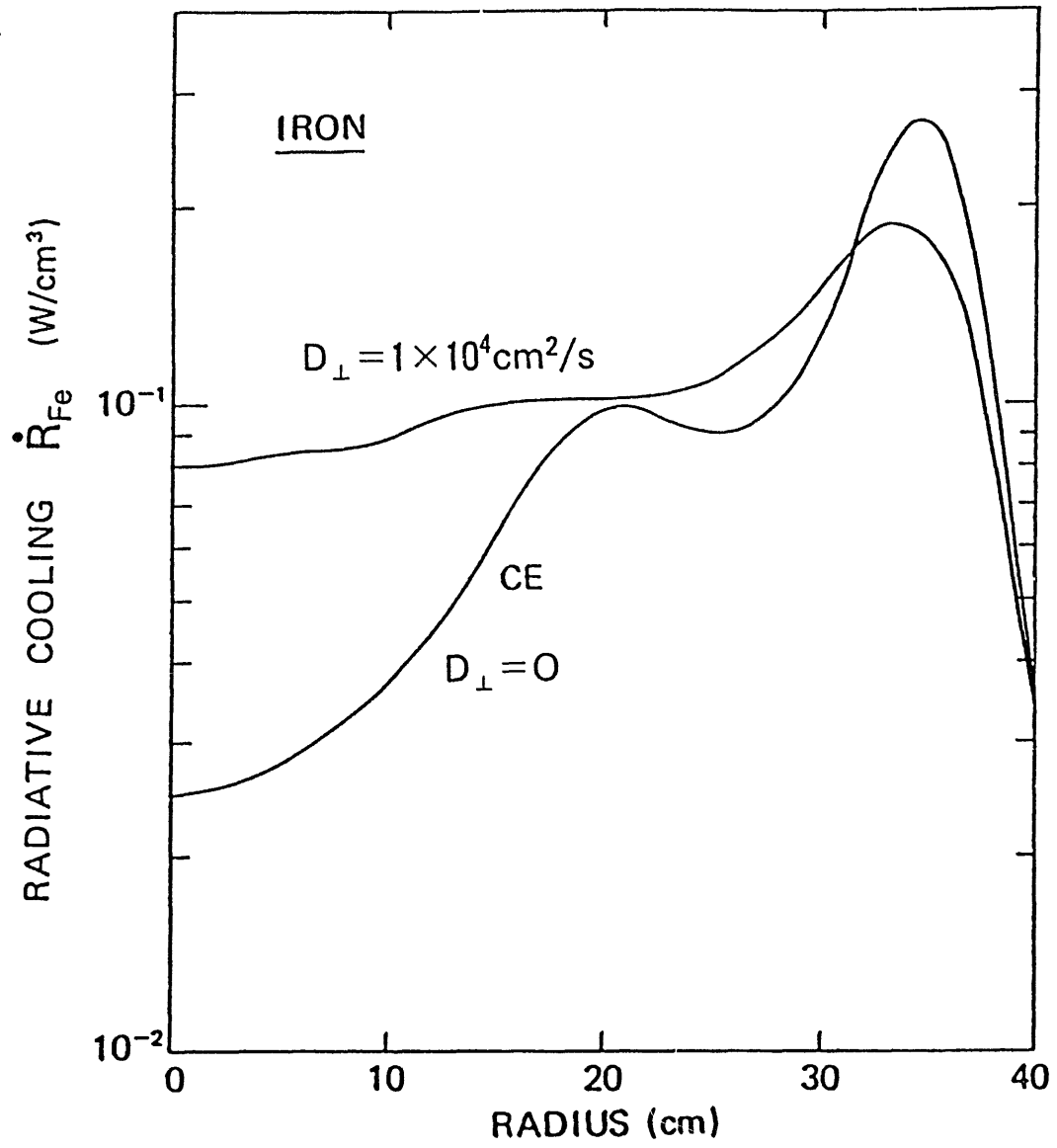


Figure 11. Power density \dot{R}_{Fe} lost by iron radiation for the radial iron ion distributions given in Figures 9.a and 9.b, after Ref. [16].

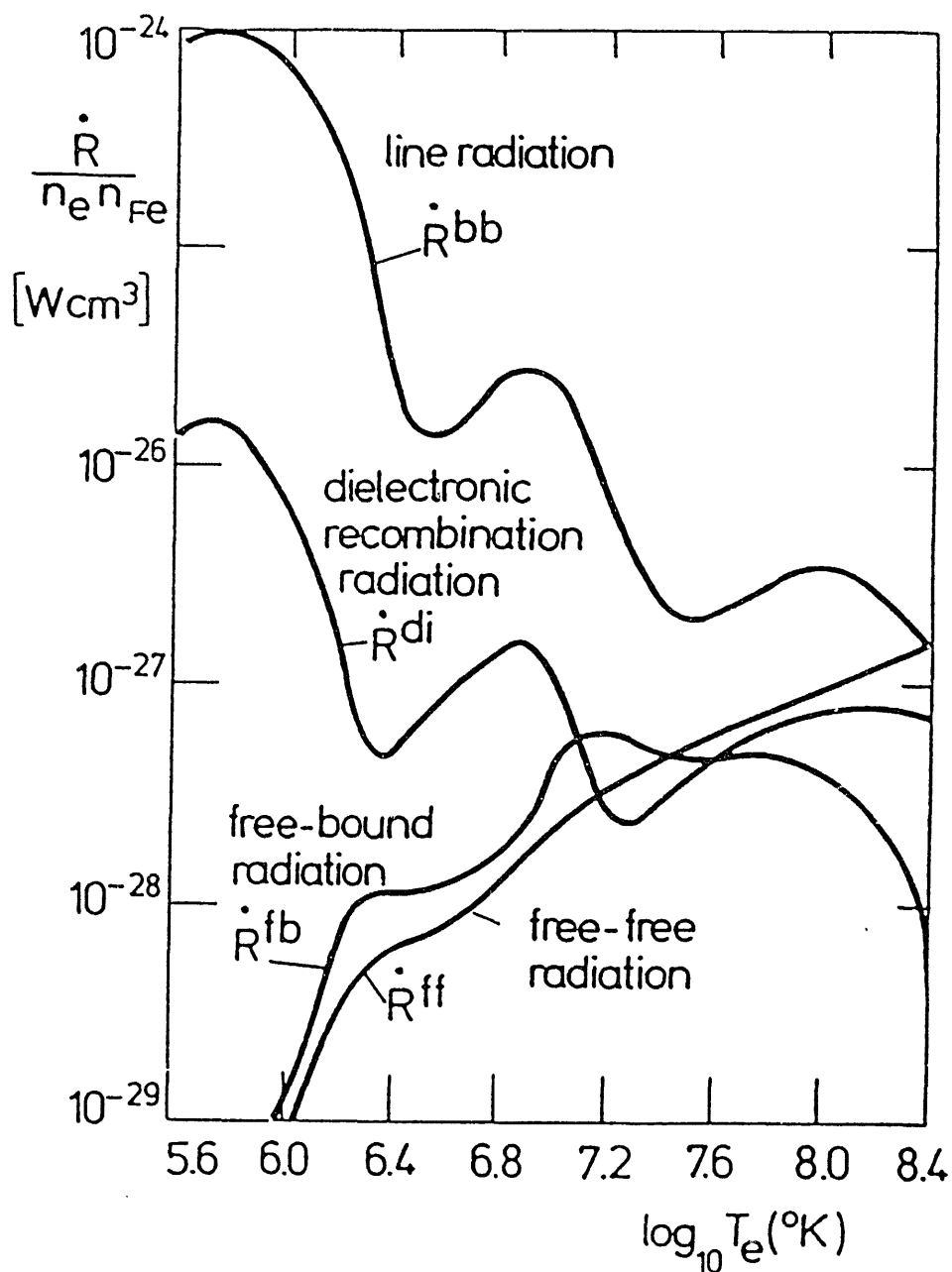


Figure 12. Power densities $\dot{R}/n_e n_{Fe}$ radiated per electron and per iron atom by a plasma in coronal ionization-recombination equilibrium at electron temperature T_e , after Ref. [19]

III. 9 Further Applications Using Atomic Species

There exist numerous other methods based on the application of atomic physics to obtain information about the plasma state. Only very few shall be mentioned, since the large variety of atomic processes would lead to a long list of application methods.

1. Application of charge exchange

The determination of the proton (ion) temperature is based on the measurement of the energy spectrum of charge exchange neutrals leaving the hot core plasma. Charge exchange can be due to intrinsic neutral hydrogen (deuterium) atoms or due to additionally injected neutrals. In this latter case one can determine local proton temperatures. When the neutral particle beam is chopped, an increased sensitivity is obtained.

Additional neutral beam-induced charge exchange with impurity species (leading to a localized excitation of impurity species) can be used to measure locally the particle density of the impurity species in different ion charge states "z". By observing the Doppler width and Doppler shift of the emitted "impurity lines" the ion temperature and the flux velocity $\langle w_1^z \rangle_{ls}$ in the direction of the line of sight (ls) can be obtained. The movement is essentially in toroidal direction ϕ . Hence, by measuring $\langle w_1^z \rangle_\phi$ in toroidal direction at different radii one obtains in addition to the toroidal rotation velocities information about $\langle w_1^z \rangle_\phi \partial \langle w_1^z \rangle_\phi / \partial r$ which determines the viscous-shear stresses in toroidal direction.

When only a limited number of impurity ion species are present, charge exchange can be applied to determine locally Z_{eff} .

Charge exchange has been applied to determine the neutral hydrogen density in the outer part of the Alcator-C tokamak [20].

2. Application of the ratio of spectral line intensities

The measurement of the ratio of spectral line intensities offers the possibility to determine either the electron temperature, or the electron density, or the proton density or temperature. The determination of one of these quantities depends on a suitable choice of couples of spectral lines. In general, a collisional-radiative model is necessary for the interpretation of the measurement and to extract the desired quantity.

Time-resolved electron temperatures have for instance been obtained from helium-like titanium spectra emitted by plasmas of the JIPP-TII U tokamak [21]. For this purpose, a collisional-radiative model was applied to compare the measured spectra with synthetic ones. The electron density has been determined by using the spectral lines of *Fe XXII* at $\lambda=114.41 \text{ \AA}$ and $\lambda=117.17 \text{ \AA}$, again by using a collisional-radiative model. The proton temperature has been determined by using the intensity ratios of a forbidden to an allowed line of *Fe XXII* [23] and *Fe XVIII* [24]. The Figure 13 shows the sensitivity of the line

intensity ratio with respect to the density as a function of temperature. To get reliable values for the proton temperature a good knowledge of $n_e (=n_+)$ is necessary.

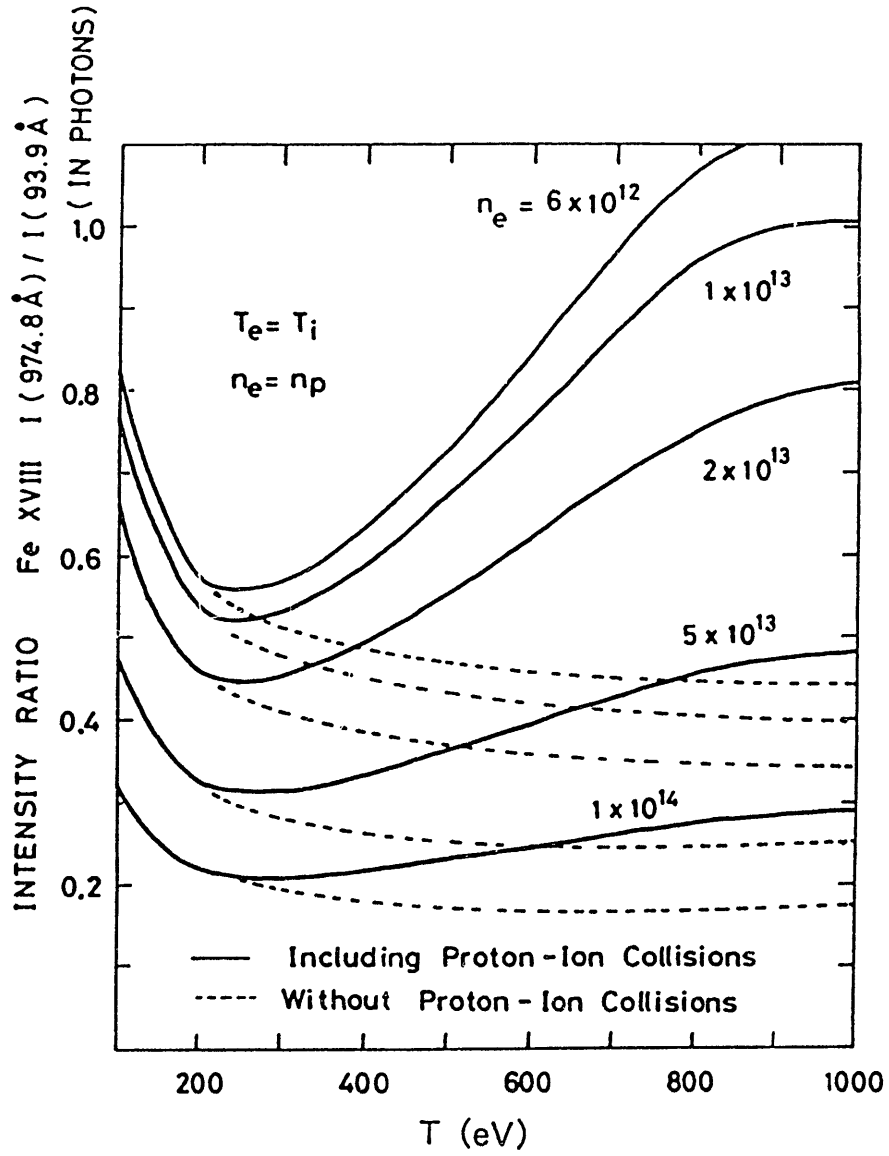


Figure 13. Intensity ratio of the forbidden ($\lambda=974.8 \text{ \AA}$) to the allowed line ($\lambda=93.4 \text{ \AA}$) of *Fe XVIII*, with and without proton-iron ion collisions. After Ref. [24]

CHAPTER IV

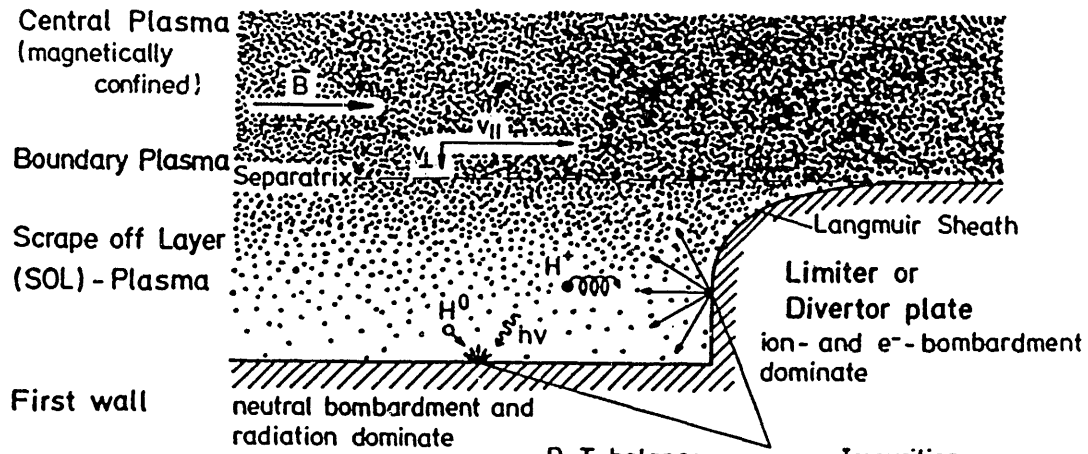
Applications To Edge And Divertor Plasmas

IV.1 Introduction

In this part, some atomic and in particular molecular physics problems shall be discussed. There exists a huge amount of articles about the Physics of Plasma-Wall Interactions. It is impossible to be exhaustive in this broad and extremely complicated field within the present context. The reader will get a good impression concerning the diversity and complexity of this field in consulting the book of Ref. [25]. The physics of atomic and molecular collisions in the plasma boundary has been reviewed and summarized in Ref. [26]. Edge plasma diagnostics based on optical methods which make use of atomic and molecular properties have extensively been described in Ref. [27]. Neutral particle transport and plasma models for impurity control experiments have, respectively, been treated in Refs. [28] and [29]. We will therefore be extremely short. Our main concern will be the treatment of molecular physics in the edge plasma region, and in particular in divertor plasmas. Molecular physics has not yet received the attention which it merits in this particular field. The temperatures of a few eV in a plasma of high density surrounded by a cold molecular gas lead to numerous molecular processes which influence this type of plasma.

IV.2 Definition of Boundary and Scrape-Off Layers and Divertor Plasmas

In Chapter III we defined the hot core plasma as that part of a toroidal plasma that lies inside the magnetic separatrix. Figure 14 shows a poloidal cut (a) and a top view (b) of a plasma in a toroidal machine. The scrape-off layer is that part of the plasma which lies outside the separatrix and which is magnetically not confined to a closed volume. The boundary of the (confined) plasma is thought to be represented by the outermost closed magnetic surface, that is the magnetic separatrix. The boundary layer is situated in the region of the separatrix. The scrape-off layer extends from the separatrix in radial direction to the walls and forms the edge plasma.



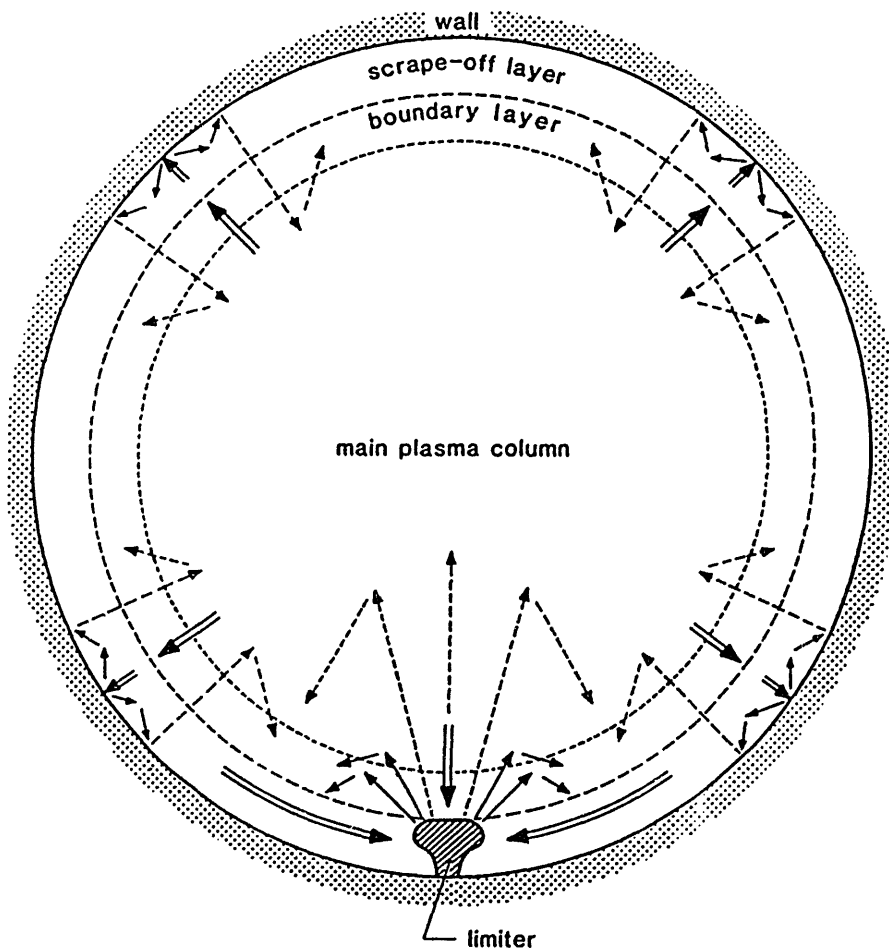
a.

D, T balance

reflection
trapping and diffusion
reemission

Impurities

sputtering
evaporation
erosion by arcs
deposition



b.

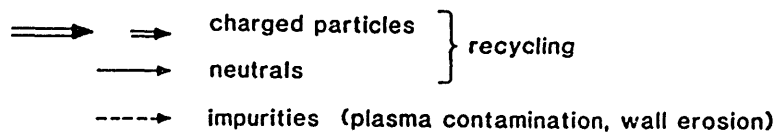


Figure 14. Definition of boundary and scrap-off layers in a toroidal plasma device, after Ref. [30] for Fig. 14.a and Ref. [31] for Fig. 14.b.

By a suitable tailoring of the magnetic field structure it is possible to guide a part of the scrape-off layer to neutralizer or target plates (Figure 15) situated inside (e. g. DOUBLET-III, PFX) or outside the main plasma chamber (DITE, ASDEX). The plasma in the scrape-off layer flows along the magnetic field lines onto the target plates where it is neutralized. A cold divertor plasma of temperature $T_e \approx 5$ to 20 eV is formed in front of the target plates. When the target plates are placed in a "closed" divertor chamber, neutral gas at relative high pressure surrounds the divertor plasma and a strong recycling in the region of the target plates takes place. It is this low-temperature high-density recycling divertor plasma which is capable of radiating off huge amounts of energy taken from the thermal energy content of the instreaming scrape-off plasma. The strongly recycling divertor plasma acts partly as an "energy transformer" which transforms thermal energy in radiation energy.

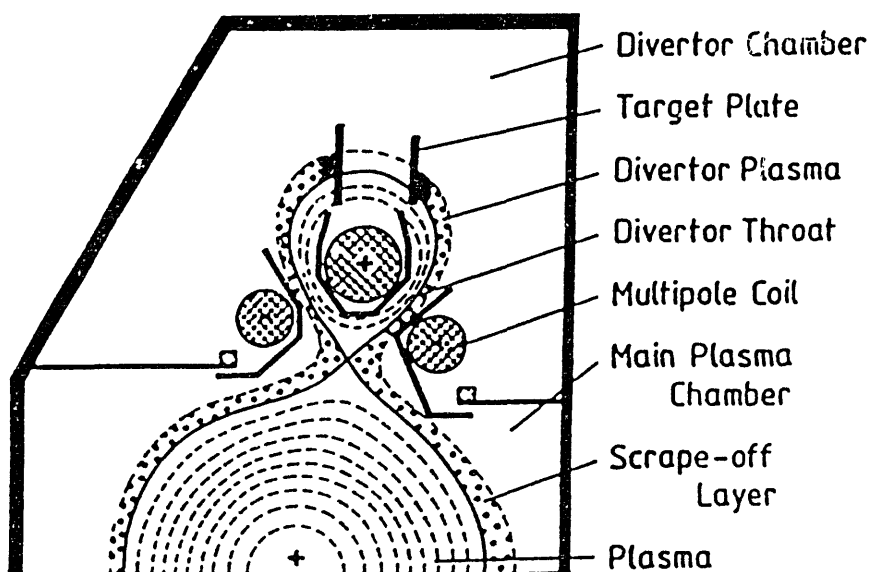


Figure 15. Magnetic divertor configuration of the ASDEX tokamak, after Ref. [32].

IV.3 Formation of the Scrape-off Layer

The edge plasma formation in the scrape-off layer in front of the wall of the main plasma chamber is due to diffusion, dissociation, ionization, recombination and charge transfer processes. It is not yet clear how molecular processes contribute to the edge plasma formation far away from carbon walls or carbon limiters. In order to simplify the physical situation we will consider a part of the scrape-off layer which is situated far away from any limiter or any target plate. We will assume that the plasma faces a metallic wall so that hydrocarbon molecules need not to be considered.

Figure 16 shows the physical processes. The two constituents of the main plasma, protons and electrons, cross the separatrix and enter the scrape-off layer. One part flows along the field lines and ends somewhere on a limiter or target plate (parallel component). The other part diffuses perpendicular to the magnetic field lines and hits the walls where the ion-electron pairs are neutralized (perpendicular component).

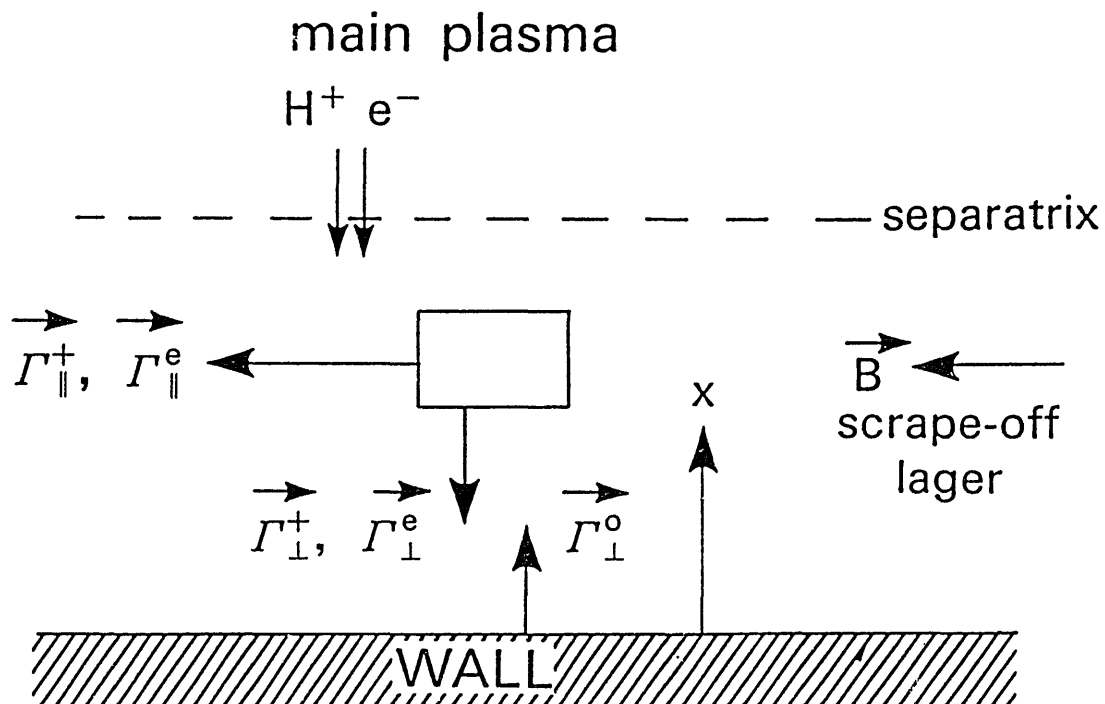


Figure 16. Diffusion fluxes in the scrape-off layer

On the wall, numerous processes occur:

- the incoming $H^+ - e^-$ pair can be reflected as a neutral atom H^0 .
- the incoming $H^+ - e^-$ pair can have the chance to encounter on the wall an adsorbed H^0 atom. The formation of an H_2^0 molecule is then possible according to the reaction $H^0 + H^0 + M \rightarrow H_2^0 + M$, where M carries off the reaction energy of 4.45 eV. M can be a wall atom or the metal grid as a whole.
- the incoming $H^+ - e^-$ pair is neutralized and adsorbed, migrates as H^0 on the wall until it finds another atom H^0 to form H_2^0 which leaves the wall as a molecule with the wall temperature.
- the incoming $H^+ - e^-$ pair is absorbed as a neutral atom, and reappears much later as a thermal molecule (retarded desorption).
- In the presence of oxygen, many $H_x - O_y$ reactions are possible.

For reasons of simplicity we will assume that the neutrals enter the edge plasma as atoms with some mean velocity $\langle w^0 \rangle_\perp$ and will keep this velocity until they are ionized and become bound to the magnetic field as $H^+ - e^-$ pairs. We will neglect charge exchange processes which do not change the ion-neutral composition, they only influence the velocity distributions of ions and neutrals. (This effect is treated by solving the Boltzmann collision equation (II.7). The ion-electron pairs have a parallel and perpendicular flux vector, $\vec{\Gamma}_\parallel^e$ and $\vec{\Gamma}_\perp^e$. Then the rate equations for the atoms and electrons write

$$\vec{\nabla} \cdot \vec{\Gamma}^0 = \langle w_1^0 \rangle_\perp \frac{\partial n_1^0}{\partial x} = \left[\frac{\partial n_1^0}{\partial t} \right]_{CR} = -n_e S_1^0 n_1^0 \quad (\text{IV.1.a})$$

$$\vec{\nabla} \cdot \vec{\Gamma}^0 = \vec{\nabla}_\parallel \cdot \vec{\Gamma}_\parallel^e + \vec{\nabla}_\perp \cdot \vec{\Gamma}_\perp^e = \left[\frac{\partial n_e}{\partial t} \right]_{CR} = +n_e S_1^0 n_1^0 \quad (\text{IV.1.b})$$

Electron-ion recombination has been neglected in the collisional-radiative terms. This approximation is permitted, since the formation of neutrals in the scrape-off layer is a rare event. Also excited neutral atoms have been omitted. (Their density can represent several per cent of the total neutral density). For the electron flux vectors we have

$$\Gamma_\parallel^e = n_e \langle w_e \rangle_\parallel \approx n_e \left[\frac{k(T_e + T_+)}{m_+} \right]^{1/2} \quad (\text{IV.2.a})$$

$$\Gamma_\perp^e = n_e \langle w_e \rangle_\perp \approx n_e \left(v_{0,\perp} + D_\perp \frac{1}{n_e} \frac{\partial n_e}{\partial x} \right) \quad (\text{IV.2.b})$$

where

$$C_s = \left[\frac{k(T_e + T_+)}{m_+} \right]^{1/2} \quad (\text{IV.2.c})$$

is the ion acoustic speed. On the *r. h. s.* of Eq. (IV.2.b) we made use of Eq. (III.51).

Eq. (IV.1.a) can formally be solved ; we obtain

$$n_1^0(x) = n_1^0(0) \exp \left\{ - \int_0^x \frac{S_1^0(x) n_e(x)}{\langle w_1^0 \rangle_{\perp}} dx \right\} \quad (\text{IV.3})$$

where $n_1^0(0)$ is the density at the wall. $n_e(x)$ is determined by Eqs. (IV.7) or (IV.8) which depend on $n_1^0(x)$. The two equations must simultaneously be solved to obtain $n_1^0(x)$ and $n_e(x)$.

One can define an attenuation length λ^0 for the neutrals, which is that length $x=\lambda^0$ for which $n_1^0(x)$ has decreased to $n_1^0(0)/e$:

$$\int_0^{x=\lambda^0} (S_1^0(x) n_e(x) / \langle w_1^0 \rangle_{\perp}) dx = 1 \quad (\text{IV.4})$$

We will define a mean value $\bar{\lambda}^0$ by assuming a mean electron density \bar{n}_e and a mean electron temperature \bar{T}_e in the edge plasma. From Eq. (IV.4) :

$$\bar{\lambda}^0 = \frac{\langle w_1^0 \rangle_{\perp}}{\bar{S}_1^0 \bar{n}_e} \quad (\text{IV.5})$$

where \bar{S}_1^0 is the ionization coefficient for \bar{T}_e and \bar{n}_e .

For neutral hydrogen atoms leaving the walls with a kinetic energy of 2.5 eV ($\langle w_1 \rangle_{\perp} = 2 \times 10^4$ m/s) and entering the edge plasma of mean temperature $\bar{T}_e = 7$ eV and mean electron density $\bar{n}_e = 1 \times 10^{13} \text{ cm}^{-3}$, the attenuation length is $\lambda^0 = 88$ cm. Thus, the neutral atoms diffuse deeply into the scrape-off layer and even into the main plasma.

To find the distribution of the electron density across the scrape-off layer we put

$$\vec{\nabla}_{\parallel} \cdot \vec{\Gamma}^e = \frac{n_e}{\tau_{\parallel}} \quad (\text{IV.6})$$

where τ_{\parallel} is a longitudinal confinement time.

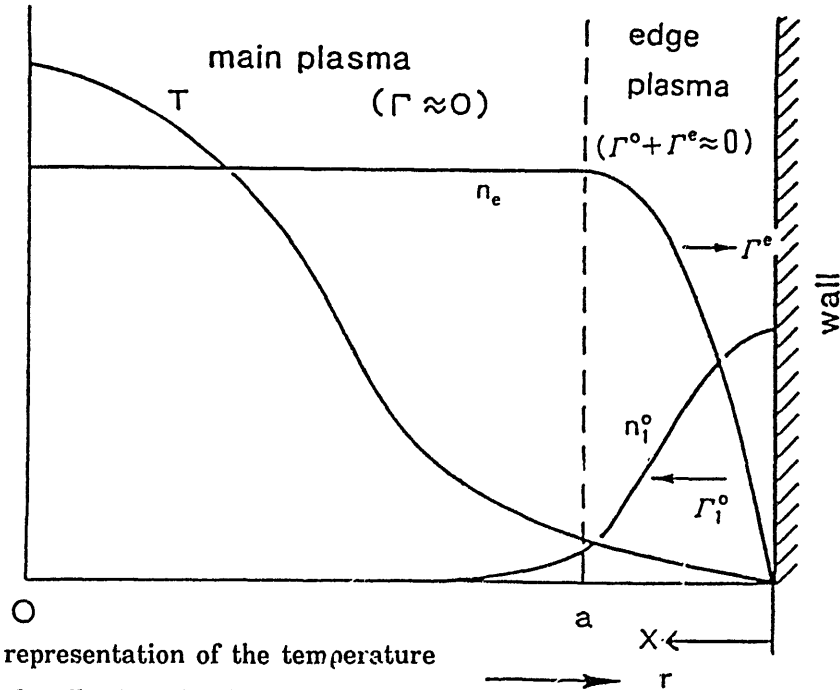


Figure 17. Qualitative representation of the temperature and density distributions in the edge plasma.

The Eq. (IV.1.b) then gives, with Γ_{\perp}^e substituted by the expression (IV.2.b):

$$\frac{\partial}{\partial x} \left\{ n_e v_{0\perp} + D_{\perp} \frac{\partial n_e}{\partial x} \right\} = n_e S_1^0 n_1^0 - \frac{n_e}{\tau_{\parallel}} \quad (\text{IV.7})$$

where $n_1^0(x)$ is determined by Eq. (IV.3). An analytic solution is only possible when further approximations are made. We assume that the perpendicular convective velocity $v_{0\perp}$ is negligible (which will close to the wall surely be a good hypothesis). We further assume that D_{\perp} is constant across the scrape-off layer. Then Eq. (IV.7) becomes

$$\frac{1}{n_e} \frac{\partial^2 n_e}{\partial x^2} = - \frac{1}{D_{\perp} \tau_{\parallel}} (1 - S_1^0 n_1^0 \tau_{\parallel}) \quad (\text{IV.8})$$

The term $S_1^0(x)n_1^0(x)$ first increases when one proceeds from the wall into the scrape-off layer (because of the temperature increase which increases S_1^0). Deep in the scrape-off layer, $S_1^0(x)n_1^0(x)$ decreases (because n_1^0 is decreasing whereas $S_1^0(x)$ changes only little at high temperatures). We will assume some mean value $\bar{S}_1^0 \bar{n}_1^0$. Then the Eq. (IV.8) yields the solution

$$n_e(x) = n_e(a) e^{-(a-x) \left[\frac{1 - \bar{S}_1^0 \bar{n}_1^0 \tau_{\parallel}}{D_{\perp} \tau_{\parallel}} \right]^{1/2}} \quad (\text{IV.9})$$

where $n_e(a)$ is the electron density at the separatrix situated at $x=a$. Figure 17 gives a qualitative representation of the density and temperature distributions. To obtain $T(x)$ one has to solve the energy equation.

In the scrape-off layer, the ion temperature is often found to be higher than the electron temperature, in particular when high concentrations of impurity species are present. This feature has its origin in the strong radiation and ionization of the impurity atoms and ions, which takes its energy from the thermal energy content of the electrons, see Eq.(II.88). Owing to the low temperatures the equipartitioning of the thermal energies of electrons and ions is slow, so that the ion temperature stays above the electron temperature. Also a high thermal conductivity can be the reason that the electron temperature is lower than the ion temperature.

IV.4 Recycling Coefficient

The proton-electron flux ($\Gamma_{\perp}^e = \Gamma_{\perp}^+$) onto the walls returns partly back to the plasma as a neutral particle flux (Γ_{\perp}^0). In Chapter III.5 we have defined a recycling coefficient R by

$$\oint \vec{\Gamma}_{0,R} \cdot d\vec{S} = -R \oint \vec{\Gamma}_e \cdot d\vec{S} = -R \frac{N_e}{\tau_{p,e}} \quad (\text{IV.10})$$

R is a quantity which averages out all poloidal and toroidal variations of the back streaming neutral particle fluxes. R is an average value for the whole inner wall. The

local value of R can be determined spectroscopically by measuring for instance the radial distribution of H_α or H_β in the edge plasma region close to the walls. R is also a function of time. It is even conceivable that R changes after some time from values $R < 1$ to $R > 1$ by a release of huge amounts of gas which has been accumulated during precedent discharges. Measurements of local R -values are important for a better understanding of plasma-wall interaction.

From the Eqs. (III. 38.a, 38.c, 40, 42) follows that R can be expressed by the total volume ionization rate $[\partial N_e / \partial t]_{CR}$ and the mean confinement time :

$$R \frac{N_e}{\tau_{p,e}} + \phi_{0,G} = \left[\frac{\partial N_e}{\partial t} \right]_{CR} + \frac{\partial N_0}{\partial t} \quad (IV.11)$$

N_e is the total number of electrons, N_0 the one of neutral atoms in the main plasma. This equation also shows that the inwardly directed neutral particle flux is the source for the ionization processes.

IV.5 Properties of Diverted Plasmas

Divertor experiments, without direct "plasma-limiter contact" – have shown [32, 33, 39] that the impurity concentration of metallic species, and also of carbon, is strongly reduced followed by a noticeable decrease of the radiation loss from the main plasma. The reduction of the impurity concentrations is mainly due to reduced "plasma-limiter interaction". In the case of a limiter discharge, the main plasma is in direct contact with the limiter surface; and also that part of the scrape-off layer which is very close to the separatrix intensely reacts with the limiter surface (see Figure 14) leading to metallic sputtering and limiter erosion. The metallic atoms (and/or carbon atoms) have a high probability to enter into the main plasma, because there is no or only a very thin scrape-off layer plasma between the location of the impurity source (limiter surface) and the main plasma [34].

In a diverted discharge – without "main plasma-limiter contact" – this source of impurity production does not exist. Only the much less violent "edge plasma-chamber wall interaction" takes place producing less impurity atoms.

Somewhere must the scrape-off layer come into contact with material walls. This contact takes place on the divertor target plates, many attenuation lengths $\bar{\lambda}^0$ (see Eq. IV.5) away from the main plasma. Owing to the relative low temperature in the scrape-off layer this "plasma-target interaction" is also less violent than the interaction with the limiter.

Measurements have further shown [32, 35–39] that there is a non-linear increase of the electron density in the divertor plasma with mean electron density \bar{n}_e of the main plasma. Also the neutral gas pressure (H_2 molecules) increases non-linearly with \bar{n}_e . For instance, far away from the divertor target plates a hydrogen molecule density of $n_{H_2}^0 \approx 3 \times 10^{13} \text{ cm}^{-3}$

was measured in the ASDEX divertor chamber for $\bar{n}_e \approx 6 \times 10^{13} \text{ cm}^{-3}$ in the main plasma [36]. The mean electron density in the divertor plasma was of same magnitude as \bar{n}_e .

The non-linear increase of the divertor densities with \bar{n}_e of the main plasma is accompanied by a non-linear increase of radiation from the divertor plasma.

Additional neutral beam heating (at relatively modest level) of diverted ASDEX discharges [38, 40] did not lead to a noticeable increase of the plasma temperature ($T_e \approx 10 \text{ eV}$) near the target plates.

All experiments with diverted discharges have shown that the temperature of the divertor plasma strongly decreases with increasing \bar{n}_e in the main plasma [32, 35, 38–40].

These features are indications that the divertor plasma is submitted to strong recycling within the divertor chamber [32, 38, 40–42].

IV.6 Molecules in Recycling Divertor Plasmas

The fact that the divertor plasma which is attached to the target plates is surrounded by a molecular gas at relative high pressure leads to high densities of the particle fluxes and intense recycling on the target plates. The conditions are such that molecules could play an important role in the divertor plasma, in particular at its periphery. In the outer shell of the divertor plasma, the plasma properties are very likely entirely determined by molecular properties.

Figure 18 shows the level system of atomic hydrogen with the most important transitions: electronic excitation followed by spontaneous de-excitation, and electronic ionization followed by radiative recombination are the main processes which transfer thermal energy to internal energy which is then lost in the form of radiation.

In Figure 19, some potential energy curves for the H_2 molecule, H_2^+ and H_2^{2+} molecular ions are shown, with the same energy scale as for the H -atom in Fig. 18. The many vibrational and rotational levels belonging to each electronic state are not shown. The H_2 molecule as a homo-nuclear linear top molecule has no permanent electric dipole moment. Therefore radiative transitions take only place when the molecule changes its electronic state (respecting the selection rules). However, for each electronic transition many rotation-vibration transitions take place (rotational and vibrational electronic bands). They represent additional radiation loss channels, thus leading to a decrease of plasma temperature.

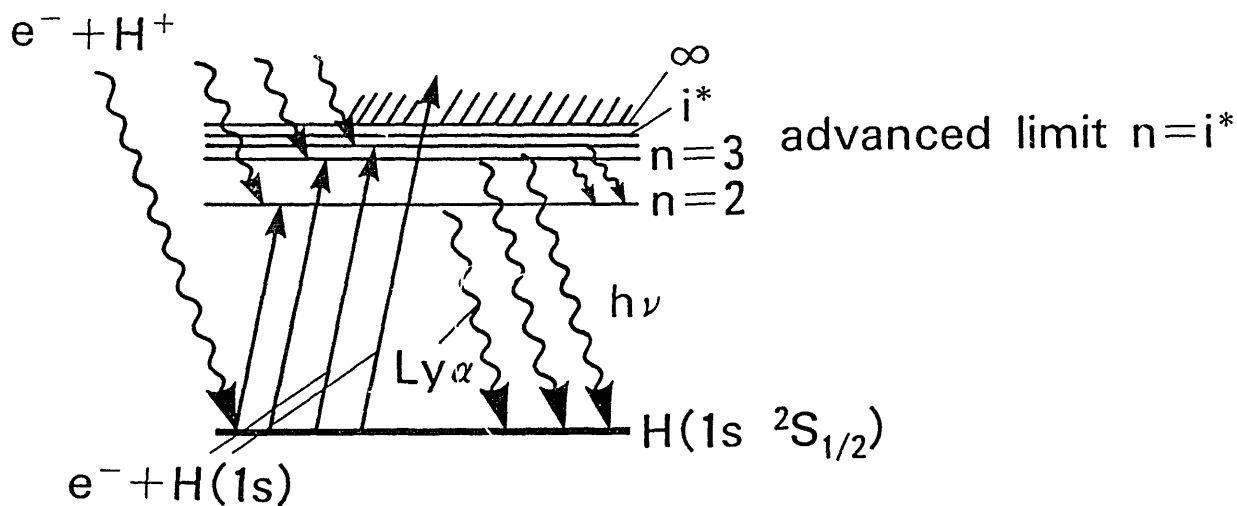


Figure 18. Level system of atomic hydrogen with some collision and radiation processes

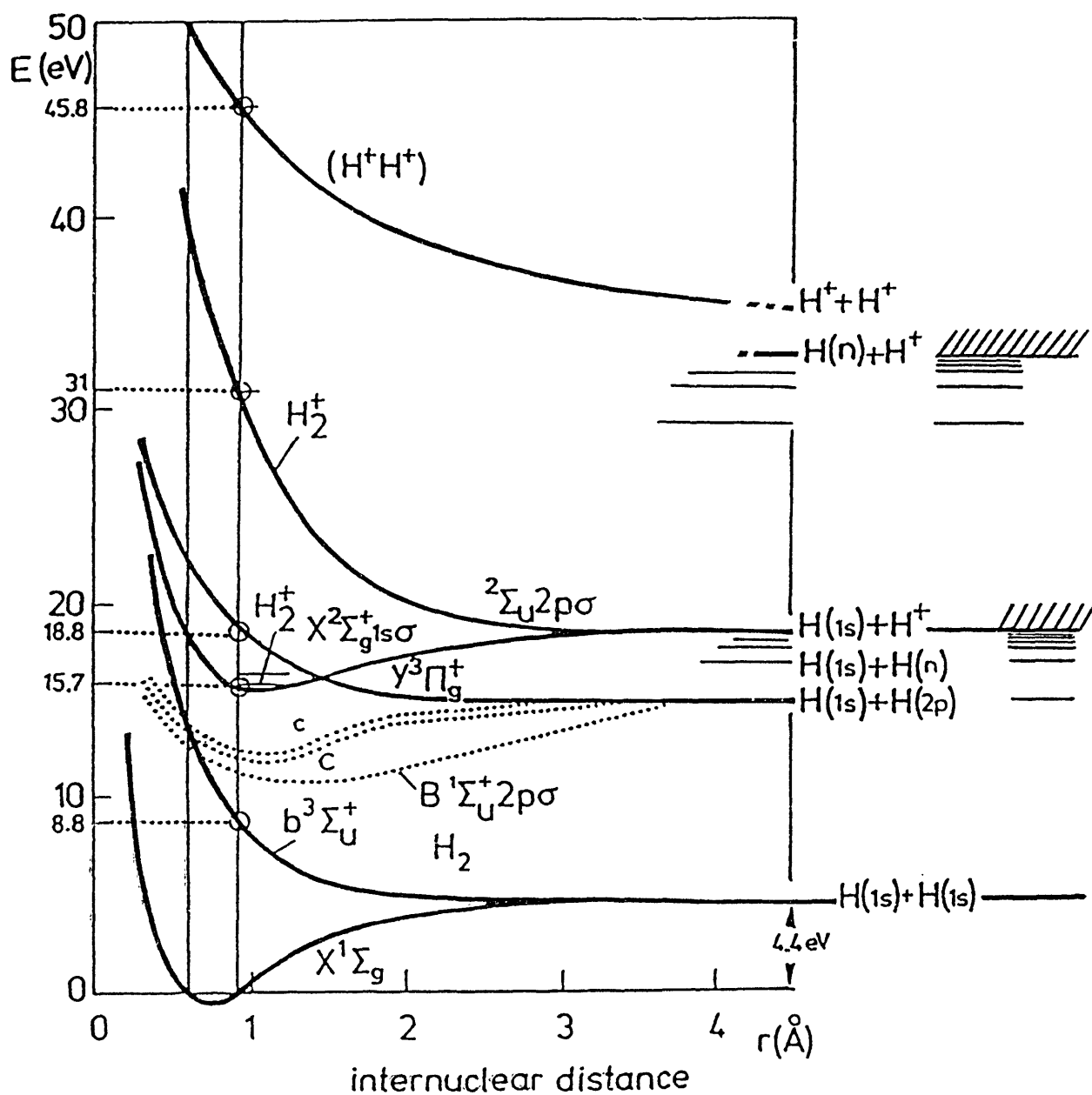


Figure 19. Potential energy curves for the H_2 , H_2^+ and H_2^{2+} molecules

The plasma electrons lose energy also in exciting the molecule to repulsive energy curves followed by dissociation. One part of this thermal electron energy is used for dissociation, the other part is used to form "Frank-Condon atoms". These atoms have kinetic energies which lie mainly in the range of $2.5-4 \text{ eV/atom}$: excitation to $9-12 \text{ eV}$, minus dissociation energy of 4.4 eV , divided by two, to give each atom the same energy.

At temperatures of 5 to 10 eV and particle densities of the order of 10^{13} to 10^{14} cm^{-3} , the transport of internal energy could eventually play a certain role in the energy transport (contribution from $\vec{\nabla} \cdot (E^{int} \vec{v}_0 + \vec{Q}^{int})$ in Eq. (II.61). The transport capability of internal energy depends on the energy which can be stocked in form of internal energy in the excited levels and as dissociation and ionization energy. The number of quantum states which are thermodynamically occupied in the state of (local) thermodynamic equilibrium (L.T.E.) is given by the (internal) partition function. Although the divertor plasma is far away from an L.T.E. state, the internal partition function can be an indication for heat removal capability. The internal partition functions of the H_2 -molecule and of the H -atom are shown in Figure 20 as a function of temperature. For the hydrogen atom, three different cut-off principal quantum numbers $n=i^*$ have been chosen. For $n_e = 5 \times 10^{13} \text{ cm}^{-3}$, $i^* \approx 18$. It can be seen that the H_2 molecule has a far larger internal partition function than the H -atom. Whether molecules play actually a role or not depends on the density ratio $n_{H_2}^0/n_H^0$.

It is difficult to avoid oxygen in tokamak plasmas. Oxygen, and eventually nitrogen, could in divertor plasmas be the "stars" for energy removal. The potential energy curves for O_2^0 , O_2^+ and O_2^- are shown in Figures 21 and 22. The particular electronic structure of the O^0 -atom yields a greater diversity of the electronic states of the O_2^0 -molecule. The H_2^+ -molecule is only stable in the electronic ground state. No stable electronically excited states of H_2 have been found. The situation is different for O_2^+ which forms many stable energy potential curves with a deep minimum leading to a large number of vibrational and rotational states and which are potential radiators.

The O_2^0 and O_2^+ molecules have also excellent capabilities for conducting huge amounts of internal energy. The same is valid for N_2^0 and N_2^+ . Figure 23 shows their internal partition functions.

The formation of oxygen and nitrogen ions of higher plasma temperatures still ensures removal of energy by radiation (and probably to a much lesser extent by conduction of internal energy) under conditions for which hydrogen does not further contribute to the energy removal because it is completely ionized.

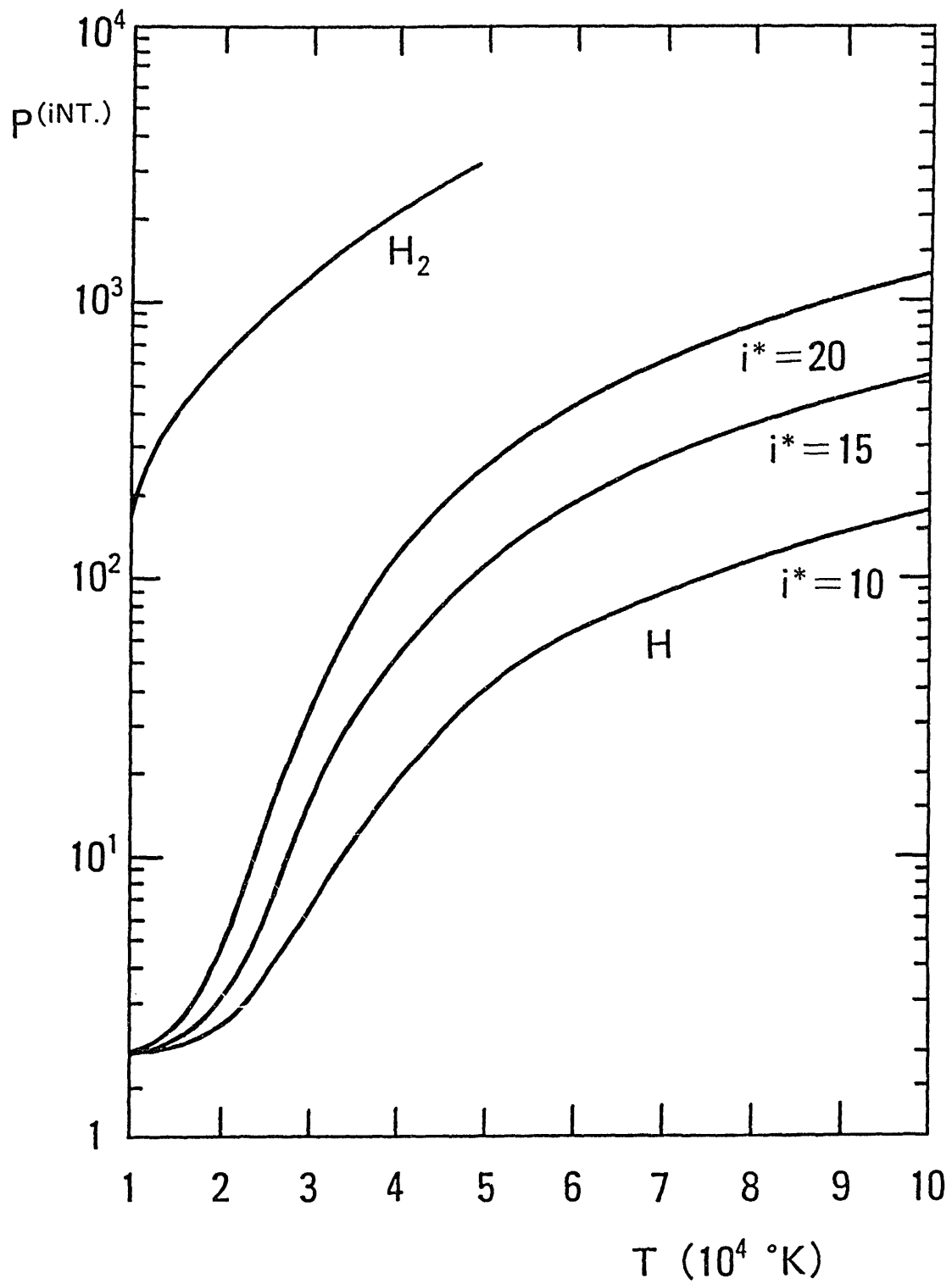


Figure 20. Internal partition function for atomic and molecular hydrogen

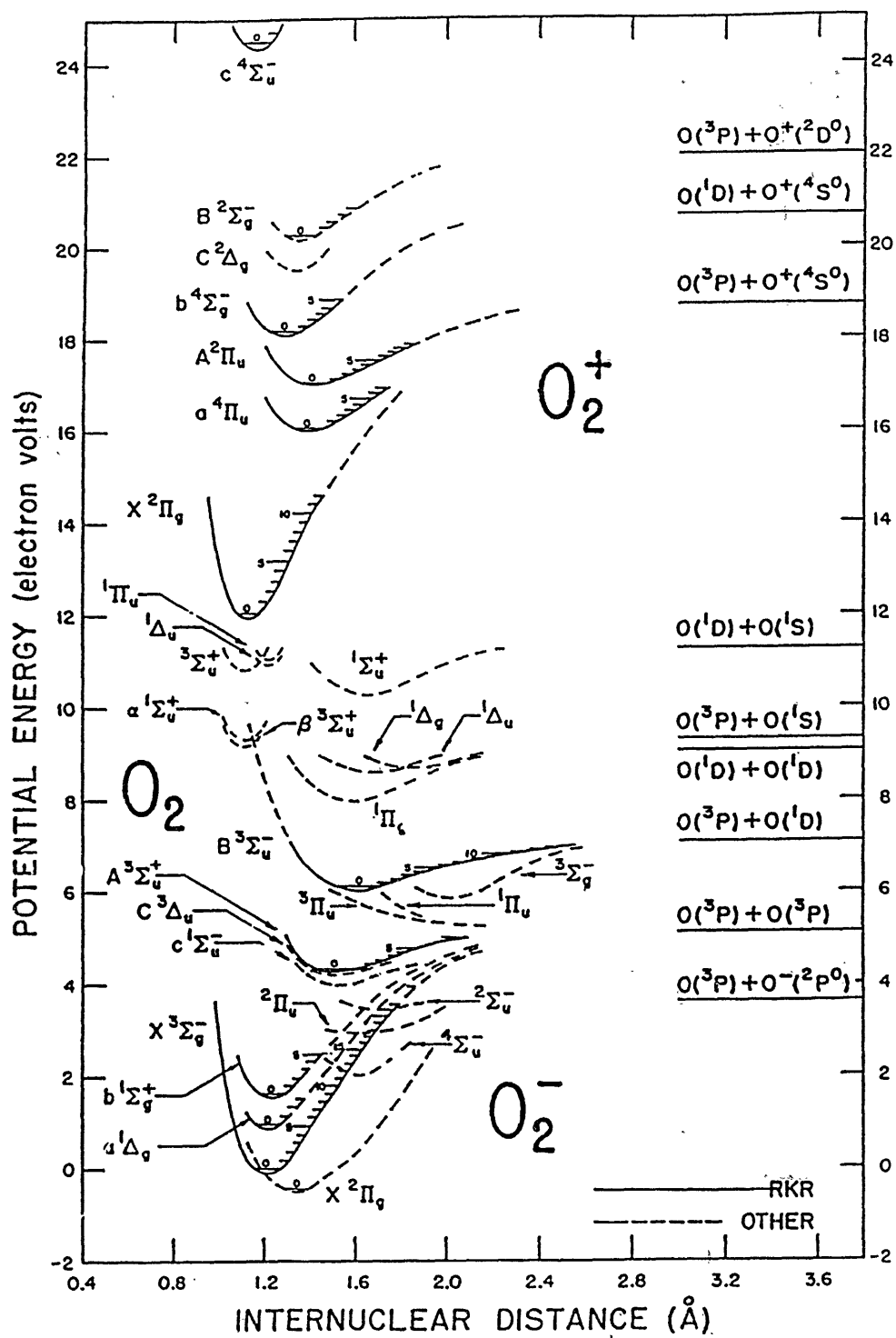
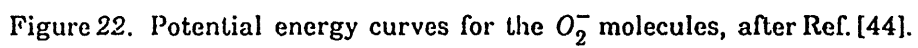


Figure 21. Potential energy curves for the O_2 , O_2^- and O_2^+ molecules, after Ref.[43].



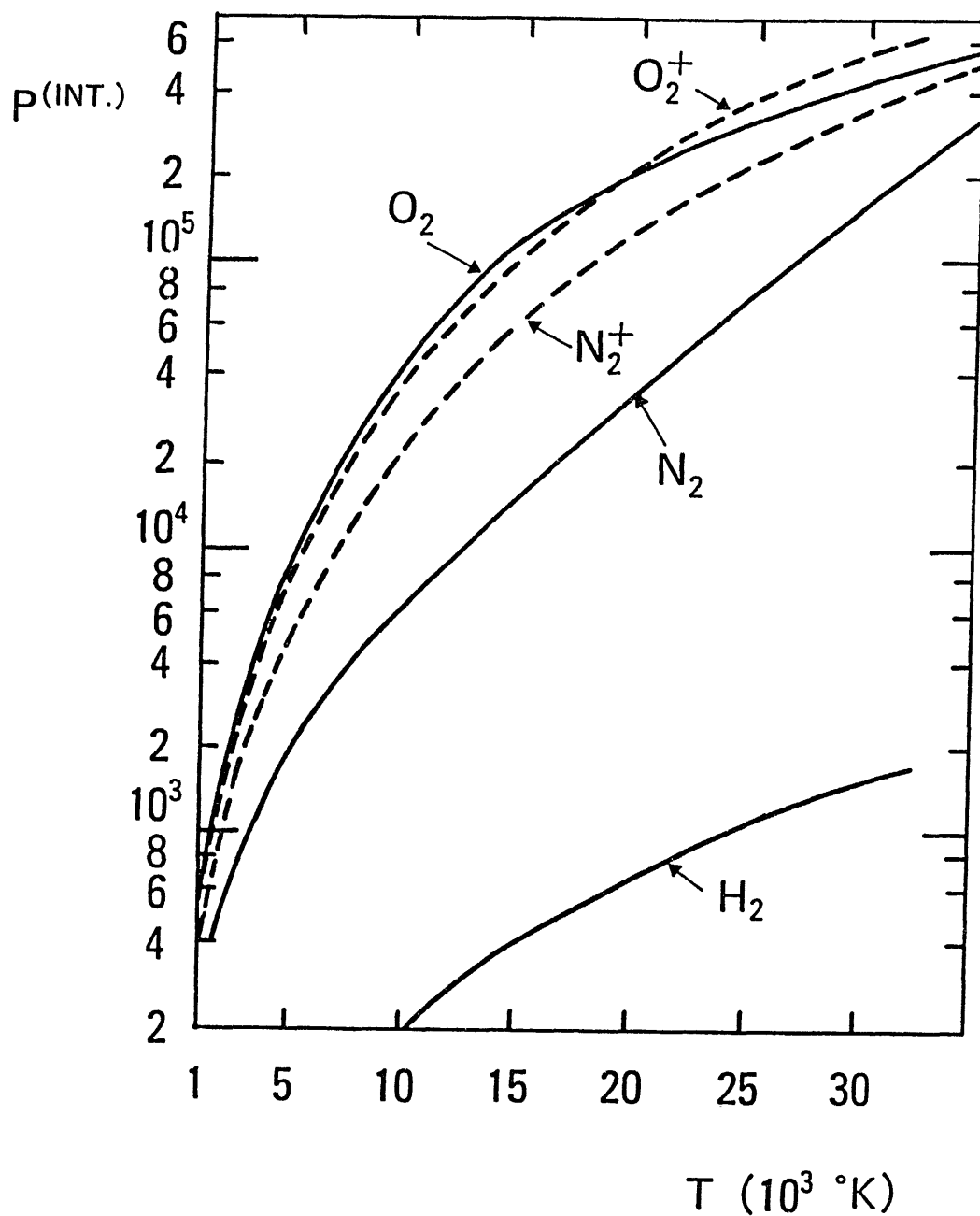


Figure 23. Internal partition functions $P(\text{int})$ for the O_2 , O_2^+ , N_2 , and N_2^+ molecules, after Ref. [45]. The partition function for H_2 of Fig. 19 is shown for comparison.

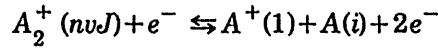
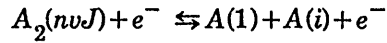
IV. 7 Collisional-Radiative Models for Molecules

All these considerations are rather qualitative. Unfortunately, not much can be said quantitatively about the role the molecules and molecular ions play in divertor plasmas. Only for L.T.E. plasmas is their influence known.

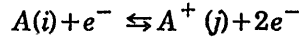
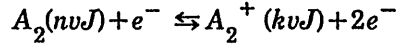
To describe the effect of molecules and molecular ions in divertor plasmas quantitatively, a collisional-radiative model is necessary which couples electrons, molecules, atoms, molecular ions and atomic ions. To ensure some consistency of such a model it is indispensable to consider both forward and backward reactions. This permits to study ionizing, stationary and recombining plasmas and to investigate the conditions for approaching local thermodynamic equilibrium.

We will consider a homo-nuclear diatomic molecule, symbolically designated by A_2 . Then the following reactions should be included in the model (nvJ designate electronic vibrational states, i and j electronic states) :

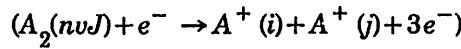
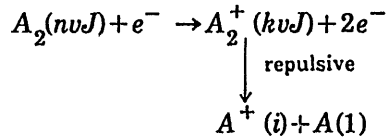
• Electron-impact dissociation and atom recombination :



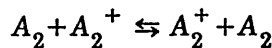
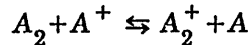
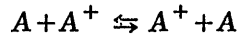
Electron-impact ionization and 3-body recombination :



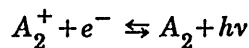
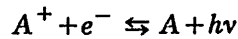
Electron-impact ionization with dissociation :



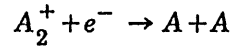
Charge exchange :



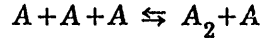
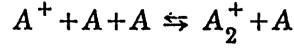
Radiative recombination and photoionization :



Dissociative recombination :



Atomic recombination and dissociation :



The reactions should as far as possible be specified by their quantum state. In addition to these reactions which link molecular species to atomic species (and their ions), the most important reactions within A_2 , A_2^+ , A and A^+ have to be taken into account, that is : electronic excitation and de-excitation of electronic and ro-vibrational levels, and spontaneous de-excitations and eventual reabsorption from the ground level. When A^{2+} -ions can be formed, the corresponding reactions must also be included in the model.

The presence of carbon and oxygen in a hydrogen plasma leads to numerous molecular associations, e. g. C_xH_y , OH, CO, CO_2 , ...and their ions. The spatial distributions of metal impurities in such an environment is strongly influenced by charge transfer reactions in which the excited atomic and molecular species play an important role.

The great variety of reactions excludes edge plasma models in which all or too many reactions are taken into account. An important task is therefore the identification of the most prominent reaction processes, assuming that they dominate the edge plasma properties. To test simplified edge plasma models, independent collisional-radiative model calculations with a larger number of reaction processes should be performed.

Whether such collisional-radiative calculations can be performed, or not, depends on the availability of the relevant atomic and molecular data and/or rate coefficients for electron and heavy particle velocity distributions which are characteristic for edge plasmas.

IV.8 Atomic And Molecular Data for Edge Plasmas

Reliable model calculations for the edge plasma require a minimum set of atomic and molecular data for the prominent atomic and molecular species and their ions. The presence of molecules and molecular ions considerably complicates the situation, since the ro-vibrational levels play an important role in the excitation, dissociation and ionization of electronic states. The existence of the molecular ion H_2 seems to have a direct influence of the formation of H ions.

Non-Franck-Condon populations have been observed for the $a^1\Delta_g$ and $b^1\Sigma_g$ states of the O_2 molecule [46]. The probable reason of this phenomenon is the existence of the intermediate resonance state $2\pi_g$ of the O_2 molecular ion which dominates the excitation of the O_2 molecular levels. According to Refs.[46,47] the following electronic states of O_2 should be affected by intermediate O_2^+ states: $X^3\Sigma_g^-$, $a^1\Delta_g$, $b^1\Sigma_g^+$, $A^3\Sigma_u^+$, $A^3\Delta_u$, $\tau^1\Sigma_u^-$, $B^3\Sigma_u^-$, $^1\Sigma_u^+$ and $^1\Delta_u$. The three lowest states have excitation energies around 6eV which corresponds to the temperature in the edge plasma close to the walls and in the divertor plasma close to the target plates.

This example shows that one has to be careful in the application of the presently known molecular data. The reader finds a discussion of the data requirements for fusion plasma edge studies in Ref. [48] with a review of the available data base of atomic and molecular data. Only for the H_2 molecule and the H_2 molecular ion is the data base relatively well established. But even for this molecule data are missing which permit to treat the collisional-radiative coupling of the molecular with the atomic states. This coupling process determines for instance the photon emission rate of H_α and H_β which is used as a diagnostic tool.

The known cross-sections (together with the rate coefficients) involving atomic and molecular hydrogen and their ions (H^+ , H^- , H_2^+ , H_2^- , H_3^+) and helium and its ions have been compiled in Refs.[49-51]. A data compilation for the O_2 molecule is given in Ref. [52]. As for hydrogen, important cross-sections are not yet known and which are necessary to couple the molecular to the atomic states.

References

- [1] YAAKOBI, B., et al. in "Laser Interaction and Related Phenomena", Vol. 7, (Eds. H. Hora and G.H. Miley) p. 89, Plenum Press 1985
- [2] YAMANAKA, C., et al., Nucl. Fusion 27 (1987) 19
- [3] KEY, M. H., in "Laser - Plasma Interactions", (Eds. R.A. Cairns and J. J. Sanderson), Scottish Universities Summer School in Physics, p. 219, Edinburgh 1979.
- [4] FELBER, F. S., MILLER, P. H., PARKS, P. B., PRATER, R. and VASLOW, D. F., Nucl. Fusion 19 (1979) 1061
- [5] SPITZER, L. jr., "Physics of Fully Ionized Gases", 2nd Ed., Interscience Publ. 1962
- [6] DELCROIX, J-L., "Physique des Plasmas, Tome 1, Dunod, Paris 1963
- [7] DRAWIN, H. W., Physics Reports 37 (1978) 125
- [8] HOLSTEIN, T., Phys. Rev. 83 (1951) 1159 ; see also MANCINI, R.C., et al., J. Phys. B: At. Mol. Phys. 20 (1987) 2975
- [9] DRAWIN, H. W., in "Progress in Plasmas and Gas Electronics", Vol. 1, (Eds. R. Rompe and M. Steenbeck, p. 591, Akademie Verlag, Berlin 1975
- [10] DRAWIN, H. W., in "Atomic and Molecular Physics of Controlled Thermonuclear Fusion" (Eds. Ch. J. Joachain and D. E. Post), p. 519, Plenum Press 1983
- [11] RAEDER, J. and SUGAR, J., Energy Levels of Iron, *Fe* I through *Fe* XXVI, J. Phys. and Chem. Reference Data 4 (1975) 353
- [12] ENGELHARDT, W., BEHRINGER, K., FUSSMANN, G. und das ASDEX - Team, Verhandlg. DPG VI 16 (1981) 875, also I.A. E. A. Technical Committee Meeting on Divertors and Impurity Control, July 6-10, Garching 1981, paper I. C6, Conference Proceedings
- [13] DRAWIN, H. W., in "Atomic and Molecular Physics of Controlled Thermonuclear Fusion" (Eds. Ch. J. Joachain and D. E. Post) p. 341, Plenum Press 1983
- [14] DE MICHELIS, C. and MATTIOLI, M., Rep. Prog. Phys. 47 (1984) 1233
- [15] ISLER, R. C., Nucl. Fusion 24 (1984) 1599

- [16] HULSE, R.A., Nuclear Techn. 3 (1983) 259
- [17] TFR - Group, Nucl. Fusion 23 (1983) 559
- [18] TFR - Group, Nucl. Fusion 25 (1985) 1767, see also Nucl. Fusion 25 (1985) 981
- [19] BRETON, C., DE MICHELIS, C. and MATTIOLI, M., Nucl. Fusion 16 (1976) 891
- [20] RICE, J. E., MARMAR, E. S., TERRY, J. L., KÄLLNE, E. and KÄLLNE, J., Phys. Rev. Lett. 56 (1986) 50
- [21] KATO, T., MORITA, S., MASAI, K. and HAYAKAWA, S., Phys. Rev. A 36 (1987) 795
- [22] MASAI, K. and KATO, T., Phys. Letts. 123 (1987) 405
- [23] SATO, K., SUCKEWER, S. and WOUTERS, A., Phys. Rev. A 36 (1987) 3312
- [24] SATO, K., MIMURA, M., OTSUKA, M., WATARI, T., ONO, M., TOI, K., KAWASUMI, Y., KAWAHATA, K. and ODA, T., Phys. Rev. Lett. 56 (1986) 151
- [25] POST, D. E. and BEHRISCH, R. (Eds.), "Physics of Plasma - Wall Interactions in Controlled Fusion", Plenum 1986
- [26] HARRISON, M. F. A., article in Ref. [25], p. 281
- [27] BOGEN, P. and HINTZ, E., article in Ref. [25], p. 211
- [28] HEIFETZ, D. B., article in Ref. [25], p. 695
- [29] POST, D. E. and LACKNER, K., article in Ref. [25], p. 627
- [30] POST, D. E., BEHRISCH, R. and STANSFIELD, B., article in Ref. [25], p. 1
- [31] ENGELMANN, F., article in Ref. [25], p. 15
- [32] WAGNER, F. and LACKNER, K., article in Ref. [25], p. 931
- [33] KEILHACKER, M., et al., article in Plasma Physics and Contr. Nucl. Fusion Research, 1980, (Proc. 8th Intern. Conf., Brussels), Vol. 2, p. 351, IAEA, Vienna, 1981
- [34] BEHRINGER, K. H., J. Nucl. Materials 145/147 (1987) 145

- [35] MAHDAVI, M. A., ARMENTROUT, C. J., BLAU, F. P., et al., J. Nucl. Materials 111 & 112 (1982) 355
- [36] ENGELHARDT, W., BECKER, G., BEHRINGER, K., et al., J. Nucl. Materials 111 & 112 (1982) 337
- [37] FONCK, R. J., BELL, M., BOL, K., et al., J. Nucl. Materials 111 & 112 (1982) 343
- [38] KAHN, C., BURREL, K. H., EJIMA, S., FAIRBANKS, E., PETRIE, T., SHIMADA, M. and WASHIZU, M., Nucl. Fusion 26 (1986) 73
- [39] SHIMADA, M., NAGAMI, M., IOKI, K., et al., Nucl. Fusion 22 (1982) 643
- [40] SHIMOMURA, Y., KEILHACKER, M., LACKNER, K. and MURMAN, H., Nucl. Fusion 23 (1983) 869
- [41] SHIMADA, M. and JAERI Team, J. Nucl. Materials 121 (1984) 184
- [42] SCHNEIDER, W., HEIFETZ, D. B., LACKNER, K., NEUHAUSER, J., POST, D. E. and RAUH, K. G., J. Nucl. Materials 121 (1984) 178
- [43] KRUPENIE, P. H., J. Phys. Chem. Ref. Data 1 (1972) 423
- [44] MICHELS, H. H., article in "The Excited State in Chemical Physics", Part 2, (Ed. J.J. McGowan) in the series: Advances in Chemical Physics, Vol. XLV, p. 225 Interscience 1981
- [45] DRELLISHAK, K. S., AESCHLIMAN, D. P. and CAMBEL, A. B., Phys. Fluids 8 (1965) 1590
- [46] TEILLET-BILLY, D., et al., Europhys. Lett. 6 (1988) 139
- [47] TEILLET-BILLY, D., MALEGAT, L. and GAUYACQ, J. P., J. Phys. B 20 (1987) 3201
- [48] TAWARA, H., and PHANEUF, R. A., Comments on Atomic and Molecul. Phys. (in the press)
- [49] TAWARA, H., et al., Report IPPJ-AM-46, Institute of Plasma Physics, Nagoya University, July 1986: "Atomic Data Involving Hydrogen Relevant to Edge Plasmas"
- [50] TAWARA, H., et al., Report IPPJ-AM-55, Nagoya University, October 1987 (supplement to Ref. [49]).

- [51] JANEV, R. K., LANGER, W. D. EVANS, K. jr. and POST, D.E. jr. :“Elementary Processes in Hydrogen-Helium Plasmas”, Springer 1987
- [52] ICHIKAWA, Y., et al., ISAS RN-374 (The Institute of Space and Astronautical Science, Dec., 1987)

APPENDIX

The mean value $\langle Q(\vec{r}, t) \rangle$ for any arbitrary function $Q(\vec{w}, \vec{r}, t)$ is given by

$$\langle Q(\vec{r}, t) \rangle = \frac{1}{n(r, t)} \int \int \int_{-\infty}^{+\infty} Q(\vec{w}) f(\vec{w}, \vec{r}, t) d^3w$$

The derivatives are calculated as follows :

$$\int \int \int_{-\infty}^{+\infty} Q(\vec{w}) \frac{\partial f}{\partial t} d^3w = \frac{\partial}{\partial t} \int \int \int_{-\infty}^{+\infty} Q(\vec{w}) f(\vec{w}, \vec{r}, t) d^3w = \frac{\partial}{\partial t} (n \langle Q \rangle)$$

The divergence of the velocity moment of $Q(\vec{w})$ is obtained as follows :

$$\int \int \int_{-\infty}^{+\infty} Q(\vec{w}) \vec{w} \cdot \vec{\nabla} f d^3w = \vec{\nabla} \cdot \int \int \int_{-\infty}^{+\infty} Q(\vec{w}) \vec{w} f(\vec{w}, \vec{r}, t) d^3w = \vec{\nabla} \cdot (n \langle Q \vec{w} \rangle)$$

The integral involving the force \vec{F} yields with an integration by parts over \vec{w}

$$\begin{aligned} \int \int \int_{-\infty}^{+\infty} Q(\vec{w}) \vec{F}(\vec{r}, \vec{w}) \cdot \vec{\nabla}_w f d^3w &= [QF]_{-\infty}^{+\infty} - \int \int \int_{-\infty}^{+\infty} f \vec{\nabla}_w \cdot (\vec{F}Q) d^3w = -n \langle \vec{\nabla}_w \cdot \vec{F}Q \rangle \\ &= -n \langle (\vec{\nabla}_w \vec{F})Q \rangle - n \langle \vec{F} \cdot \vec{\nabla}_w Q \rangle \end{aligned}$$

because of $f=0$ for $w=\pm\infty$.

For magnetic forces : $\vec{\nabla}_w \cdot \vec{F} = 0$

For $Q(w)=w$: $\langle \vec{F} \cdot \vec{\nabla}_w \vec{w} \rangle = \langle \vec{F} \rangle$

For $Q(w)=ww$: $\langle \vec{F} \cdot \vec{\nabla}_w \vec{w} \vec{w} \rangle = 2 \langle \vec{F} \vec{w} \rangle$

$\vec{\nabla}_w$ is the gradient operator with respect to \vec{w} : $\frac{\partial}{\partial w_x} \vec{i}, \frac{\partial}{\partial w_y} \vec{j}, \frac{\partial}{\partial w_z} \vec{k}$.

LIST OF IPPJ-AM REPORTS

- IPPJ-AM-1 * "Cross Sections for Charge Transfer of Hydrogen Beams in Gases and Vapors in the Energy Range 10 eV–10 keV"
H. Tawara (1977) [Published in Atomic Data and Nuclear Data Tables 22, 491 (1978)]
- IPPJ-AM-2* "Ionization and Excitation of Ions by Electron Impact –Review of Empirical Formulae–"
T. Kato (1977)
- IPPJ-AM-3 "Grotrian Diagrams of Highly Ionized Iron FeVIII-FeXXVI"
K. Mori, M. Otsuka and T. Kato (1977) [Published in Atomic Data and Nuclear Data Tables 23, 196 (1979)]
- IPPJ-AM-4 "Atomic Processes in Hot Plasmas and X-Ray Emission"
T. Kato (1978)
- IPPJ-AM-5* "Charge Transfer between a Proton and a Heavy Metal Atom"
S. Hiraide, Y. Kigoshi and M. Matsuzawa (1978)
- IPPJ-AM-6* "Free-Free Transition in a Plasma –Review of Cross Sections and Spectra–"
T. Kato and H. Narumi (1978)
- IPPJ-AM-7* "Bibliography on Electron Collisions with Atomic Positive Ions: 1940 Through 1977"
K. Takayanagi and T. Iwai (1978)
- IPPJ-AM-8 "Semi-Empirical Cross Sections and Rate Coefficients for Excitation and Ionization by Electron Collision and Photoionization of Helium"
T. Fujimoto (1978)
- IPPJ-AM-9 "Charge Changing Cross Sections for Heavy-Particle Collisions in the Energy Range from 0.1 eV to 10 MeV I. Incidence of He, Li, Be, B and Their Ions"
Kazuhiko Okuno (1978)
- IPPJ-AM-10 "Charge Changing Cross Sections for Heavy-Particle Collisions in the Energy Range from 0.1 eV to 10 MeV II. Incidence of C, N, O and Their Ions"
Kazuhiko Okuno (1978)
- IPPJ-AM-11 "Charge Changing Cross Sections for Heavy-Particle Collisions in the Energy Range from 0.1 eV to 10 MeV III. Incidence of F, Ne, Na and Their Ions"
Kazuhiko Okuno (1978)
- IPPJ-AM-12* "Electron Impact Excitation of Positive Ions Calculated in the Coulomb-Born Approximation –A Data List and Comparative Survey–"
S. Nakazaki and T. Hashino (1979)
- IPPJ-AM-13 "Atomic Processes in Fusion Plasmas – Proceedings of the Nagoya Seminar on Atomic Processes in Fusion Plasmas Sept. 5-7, 1979"
Ed. by Y. Itikawa and T. Kato (1979)
- IPPJ-AM-14 "Energy Dependence of Sputtering Yields of Monatomic Solids"
N. Matsunami, Y. Yamamura, Y. Itikawa, N. Itoh, Y. Kazumata, S. Miyagawa, K. Morita and R. Shimizu (1980)

- IPPJ-AM-15 "Cross Sections for Charge Transfer Collisions Involving Hydrogen Atoms"
Y. Kaneko, T. Arikawa, Y. Itikawa, T. Iwai, T. Kato, M. Matsuzawa, Y. Nakai,
K. Okubo, H. Ryufuku, H. Tawara and T. Watanabe (1980)
- IPPJ-AM-16 "Two-Centre Coulomb Phaseshifts and Radial Functions"
H. Nakamura and H. Takagi (1980)
- IPPJ-AM-17 "Empirical Formulas for Ionization Cross Section of Atomic Ions for Elec-
tron Collisions –Critical Review with Compilation of Experimental Data–"
Y. Itikawa and T. Kato (1981)
- IPPJ-AM-18 "Data on the Backscattering Coefficients of Light Ions from Solids"
T. Tabata, R. Ito, Y. Itikawa, N. Itoh and K. Morita (1981) [Published in
Atomic Data and Nuclear Data Tables 28, 493 (1983)]
- IPPJ-AM-19 "Recommended Values of Transport Cross Sections for Elastic Collision and
Total Collision Cross Section for Electrons in Atomic and Molecular Gases"
M. Hayashi (1981)
- IPPJ-AM-20 "Electron Capture and Loss Cross Sections for Collisions between Heavy
Ions and Hydrogen Molecules"
Y. Kaneko, Y. Itikawa, T. Iwai, T. Kato, Y. Nakai, K. Okuno and H. Tawara
(1981)
- IPPJ-AM-21 "Surface Data for Fusion Devices – Proceedings of the U.S–Japan Work-
shop on Surface Data Review Dec. 14-18, 1981"
Ed. by N. Itoh and E.W. Thomas (1982)
- IPPJ-AM-22 "Desorption and Related Phenomena Relevant to Fusion Devices"
Ed. by A. Koma (1982)
- IPPJ-AM-23 "Dielectronic Recombination of Hydrogenic Ions"
T. Fujimoto, T. Kato and Y. Nakamura (1982)
- IPPJ-AM-24 "Bibliography on Electron Collisions with Atomic Positive Ions: 1978
Through 1982 (Supplement to IPPJ-AM-7)"
Y. Itikawa (1982) [Published in Atomic Data and Nuclear Data Tables 31,
215 (1984)]
- IPPJ-AM-25 "Bibliography on Ionization and Charge Transfer Processes in Ion-Ion
Collision"
H. Tawara (1983)
- IPPJ-AM-26 "Angular Dependence of Sputtering Yields of Monatomic Solids"
Y. Yamamura, Y. Itikawa and N. Itoh (1983)
- IPPJ-AM-27 "Recommended Data on Excitation of Carbon and Oxygen Ions by Electron
Collisions"
Y. Itikawa, S. Hara, T. Kato, S. Nakazaki, M.S. Pindzola and D.H. Crandall
(1983) [Published in Atomic Data and Nuclear Data Tables 33, 149 (1985)]
- IPPJ-AM-28 "Electron Capture and Loss Cross Sections for Collisions Between Heavy
Ions and Hydrogen Molecules (Up-dated version of IPPJ-AM-20)
H. Tawara, T. Kato and Y. Nakai (1983) [Published in Atomic Data and
Nuclear Data Tables 32, 235 (1985)]

- IPPJ-AM-29 "Bibliography on Atomic Processes in Hot Dense Plasmas"
T. Kato, J. Hama, T. Kagawa, S. Karashima, N. Miyanaga, H. Tawara,
N. Yamaguchi, K. Yamamoto and K. Yonei (1983)
- IPPJ-AM-30 "Cross Sections for Charge Transfers of Highly Ionized Ions in Hydrogen
Atoms (Up-dated version of IPPJ-AM-15)"
H. Tawara, T. Kato and Y. Nakai (1983) [Published in Atomic Data and
Nuclear Data Tables 32, 235 (1985)]
- IPPJ-AM-31 "Atomic Processes in Hot Dense Plasmas"
T. Kagawa, T. Kato, T. Watanabe and S. Karashima (1983)
- IPPJ-AM-32 "Energy Dependence of the Yields of Ion-Induced Sputtering of Monatomic
Solids"
N. Matsunami, Y. Yamamura, Y. Itikawa, N. Itoh, Y. Kazumata, S. Miyagawa,
K. Morita, R. Shimizu and H. Tawara (1983) [Published in Atomic Data and
Nuclear Data Tables 31, 1 (1984)]
- IPPJ-AM-33 "Proceedings on Symposium on Atomic Collision Data for Diagnostics and
Modelling of Fusion Plasmas, Aug. 29 – 30, 1983"
Ed. by H. Tawara (1983)
- IPPJ-AM-34 "Dependence of the Backscattering Coefficients of Light Ions upon Angle of
Incidence"
T. Tabata, R. Ito, Y. Itikawa, N. Itoh, K. Morita and H. Tawara (1984)
- IPPJ-AM-35 "Proceedings of Workshop on Synergistic Effects in Surface Phenomena
Related to Plasma-Wall Interactions, May 21 – 23, 1984"
Ed. by N. Itoh, K. Kamada and H. Tawara (1984) [Published in Radiation
Effects 89, 1 (1985)]
- IPPJ-AM-36 "Equilibrium Charge State Distributions of Ions ($Z_1 \geq 4$) after Passage
through Foils – Compilation of Data after 1972"
K. Shima, T. Mikumo and H. Tawara (1985) [Published in Atomic Data and
Nuclear Data Tables 34, 357 (1986)]
- IPPJ-AM-37 "Ionization Cross Sections of Atoms and Ions by Electron Impact"
H. Tawara, T. Kato and M. Ohnishi (1985) [Published in Atomic Data and
Nuclear Data Tables 36, 167 (1987)]
- IPPJ-AM-38 "Rate Coefficients for the Electron-Impact Excitations of C-like Ions"
Y. Itikawa (1985)
- IPPJ-AM-39 "Proceedings of the Japan-U.S. Workshop on Impurity and Particle Control,
Theory and Modeling, Mar. 12 – 16, 1984"
Ed. by T. Kawamura (1985)
- IPPJ-AM-40 "Low-Energy Sputterings with the Monte Carlo Program ACAT"
Y. Yamamura and Y. Mizuno (1985)
- IPPJ-AM-41 "Data on the Backscattering Coefficients of Light Ions from Solids (a
Revision)"
R. Ito, T. Tabata, N. Itoh, K. Morita, T. Kato and H. Tawara (1985)

- IPPJ-AM-42 "Stopping Power Theories for Charged Particles in Inertial Confinement Fusion Plasmas (Emphasis on Hot and Dense Matters)"
S. Karashima, T. Watanabe, T. Kato and H. Tawara (1985)
- IPPJ-AM-43 "The Collected Papers of Nice Project/IPP, Nagoya"
Ed. by H. Tawara (1985)
- IPPJ-AM-44 "Tokamak Plasma Modelling and Atomic Processes"
Ed. by T. Kawamura (1986)
- IPPJ-AM-45 Bibliography of Electron Transfer in Ion-Atom Collisions
H. Tawara, N. Shimakura, N. Toshima and T. Watanabe (1986)
- IPPJ-AM-46 "Atomic Data Involving Hydrogens Relevant to Edge Plasmas"
H. Tawara, Y. Itikawa, Y. Itoh, T. Kato, H. Nishimura, S. Ohtani, H. Takagi, K. Takayanagi and M. Yoshino (1986)
- IPPJ-AM-47 "Resonance Effects in Electron-Ion Collisions"
Ed. by H. Tawara and G. H. Dunn (1986)
- IPPJ-AM-48 "Dynamic Processes of Highly Charged Ions (Proceedings)"
Ed. by Y. Kanai and S. Ohtani (1986)
- IPPJ-AM-49 "Wavelengths of K X-Rays of Iron Ions"
T. Kato, S. Morita and H. Tawara (1987)
- IPPJ-AM-50 "Proceedings of the Japan-U.S. Workshop P-92 on Plasma Material Interaction/High Heat Flux Data Needs for the Next Step Ignition and Steady State Devices, Jan. 26 – 30, 1987"
Ed. by A. Miyahara and K. L. Wilson (1987)
- IPPJ-AM-51 "High Heat Flux Experiments on C-C Composite Materials by Hydrogen Beam at the 10MW Neutral Beam Injection Test Stand of the IPP Nagoya"
H. Bolt, A. Miyahara, T. Kuroda, O. Kaneko, Y. Kubota, Y. Oka and K. Sakurai (1987)
- IPPJ-AM-52 "Energy Dependence of Ion-Induced Sputtering Yields of Monatomic Solids in the Low Energy Region"
N. Matsunami, Y. Yamamura, N. Itoh, H. Tawara and T. Kawamura (1987)
- IPPJ-AM-53 "Data Base on the High Heat Flux Behaviour of Metals and Carbon Materials for Plasma Facing Components – Experiments at the 10 MW Neutral Beam Injection Test Stand of the IPP Nagoya"
H. Bolt, C. D. Croessmann, A. Miyahara, T. Kuroda and Y. Oka (1987)
- IPPJ-AM-54 "Final (n, ℓ) State-Resolved Electron Capture by Multiply Charged Ions from Neutral Atoms"
N. Shimakura, N. Toshima, T. Watanabe and H. Tawara (1987)
- IPPJ-AM-55 "Atomic Data for Hydrogens in Collisions with Electrons – Addenda to IPPJ-AM-46"
H. Tawara, Y. Itikawa, H. Nishimura and M. Yoshino (1987)

- IPPJ-AM-56 "Total and Partial Cross Sections for Electron Capture for C^{q+} ($q=6-2$) and O^{q+} ($q=8-2$) Ions in Collisions with H, H_2 and He Atoms"
H. Tawara (1987)
- IPPJ-AM-57 "Atomic Models for Hot Dense Plasmas"
K. Fujima (1988)
- IPPJ-AM-58 "Recommended Data for Excitation Rate Coefficients of Helium Atoms and Helium-Like Ions by Electron Impact"
T. Kato and S. Nakazaki (1988)
- IPPJ-AM-59 "Atomic and Molecular Processes in Edge Plasmas Including Hydrocarbon Molecules"
Ed. by H. Tawara (1988)
- IPPJ-AM-60 "Theory of Threshold Energy of Ion-Induced Desorption by a Few-Collision Model"
Y. Yamamura, J. Bohdansky and E. Taglauer (1988)
- IPPJ-AM-61 "The Application of Atomic and Molecular Physics in Fusion Plasma Diagnostics"
H. W. Drawin (1988)

Available upon request to Research Information Center, Institute of Plasma Physics, Nagoya University, Nagoya 464, Japan, except for the reports noted with*.